# Probing some beyond Standard Model scenarios in different sectors of flavour physics

*By*
**Anirban Karan**

**PHYS10201205008**

**The Institute of Mathematical Sciences, Chennai**

*A thesis submitted to the*

*Board of Studies in Physical Sciences*

*In partial fulfillment of requirements*

*For the Degree of*

**DOCTOR OF PHILOSOPHY**

*of*

**HOMI BHABHA NATIONAL INSTITUTE**



**May, 2019**

# Homi Bhabha National Institute

## Recommendations of the Viva Voce Board

As members of the Viva Voce Board, we certify that we have read the dissertation prepared by Anirban Karan entitled "Probing some beyond Standard Model scenarios in different sectors of flavour physics" and recommend that it maybe accepted as fulfilling the dissertation requirement for the Degree of Doctor of Philosophy.

_____ Date: 25.10.19

Chair - V. RAVINDRAN

_____ Date: 25.10.19 .

Guide/Convener - RAHUL SINHA

_____ Date: 25.10.19

Examiner - ANIRBAN KUNDU

_____ Date: 25.10.19

Member 1 - D. INDUMATHI

_____ Date: 25.10.19

Member 2 - SHRIHARI GOPALAKRISHNA

_____ Date: 25/10/2019

Member 3 - SIBASISH GHOSH

Final approval and acceptance of this dissertation is contingent upon the candidate's submission of the final copies of the dissertation to HBNI.

I hereby certify that I have read this dissertation prepared under my direction and recommend that it may be accepted as fulfilling the dissertation requirement.

Date: 25.10.19

Place: Chennai

Guide

i

# STATEMENT BY AUTHOR

This dissertation has been submitted in partial fulfillment of requirements for an advanced degree at Homi Bhabha National Institute (HBNI) and is deposited in the Library to be made available to borrowers under rules of the HBNI.

Brief quotations from this dissertation are allowable without special permisiion, provided that accurate acknowledgement of source is made. Requests for permisiion for extended quotation from or reproduction of this manuscriptin whole or in part may be granted by the Competent Authority of HBNI when in his or her judgement the proposed use of the material is in the interests of scholarship. In all other instances, however, permission must be obtained from the author.

Anirban Karan

# DECLARATION

I, hereby declare that the investigtion presented in the thesis has been carried out by me. The work is original and has notbeen submitted eralier as a whole or in part for a degree / diploma at this or any other Institution / University.

Anirban Karan

*Dedicated To,*

*My Parents And Grand Parents.*

# ACKNOWLEDGEMENTS

# List of Publications

- ## <u>Publications included in the thesis:</u>

  1. *"Using time-dependent indirect CP asymmetries to measure T and CPT violation in $B^0 - \bar{B}^0$ mixing"*, **Anirban Karan**, Abinash Kumar Nayak, Rahul Sinha, David London, *Phys. Lett. B 781 (2018) 459-463*.

  2. *"Testing $WW\gamma$ vertex in radiative muon decay"*, **Anirban Karan**, Rusa Mandal, Rahul Sinha, *Phys. Rev. D 99, 033006 (2019)*.

- ## <u>Other publications:</u>

  1. *"Signal of right-handed currents using $B \to K^* l^+ l^-$ observables at the kinematic endpoint"*, **Anirban Karan**, Rusa Mandal, Abinash Kumar Nayak, Rahul Sinha, Thomas E. Browder, *Phys. Rev. D 95, 114006 (2017)*.

  2. *"Simulating Dirac Hamiltonian in curved space-time by split-step quantum walk"*, Arindam Mallick, Sanjoy Mandal, **Anirban Karan**, C M Chandrashekar, *J. Phys. Commun. 3, 015012 (2019)*.

# Seminars Presented

1. *"T & CPT violation in B meson mixing"*, 7$^{th}$ Belle Analysis Workshop (BAW-2017), **Malaviya National Institute of Technology, Jaipur**, 29th November - 3rd December 2017.

2. *"Using indirect CP asymmetry to measure T & CPT violation in B meson mixing"*, Institute Seminar Days 2018, **The Institute of Mathematical Sciences, Chennai**, 9th April 2018.

3. *"Estimation of T and CPT violation in $B^0 - \bar{B}^0$ mixing from time dependent CP asymmetry"* 16$^{th}$ Conference on Flavor Physics & CP Violation (FPCP 2018), **University of Hyderabad, Hyderabad**, 14th - 18th July 2018.

4. *"T & CPT violation in $B^0 - \bar{B}^0$ mixing"*, **Jožef Stefan Institute, Ljubljana, Slovenia**, 10th September 2018.

5. *"T & CPT violation in $B^0 - \bar{B}^0$ mixing"*, **Mainz Institute for Theoretical Physics, Mainz, Germany**, 25th September 2018.

6. *"Measuring T & CPT violation in $B^0 - \bar{B}^0$ mixing"*, **Universität Regensburg, Regensburg, Germany**, 28th September 2018.

# CONTENTS

# Contents

# Introduction and Motivation

In last few decades, experiments involving precision measurements at LEP, consistency of the top quark, discovery of Higgs boson etc., established the acceptability of standard model (SM) as the theory of elementary particles. However, there are several reasons to believe that the SM is not a complete theory, rather just an effective one. Among the reasons are the theoretical argument of naturalness protecting the Higgs mass from radiative corrections and the nature of Higgs vacuum. Experimentally, the observed matter-antimatter asymmetry arising with SM is inconsistent with the observed baryon over photon density. Neutrino oscillations are also regarded as the first evidence beyond SM. One also envisages that extensions beyond the SM will also eventually explain the nature of dark matter and dark energy. To understand the actual underlying theory, direct evidences for various beyond standard model (BSM) particles have been searched in collider experiments; but unfortunately, no success in this direction has been achieved to date. In this situation,

precise measurement of various theoretical parameters that are uniquely predicted in SM is indispensable. Any deviation observed from their predictions in SM will act as indirect evidence for the existence of BSM physics. Along with increase in the luminosity of beams and advancements in experimental techniques, new measurement methods are also required in this regard. In this thesis, we have studied new measurement procedures for two different types of theoretical parameters: a) T and CPT violation in $B^0 - \bar{B}^0$ mixing, b) C and P conserving dimension four $WW\gamma$ vertex.

CPT invariance is one of the pillars of quantum field theory (QFT) as its violation necessitates breaking of Lorentz symmetry [1] and hence, it must be tested in experiments with high precision. Direct searches for CPT violation through difference in masses or life-times of particle and antiparticle have been performed in several experiments; nevertheless, they are observed to be extremely insignificant in every case since they are mostly dominated by strong or electromagnetic interactions. Neutral pseudoscalar meson mixing, which is a second order weak process governed by box diagrams, seems to be a very promising candidate in this regard [2]. Though all experimental results to date are consistent with CPT conservation, an important improvement in statistics is expected in near future. In this thesis, we investigate the possibilities for indirect measurement of T and CPT violating parameters in $B^0 - \bar{B}^0$ mixing using the time-dependent indirect CP asymmetry in decays of $B^0$ or $\bar{B}^0$ to a CP eigenstate.

On the other hand, triple gauge boson interaction is a key feature of non-Abelian gauge theories which have been used in SM to describe weak and strong interactions. Nonetheless, triple gauge boson couplings in electroweak sector are yet to be measured with a sufficient accuracy for scrutinizing at least one loop correction to it within the SM framework. Radiative muon decay ($\mu \to e\nu_\mu\bar{\nu}_e\gamma$), which are expected to be produced in a large number as the background of experiments to probe lepton-flavour-violating process $\mu \to e\gamma$ (like COMET, MEG, Mu2e [3]), appears to be a promising mode for probing C- and P-conserving dimension-four $WW\gamma$ vertex. In this decay mode, we have studied a *new*

*type of zero* (other than the zeros of radiation amplitude [4]) which has not been studied so far and it enables us a sensitive probe for $WW\gamma$ vertex beyond the SM.

# Measuring T and CPT violation in $B^0 - \bar{B}^0$ mixing

The most general hamiltonian ($\mathcal{H}$) describing the mixing between two flavour states $B^0$ and $\bar{B}^0$ is given in terms of two $2 \times 2$ hermitian matrices $\mathbf{M}$ and $\mathbf{\Gamma}$, respectively the mass and decay matrices, as:

$$\mathcal{H} = \mathbf{M} - \frac{i}{2}\mathbf{\Gamma} . \tag{1}$$

The light (L) and heavy (H) physical states, which are actually the eigenstates of the mixing hamiltonian $\mathcal{H}$, can be expressed as linear combinations of flavour states in the following way:

$$|B_L\rangle = \cos\frac{\theta}{2}|B^0\rangle + e^{i\phi}\sin\frac{\theta}{2}|\bar{B}^0\rangle , \qquad |B_H\rangle = \sin\frac{\theta}{2}|B^0\rangle - e^{i\phi}\cos\frac{\theta}{2}|\bar{B}^0\rangle , \tag{2}$$

where $\theta$ and $\phi$ are mixing parameters and they are complex numbers in general.

Defining $g_\pm$ as following:

$$g_+ = e^{-it\left(M-i\frac{\Gamma}{2}\right)}\cos\left[\left(\Delta M - i\frac{\Delta\Gamma}{2}\right)\frac{t}{2}\right] , \quad g_- = e^{-it\left(M-i\frac{\Gamma}{2}\right)}i\sin\left[\left(\Delta M - i\frac{\Delta\Gamma}{2}\right)\frac{t}{2}\right] , \tag{3}$$

one can find the time-dependent decay amplitudes for uncorrelated or tagged neutral mesons (both $B^0$ and $\bar{B}^0$) decaying to a final state $f$ to be:

$$\begin{aligned} \mathcal{A}(B^0(t) \to f) &= (g_+ + g_-\cos\theta)\mathcal{A}_f + e^{i\phi}g_-\sin\theta\bar{\mathcal{A}}_f , \\ \mathcal{A}(\bar{B}^0(t) \to f) &= e^{-i\phi}g_-\sin\theta\mathcal{A}_f + (g_+ - g_-\cos\theta)\bar{\mathcal{A}}_f , \end{aligned} \tag{4}$$

where $M \equiv (M_H + M_L)/2$, $\Delta M \equiv M_H - M_L$, $\Gamma \equiv (\Gamma_H + \Gamma_L)/2$ and $\Delta\Gamma \equiv \Gamma_H - \Gamma_L$, $\mathcal{A}_f \equiv \langle f|\mathcal{H}_{\Delta F=1}|B^0\rangle$ and $\bar{\mathcal{A}}_f \equiv \langle f|\mathcal{H}_{\Delta F=1}|\bar{B}^0\rangle$ with $\mathcal{H}_{\Delta F=1}$ being the decaying hamiltonian.

The time-dependent indirect CP asymmetry $\mathcal{A}_{CP}^{f}(t)$ involving B-meson decays to a CP eigenstate $f$ is defined as:

$$\mathcal{A}_{CP}^{f}(t) = \frac{\frac{d\Gamma}{dt}\left(\bar{B}_d^0(t) \to f\right) - \frac{d\Gamma}{dt}\left(B_d^0(t) \to f\right)}{\frac{d\Gamma}{dt}\left(\bar{B}_d^0(t) \to f\right) + \frac{d\Gamma}{dt}\left(B_d^0(t) \to f\right)} = \frac{\left|\mathcal{A}\left(\bar{B}_d^0(t) \to f\right)\right|^2 - \left|\mathcal{A}\left(B_d^0(t) \to f\right)\right|^2}{\left|\mathcal{A}\left(\bar{B}_d^0(t) \to f\right)\right|^2 + \left|\mathcal{A}\left(B_d^0(t) \to f\right)\right|^2} \; . \tag{5}$$

Using the T and CPT properties of $\mathbf{M}$ and $\mathbf{\Gamma}$, discussed in Ref. [5], we find that

- if CPT invariance holds, then, independently of T symmetry, $\boldsymbol{\theta = \pi/2}$ .

- if T invariance holds, then, independently of CPT symmetry, $\mathbf{Im}\,\boldsymbol{\phi} = \mathbf{0}$ .

This shows that though $|e^{i\phi}| = 1$ is usually taken to be the condition for absence of CP violation, it actually signifies the absence of T violation. Now, incorporating T and CPT violation in mixing. we express the mixing parameters as:

$$\theta = \frac{\pi}{2} + \epsilon_1 + i\epsilon_2 \quad \text{and} \quad \phi = -2\beta^{\text{mix}} + i\epsilon_3 \; , \tag{6}$$

where $\beta^{mix}$ is the weak phase describing $B^0 - \bar{B}^0$ mixing. Thus $\epsilon_1$ and $\epsilon_2$ are CPT violating parameters whereas non-zero value of $\epsilon_3$ indicates T violation. Though the values for $\epsilon_1$, $\epsilon_2$ and $\epsilon_3$ have already been reported by the BaBar and Belle Collaborations [6], the errors are too large to infer their existence.

For $B_d^0$ system (taking $\Delta\Gamma_d = 0$), the indirect CP asymmetry takes the familiar expression in the absence of T and CPT violation:

$$\mathcal{A}_{CP}^{f}(t) = S \sin\left(\Delta M_d t\right) - C \cos\left(\Delta M_d t\right), \tag{7}$$

where, $\quad S \equiv \sqrt{1 - C^2} \, \sin\varphi \; , \; C \equiv \dfrac{|\mathcal{A}_f|^2 - |\bar{\mathcal{A}}_f|^2}{|\mathcal{A}_f|^2 + |\bar{\mathcal{A}}_f|^2} \; , \; \varphi \equiv -2\beta^{mix} - \arg[\mathcal{A}_f] + \arg[\bar{\mathcal{A}}_f] \; . \tag{8}$

Here, $C$ is called direct CP asymmetry and $\varphi$ is the measured weak phase.

However, if T and CPT violations are present in mixing, the time dependent CP asymmetry

takes a very complicated form. Nevertheless, since $\epsilon_{1,2,3}$ and $y_d$ ($\equiv \Delta\Gamma_d/2\Gamma_d$) are expected as well as measured to be very small [6, 7], the CP asymmetry can be expanded in a relatively easier expression by keeping only terms at most linear in those parameters as follows:

$$
\begin{aligned}
\mathcal{A}_{CP/CPT}^{f}(t) \simeq{} & c_0 + c_1 \cos(\Delta M_d t) + c_2 \cos(2\Delta M_d t) + s_1 \sin(\Delta M_d t) \\
& + s_2 \sin(2\Delta M_d t) + c_1' \, \Gamma_d \, t \cos(\Delta M_d t) + s_1' \, \Gamma_d \, t \sin(\Delta M_d t)
\end{aligned}
\tag{9}
$$

The coefficients of various time dependent terms in the CP asymmetry act as observables. Using the five observables $c_0, c_1, c_2, s_1$ and $s_2$ one can analytically solve for five unknown parameters $C, \sin\varphi$ and $\epsilon_{1,2,3}$ from the following equations:

$$
C = -(c_0 + c_1 + c_2) \,,
\tag{10}
$$

$$
\sin^4\varphi - 2\left(\frac{s_1 + 2s_2}{2 - C^2}\right)\sin^3\varphi + 4C\left(C + \frac{c_2}{2 - C^2}\right)\sin^2\varphi
$$
$$
- 4\left(\frac{2C^2(s_1 + s_2) - s_2}{2 - C^2}\right)\sin\varphi - \left(\frac{8C\,c_2}{2 - C^2}\right) = 0 \,,
\tag{11}
$$

$$
\epsilon_1 = c_0 \sec\varphi - \frac{(2 - \sin^2\varphi)(c_2 \sin\varphi + 2C\,s_2)}{(4C^2 + \sin^2\varphi)\,\sin\varphi\,\cos\varphi} \,,
\tag{12}
$$

$$
\epsilon_2 = \frac{2\,(2C\,c_2 - s_2\,\sin\varphi)}{(4C^2 + \sin^2\varphi)\,\sin\varphi} \,,
\tag{13}
$$

$$
\epsilon_3 = \frac{2\,(c_2\,\sin\varphi + 2C\,s_2)}{(4C^2 + \sin^2\varphi)\,\sin\varphi} \,.
\tag{14}
$$

The observables $c_1'$ or $s_1'$ can be used for alternative measurement of $y_d$ .

In the absence of CPT violation ($\epsilon_1 = \epsilon_2 = 0$), the coefficients $c_0, c_2$ and $s_2$ can be expressed in terms of the measured quantities $c_1, s_1$ and $\epsilon_3$ by eliminating $C$ and $\sin\varphi$ as follows:

$$
c_0 = \epsilon_3\left[1 - \frac{2s_1^2}{(2 - c_1^2 + \epsilon_3^2)^2}\right], \quad c_2 = \frac{2s_1^2\,\epsilon_3}{(2 - c_1^2 + \epsilon_3^2)^2} \,, \quad s_2 = -\frac{2s_1\,(c_1 + \epsilon_3)\,\epsilon_3}{(2 - c_1^2 + \epsilon_3^2)} \,.
\tag{15}
$$

As an example, using the measured values of $c_1$, $s_1$ and $\epsilon_3$ [6] for final state $J/\psi K_S$, we find: $c_0 = (-15.18 \pm 15.50) \times 10^{-4}$ , $c_2 = (-4.31 \pm 4.41) \times 10^{-4}$ , $s_2 = (0.29 \pm 0.43) \times 10^{-4}$ . Should the measurements of $c_0$, $c_2$ and $s_2$ deviate significantly from the above values, this

would indicate the presence of CPT violation in $B_d^0 - \bar{B}_d^0$ mixing.

For $B_s^0 - \bar{B}_s^0$ oscillation, one should not repeat same procedure exactly since $\Delta\Gamma_s$ is not so small as $\Delta\Gamma_d$; however, it can be treated in a similar fashion with some slight modifications in the procedure.

# Measuring C & P conserving dimension four $WW\gamma$ vertex

The most general effective Lagrangian which describes $WW\gamma$ vertex [8] contains several dimension four and dimension six operators; among them, the coupling strengths of CP violating interactions are constrained to be less than $(10^{-4})$ [9] from measurements of neutron electric dipole moment. On the other hand, dimension six operators cannot be probed in low energy experiments like radiative muon decay due to an additional suppression proportional to inverse mass square of $W$ (i.e. $1/m_W^2$). Thus the effective $WW\gamma$ vertex, sensitive to radiative muon decay, contains only the C- and P- conserving dimension four interaction and in momentum space it can be expressed as:

$$\Gamma_{\rho\sigma\delta}(q_2, q_1, p) = g_{\rho\sigma}(q_2 + q_1)_\delta + g_{\sigma\delta}(p - q_1)_\rho - g_{\delta\rho}(p + q_2)_\sigma + \eta_\gamma(p_\rho g_{\sigma\delta} - p_\sigma g_{\rho\delta}), \quad (16)$$

where $\eta_\gamma \equiv \kappa_\gamma - 1$ with $\kappa_\gamma$ being the coupling constant for the mentioned operator in the unit of electron's charge and $q_2, q_1, p$ are the four momenta of incoming $W^-$, outgoing $W^-$ and outgoing photon respectively. In SM, $\kappa_\gamma = 1$ at tree level and the absolute value of one-loop corrections to it is restricted to be less than $1.5 \times 10^{-2}$ [10]; however, the current global average $\kappa_\gamma = 0.982 \pm 0.042$ [7] has too large an uncertainty to probe the SM up to one-loop accuracy. Radiative muon decay which proceeds through three Feynman diagrams, shown in Fig. 1, can be used to measure this coupling with higher precision through construction of suitable observable.

For this purpose, we define effective Mandelstam-like variables $t$ and $u$ where $t = (p_e + q)^2$
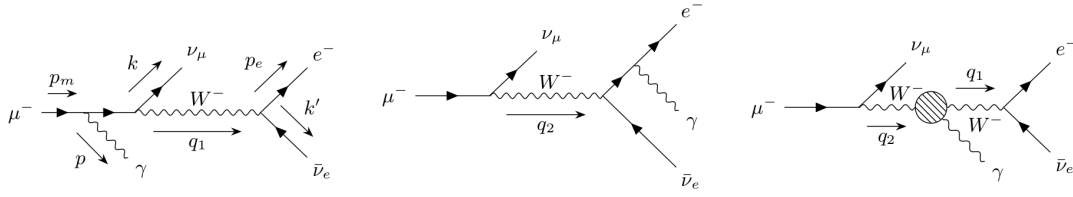
Figure 1: Feynman diagrams for radiative muon decay.

and $u = (p_\gamma + q)^2$ with $p_e^\mu$ and $p_\gamma^\mu$ being four momenta of electron and photon respectively whereas $q^\mu$ being the invariant four momentum of $\nu_\mu \bar{\nu}_e$ system . However, it is more convenient to work with three normalized parameters defined as:

$$x_p = \frac{t+u}{2(q^2+m_\mu^2)}\,, \quad y_p = \frac{t-u}{2(q^2+m_\mu^2)}\,, \quad q_p^2 = \frac{q^2}{(q^2+m_\mu^2)}\,, \tag{17}$$

where $m_\mu$ is the mass of muon. These parameters can easily be inverted in terms of the observables like energy of electron $(E_e)$, energy of photon $(E_\gamma)$ and the angle between them $(\theta)$ as:

$$E_e = \frac{m_\mu}{2}\left(\frac{1-q_p^2-x_p+y_p}{1-q_p^2}\right)\,, \quad E_\gamma = \frac{m_\mu}{2}\left(\frac{1-q_p^2-x_p-y_p}{1-q_p^2}\right)\,,$$
$$\cos\theta = \frac{(q_p^2-x_p)^2+2x_p-y_p^2-1}{(1-q_p^2-x_p)^2-y_p^2}\,. \tag{18}$$

In terms of these new normalized variables, the phase space for this process is bounded by three surfaces: $q_p^2 = 0$, $x_p = 1/2$ and $(q_p^4 - q_p^2 + x_p^2 - y_p^2) = 0$. It is easily seen from Eq. (5.16) that the plane $x_p = 1/2$ corresponds to $\theta = 0°$ and the curved surface $(q_p^4 - q_p^2 + x_p^2 - y_p^2) = 0$, which we denote as $C$, signifies $\theta = 180°$. It should also be noticed that replacement of $y_p$ with $-y_p$ while keeping $q_p^2$ and $x_p$ unchanged actually results in interchange between the energies of photon and electron keeping the angle between them unaltered.

After integrating the momenta of $\nu_\mu$ and $\bar{\nu}_e$, we consider the normalized differential decay rate $\overline{\Gamma}(x_p, y_p, q_p^2)$, defined as follows:

$$\overline{\Gamma}(x_p, y_p, q_p^2) = \frac{1}{\Gamma_\mu} \cdot \frac{d^3\Gamma}{dq_p^2\,dx_p\,dy_p}\,, \tag{19}$$

where $\Gamma_\mu$ is the total decay width of muon. The 'odd' and 'even' part of the normalized differential decay rate with respect to $y_p$ are defined in the following way respectively:

$$\overline{\Gamma}_o(x_p, y_p, q_p^2) = \frac{1}{2}\left[\overline{\Gamma}(x_p, y_p, q_p^2) - \overline{\Gamma}(x_p, -y_p, q_p^2)\right] \approx F_o(x_p, y_p, q_p^2) + \eta_\gamma\, G_o(x_p, y_p, q_p^2), \quad (20)$$

$$\overline{\Gamma}_e(x_p, y_p, q_p^2) = \frac{1}{2}\left[\overline{\Gamma}(x_p, y_p, q_p^2) + \overline{\Gamma}(x_p, -y_p, q_p^2)\right] \approx F_e(x_p, y_p, q_p^2) + \eta_\gamma\, G_e(x_p, y_p, q_p^2), \quad (21)$$

where the small $\eta_\gamma^2$ terms are ignored. We define an observable, $\mathcal{R}_\eta$, and the corresponding asymmetry , $\mathcal{A}_\eta(x_p, y_p, q_p^2)$, as:

$$\mathcal{R}_\eta(x_p, y_p, q_p^2) = \frac{\overline{\Gamma}_o}{\overline{\Gamma}_e} \approx \frac{F_o}{F_e}\left[1 + \eta_\gamma\left(\frac{G_o}{F_o} - \frac{G_e}{F_e}\right)\right], \quad (22)$$

$$\mathcal{A}_\eta(x_p, y_p, q_p^2) = \left(\frac{\mathcal{R}_\eta}{\mathcal{R}_{\text{SM}}} - 1\right) \approx \eta_\gamma\left(\frac{G_o}{F_o} - \frac{G_e}{F_e}\right), \quad (23)$$

where, $\mathcal{R}_{\text{SM}} = \left.(\overline{\Gamma}_o/\overline{\Gamma}_e)\right|_{\eta_\gamma=0} = (F_o/F_e)$ .
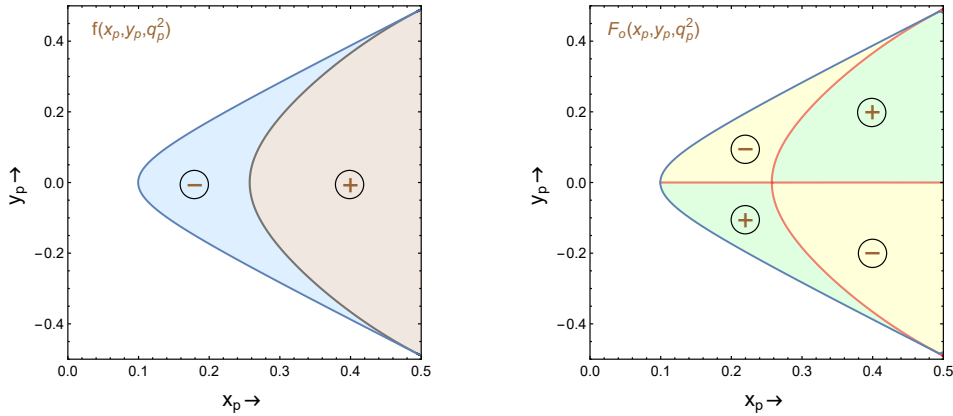


Figure 2: The variations of $f(x_p, y_p, q_p^2)$ and $F_o(x_p, y_p, q_p^2)$ are shown in $x_p - y_p$ plane in left and right panel, respectively, with $q_p^2 = 0.01$. The blue line in both the panels indicates the curve C. In the left panel, the bluish region signifies $f < 0$, the brown region symbolizes $f > 0$ and the black curve indicates $f = 0$. In the right panel, the yellow regions signify $F_o < 0$, the green regions symbolize $F_o > 0$ and the red curve indicates $F_o = 0$.

Now, $F_o(x_p, y_p, q_p^2)$, the odd part of normalized differential decay rate in SM scenario, can be expressed as:

$$F_o \propto y_p\, h(x_p, y_p, q_p^2)\, f(x_p, y_p, q_p^2) \quad (24)$$

where, $h(x_p, y_p, q_p^2)$ is a positive valued function inside the physical region. Hence, the

deciding factor on the sign of $F_o(x_p, y_p, q_p^2)$ is $f(x_p, y_p, q_p^2)$. Retaining only relevant terms up to $O(1/m_W^4)$, it can be easily shown that (as depicted in Fig. 5.4)

- on $x_p = 1/2$ surface, we have $f\left(\frac{1}{2}, y_p, q_p^2\right) \geq 0$,

- on the curved surface $C$, we have $f(x_p, y_p, q_p^2)\big|_C \leq 0$.

It is obvious therefore that there must be at least one surface within the allowed phase space region where $f(x_p, y_p, q_p^2) = 0$; we refer to this surface corresponding to the *'new type of zero'* as "null-surface". Hence, $\mathcal{A}_\eta(x_p, y_p, q_p^2)$ diverges on this null-surface for any non-zero value of $\eta_\gamma$ and becomes zero everywhere in the phase space for $\eta_\gamma$ being zero. However, this divergence has nothing to do with the usual divergences arising from soft photon or neglect of electron mass or collinearity of photon and electron since these events lie at top right corner, at bottom right corner and on $x_p = 1/2$ line in Fig. 5.4 respectively. The sign of $\eta_\gamma$ can be determined from the change in sign of $\mathcal{A}_\eta$ while crossing the null-surface.

To study the sensitivity, error analysis has been done taking the resolutions for energy of photon, energy of electron and the angle between them to be 2%, 0.5% and 10 Milli-radian, respectively [11]. For this purpose, we divide the phase space region $0 \leq q_p^2 \leq 1/2$, $0 \leq x_p \leq 1/2$, $-1/2 \leq y_p \leq 1/2$ into $62,500$ number of equisized bins. To determine the error in measurement of $\eta_\gamma = 0.01$, we consider only those bins which satisfy the cut $\left(\delta|\mathcal{A}_\eta|_i / |\mathcal{A}_\eta|_i\right) \leq 10$ and it turns out that only the bins close to null-surface obey the above cut. Taking a total of $10^{19}$ muons, which is aimed in long term future, we estimate an error of $\delta\eta_\gamma = 2.6 \times 10^{-3}$ implying a $3.9\sigma$ significance for the measurement $\eta_\gamma$. However, the next-round of experiments are aiming at $10^{18}$ muons /year which reduces the sensitivity to $1.4\sigma$; still this approach gives better significance than that of current global average. This whole analysis can be repeated keeping electron mass to be non-zero, but it gives only a correction $O(10^{-4})$ to $\eta_\gamma$.

# Conclusions

In this thesis we have investigated techniques to measure parameters arising in two different classes of possible extensions beyond the SM. Firstly, we have focused on measuring T and CPT violating parameters in $B^0 - \bar{B}^0$ mixing through time dependent indirect CP asymmetry. There is no need to neglect penguin pollution in the decay, and the method can be applied to both $B^0_d$ or $B^0_s$ meson decays.

Next, we have proposed a new method to probe C and P conserving dimension four $WW\gamma$ vertex with higher accuracy using radiative muon decay. We establish the appearance of a *'new type of zero'* (other than zeros of radiation amplitude) in the odd part of normalised differential decay rate under the exchange of electron and photon energies within the framework of SM. A suitably constructed asymmetry based on this fact enables us a sensitive probe for $WW\gamma$ vertex beyond SM.

# LIST OF FIGURES

LIST OF FIGURES

# LIST OF TABLES

# CHAPTER 1

## INTRODUCTION

> *The task is not so much to see what no one has yet seen; but to think what nobody has yet thought, about that which everybody sees.*
>
> — **Erwin Schrödinger**

Human minds have been questing through ages for the ultimate reality about the existence and functioning of everything in this entire universe. In this regard, one of the biggest concerns was discerning the elementary building blocks of our cosmos. Historically, this inquisition originated in the minds of philosophers from ancient India and Greece during first millennium BC, which begot *atomism*. In modern era, the journey recommenced with Avogadro's *molecular theory* and Dalton's *atomic theory* during early nineteenth century. The first experimental discovery of any subatomic particle was done by J. J. Thomson when he detected electron in 1897. After that science has travelled a long way. Thanks to numerous experimental and theoretical endeavours in last century, we are now living in era when even the length of $10^{-18}$ metre can be probed in experiments.

In the beginning of twentieth century, there emerged two beautiful theories: Planck's

*quantum theory* and Einstein's *special theory of relativity*. Attempts taken by Dirac to mingle these two theories in the late 1920s engendered *quantum field theory* (QFT) or more specifically *quantum electrodynamics* (QED) that describes quantized version of electromagnetic interactions. However, it took two decades involving many eminent scientists like Pauli, Wigner, Jordon, Heisenberg, Fermi, Bethe, Tomonaga, Schwinger, Feynman, Dyson and others to convey QED as a *renormalizable Abelian gauge theory* with extremely accurate theoretical predictions. The theory of another fundamental force named weak interaction was first given by Fermi [12] in 1934 in the context of nuclear $\beta$-decay. But major developments on this topic started only in late 1950s. Finally Glashow, Weinber and Salam [13–15] unified it with the electromagnetic force by showing them to be two aspects of a single gauge theory named *electroweak gauge symmetry*. The renormalizability of this theory was proved by 't Hooft [16] in 1971. To talk about the third fundamental force called strong interaction, we must acknowledge that until 1970s physicists were in absolute quandary about how protons are bound together while comprising the atomic nuclei despite their mutual electromagnetic repulsion. A brilliant step was taken forward by Gell-Mann and Zweig [17, 18] in 1964 when they proposed that hadrons are made up of *quarks*. To unravel the conundrum about formation of baryons out of three fermionic quarks, which seemed impossible according to Pauli's *exclusion principle* [19], Greenberg, Han and Nambu [20, 21] propounded an additional $SU(3)$ gauge degree of freedom for quarks. It paved the way for Fritzsch, Leutwyler and Gell-Mann [22] to establish *quantum chromodynamics* (QCD), a special version of Yang Mills theory [23], as the doctrine of strong interaction. Along with theoretical developments, numerous experimental discoveries were also going on in parallel to shape the dogmas of elementary particles. Thus emerges the most accepted theory of elementary particles: the Standard Model (SM).

According to SM, total number of elementary particles to date is sixty one; among them there are twenty four particles in each of the groups containing fermions and anti-fermions, twelve of them are gauge bosons, and the last one discovered was a scalar. The dynamics

of these particles are governed by the gauge group $SU(3)_C \otimes SU(2)_L \otimes U(1)_Y$; the group $SU(3)_C$ describes *strong interaction* and the remaining group $SU(2)_L \otimes U(1)_Y$ represents *electroweak interaction*. The strong interaction is mediated by eight gluons which are massless as well as neutral in electric charge, the weak interaction is governed by one neutral and two charged massive gauge bosons whereas the electromagnetic interaction is carried by massless neutral photon. Depending on whether the fermions (as well as the anti-fermions) take part in strong interaction or not, they can be divided into two subcategories further named quarks and leptons, each consisting of six flavours of them. On the other hand, weak interaction differentiates between left and right handed components of fermionic fields by interacting only with the former one. The scalar particle gives masses to others (not all of them) by *breaking* the $SU(2)_L \otimes U(1)_Y$ symmetry of its vacuum *spontaneously* through *Higgs mechanism*. These essential concepts summarize the key features of SM.

Though experiments in last few decades involving precision measurements at LEP [24, 25], consistency of the top quark [26, 27], detection of $\tau$-neutrino [28], discovery of Higgs boson [29, 30], etc., established the acceptability of SM as the universal theory of elementary particles, there are several reasons to believe that it is not a complete theory. Neutrino oscillation is regarded as the first unarguable evidence for beyond SM scenario since it ensures non-vanishing masses for neutrinos. Second, due to absence of any notion about dark matter or dark energy, the SM is incapable of explaining the large amount of observed cold dark matter (CDM) and its contributions to dark energy, which in turn makes it inconsistent with the $\Lambda CDM$ *model (i.e. the standard model of Big Bang cosmology)*. The matter-antimatter asymmetry arising within SM is also not compatible with the observed baryon over photon density. Third, there are theoretical complications regarding the nature of Higgs vacuum and the naturalness protecting the Higgs mass from radiative corrections. Fourth, despite lots of attempts, physicists are still struggling with assimilation of the last fundamental force gravitation into the SM in a consistent way. There are also other theoretical issues concerning the number of generations for fermions, the number

of unrelated numerical constants, Yang–Mills existence and mass gap, etc., which are unanswered yet. All of these facts suggest that SM is just an effective theory, a subset of another bigger model.

To understand the actual underlying theory, the best way would be investigating direct evidences for beyond standard model (BSM) particles in collider experiments. But, after a thorough and prolonged search over last ten years, no sign for this kind of particle has been detected. In this situation, precise measurement of various theoretical parameters that are uniquely predicted in SM can play a major role. Presence of new heavy particles in the loops can alter the measurement of these parameters significantly. Hence, any deviation observed from their predicted values in SM will act as indirect evidence for the existence of BSM physics. However, to capture these loop induced effects, one must choose the modes very cleverly. Moreover, new measurement techniques are also required along with increase in the luminosity of beams and advancements in experimental methods. In this thesis, we have studied new measurement procedures for two different types of such theoretical parameters: a) **T** and **CPT** violation in $B^0 - \bar{B}^0$ mixing, b) **C** and **P** conserving dimension four $WW\gamma$ vertex.

Before 1950s, physicists presumed charge conjugation (**C**), parity (**P**) and time reversal (**T**) to be independent symmetries of nature. However, during mid-50s, parity and charge conjugation [31–33] were found to be violated in weak interactions. To handle the situation, **CP** was proposed to be a good symmetry [34, 35], but it was also discovered to be broken [36]. Presently, we believe that **CPT** is an imperishable symmetry since its has a deep connection with Lorentz invariance [1]. Nonetheless, pondering over past experiences, it is a good idea to test its validity in experiments with high precision. Direct searches for **CPT** violation through difference in masses or life-times of particle and antiparticle have been performed in several experiments; nevertheless, they are observed to be extremely insignificant in every case since they are mostly dominated by strong or electromagnetic interactions. Neutral pseudoscalar meson mixing, which is a second order weak process

governed by box diagrams, seems to be a very promising candidate in this regard [2]. Though all experimental results to date are consistent with **CPT** conservation, an important improvement in statistics is expected in near future. After discussing the general properties of **C**, **P** and **T** symmetries in chapter 2, we have investigated the possibilities for indirect measurement of **T** and **CPT** violation in $B^0 - \bar{B}^0$ mixing using the time-dependent indirect **CP** asymmetry for decays of $B^0$ or $\bar{B}^0$ to a **CP** eigenstate, in chapter 4.

On the other hand, triple gauge boson interaction is a unique attribute of non-Abelian gauge theories which have been used in SM to describe weak and strong interactions. Nonetheless, triple gauge boson couplings in electroweak sector are yet to be measured with a sufficient accuracy for scrutinizing at least one loop correction to it within the SM framework. Among these multi-boson vertices, $WW\gamma$ vertex is of special interest since it dictates the electromagnetic properties of $W$-boson. Radiative muon decay ($\mu \rightarrow e\nu_\mu\bar{\nu}_e\gamma$), which are expected to be produced in a large number as the background of experiments to probe lepton-flavour-violating process $\mu \rightarrow e\gamma$ (like COMET, MEG, Mu2e [3]), appears to be a promising mode for probing **C** and **P** conserving dimension-four $WW\gamma$ vertex. After summarizing all SM interactions in chapter 3, we scrutinize a *new type of zero* (other than the zeros of radiation amplitude [4]) in chapter 5 for this decay mode. We also establish that a suitably constructed asymmetry using this fact can enable us a sensitive probe for $WW\gamma$ vertex beyond the SM.

❖ ❖ ❖ ❖ ❖ ❖ ❖ ❖

C, P & T SYMMETRIES

,,

*Maybe the nature is fundamentally ugly, chaotic and*

*complicated. But if it's like that, then I want out.*

— Steven Weinberg

If all the governing laws and equations of a theory (more specifically action or Lagrangian or Hamiltonian) remain invariant under any transformation, then the mentioned transformation is often said to be a "symmetry" of that theory. There are two types of transformations:

(a) **Continuous transformation:** Starting from any specific initial state, if it is possible to reach any particular final state by applying the laws of transformation infinitely many times with infinitesimal transformation parameters, then the transformation is called a *continuous transformation*. Some examples for this type of transformation are translation, rotation, $SU(N)$ gauge transformation, etc. According to Noether's theorem, if this type of transformation becomes "symmetry" of a system, there must be an associated conserved quantity. For example, translational invariances of Lagrangian in spatial and temporal directions result in conservations of linear momentum and energy respectively, rotational invariance of Lagrangian gives rise to

conservation of angular momentum, etc.

(b) **Discrete transformation:** Starting from any specific initial state, if it is not possible to reach any particular final state in a continuous process through the laws of transformation, then the mentioned transformation is said to be *discrete*. Charge conjugation (**C**), parity (**P**) and time reversal (**T**) are some examples for this type of transformation. In condensed matter physics, crystallography, chemistry and other fields discrete symmetry plays important role. In case of quantum theory, discrete symmetry was first realized through the symmetry under permutation of identical particles, namely Bose-Einstein and Fermi-Dirac statistics.

Let us first discuss the basic properties of **C**, **P** and **T** transformations.

- **Charge conjugation**: This discrete transformation, usually symbolized by **C**, changes a particle into its antiparticle with same mass, momentum and spin but opposite quantum numbers like electric charge, lepton number, baryon number etc.

- **Parity transformation:** This discrete transformation, usually denoted as **P**, alters all the space coordinates $\vec{x}$ to $-\vec{x}$. It is equivalent to a reflection about an axis followed by a rotation around origin.

  Any polar vector, like three momentum $\vec{p}$, changes its sign under parity ($\vec{\mathbb{V}} \xrightarrow{\mathbf{P}} -\vec{\mathbb{V}}$) whereas any axial vector, like angular momentum $\vec{J}$, does not ($\vec{\mathbb{A}} \xrightarrow{\mathbf{P}} \vec{\mathbb{A}}$). Similarly, scalars remain invariant under parity transformation ($\mathbb{S} \xrightarrow{\mathbf{P}} \mathbb{S}$), but pseudoscalars change sign ($\mathbb{P} \xrightarrow{\mathbf{P}} \mathbb{P}$).

  The notion of handedness is also related to parity. By applying parity, any right handed coordinate system can be transformed into a left handed one or vice versa.

- **Time reversal:** This discrete transformation, usually indicated by **T**, changes the direction of time, i.e. reflects $t$ to $-t$ leaving all the spatial coordinates unaltered. Under its action, both linear and angular momenta change their sign.

## 2.1  Classical Physics

Microscopically, all the laws and equations of classical physics (like classical mechanics, classical electrodynamics, etc.) are invariant under **C**, **P** and **T** separately.

For example, let us test it on Maxwell's equations. At first, we need to know the transformation properties of electric and megnetic fields under **C**, **P** and **T**. For this purpose, it is sufficient to use *Coulomb's law* and *Biot Savart law* from electrostatics and magnetostatics respectively:

$$\vec{E}(\vec{r}) = \frac{1}{4\pi\varepsilon_0} \int \frac{(\vec{r} - \vec{r}')}{|\vec{r} - \vec{r}'|^3}\, \rho(\vec{r}')\, dV' \quad \text{and} \quad \vec{B}(\vec{r}) = \frac{\mu_0}{4\pi} \int \frac{\vec{J}(\vec{r}'') \times (\vec{r} - \vec{r}'')}{|\vec{r} - \vec{r}''|^3}\, dV'' \quad (2.1)$$

where, electric field $\vec{E}$ and magnetic field $\vec{B}$ at a point $\vec{r}$ are given for static charge density $\rho(\vec{r}')$ inside the volume $V'$ and steady current density $\vec{J}(\vec{r}'')$ through the volume $V''$ respectively. Hence, the action of **C**, **P** and **T** can be visualised in the following way:

- $\{\vec{r}, \vec{r}', \vec{r}''\} \xrightarrow{\mathbf{C}} \{\vec{r}, \vec{r}', \vec{r}''\}, \quad \rho \xrightarrow{\mathbf{C}} -\rho, \quad \vec{J} \xrightarrow{\mathbf{C}} -\vec{J}$

  $\implies \quad \vec{E} \xrightarrow{\mathbf{C}} -\vec{E} \ \text{and} \ \vec{B} \xrightarrow{\mathbf{C}} -\vec{B}$

- $\{\vec{r}, \vec{r}', \vec{r}''\} \xrightarrow{\mathbf{P}} \{-\vec{r}, -\vec{r}', -\vec{r}''\}, \quad \rho \xrightarrow{\mathbf{P}} \rho, \quad \vec{J} \xrightarrow{\mathbf{P}} -\vec{J}$

  $\implies \vec{E} \xrightarrow{\mathbf{P}} -\vec{E} \ \text{and} \ \vec{B} \xrightarrow{\mathbf{P}} \vec{B}$

- $\{\vec{r}, \vec{r}', \vec{r}''\} \xrightarrow{\mathbf{T}} \{\vec{r}, \vec{r}', \vec{r}''\}, \quad \rho \xrightarrow{\mathbf{T}} \rho, \quad \vec{J} \xrightarrow{\mathbf{T}} -\vec{J}$

  $\implies \quad \vec{E} \xrightarrow{\mathbf{T}} \vec{E} \ \text{and} \ \vec{B} \xrightarrow{\mathbf{T}} -\vec{B}$

Now, let us look at Maxwell's equations in free space with sources being present:

$$\vec{\nabla} \cdot \vec{E} = \frac{\rho}{\varepsilon_0}, \quad \vec{\nabla} \times \vec{E} = -\frac{\partial \vec{B}}{\partial t},$$

$$\vec{\nabla} \cdot \vec{B} = 0, \quad \vec{\nabla} \times \vec{B} = \mu_0 \left( \vec{J} + \varepsilon_0 \frac{\partial \vec{E}}{\partial t} \right). \tag{2.2}$$

In this case, the charge density and current density varies with time making the electric and magnetic field time-dependent. Using the transformation properties of $\vec{E}$, $\vec{B}$, $\rho$ and

$\vec{J}$, as discussed above, along with $\vec{\nabla} \xrightarrow{\textbf{P}} -\vec{\nabla}$ and $t \xrightarrow{\textbf{T}} -t$, it can be shown easily that Maxwell's equations remain invariant under the actions of **C**, **P** and **T** individually.

Since the potential energy appears to be even under **C** and **P** transformations, they become symmetries of the Lagrangian in classical physics. However, if it is somehow possible to generate any potential energy that is odd under **C** and **P** then only these two symmetries can be violated. On the other hand, time reversal transformation sometimes shows apparent macroscopic asymmetry depending on the likelihood for the occurrences of initial and final state. For example, let us consider a scenario where some billiard balls have been accumulated at a particular position on a table and someone hits them with the white cue-ball; as a result, all the balls will move in different directions. Now, contemplate the time-reversed situation: some balls, coming from different directions, collide with each other and get piled up around a particular position and after all the collisions, only the white cue ball keeps moving. Though the dynamics involved in the motion for individual ball obeys **T** symmetry, we know from our experience that the time-reversed scenario is *very less likely* to happen in reality. Actually, the movement of each ball is governed not only by the equation of motion, but also by the initial condition. So, the time-reversed situation will occur only when the initial conditions for that process is prepared very precisely. This lowers the likelihood of the time-reversed version of a complex process to happen in classical physics. Moreover, in the presence of any dissipative force, the time reversed process looks impossible. For instance, let us consider a ball moving on a rough horizontal plane. After sometime, it will loose all its energy and come to rest because of friction. In this case, the time-reversed situation, where the ball starts from rest and accelerates just by gaining energy from the ground, is literally impractical. In the context of classical thermodynamics, we usually connect this *less likelihood* of time-reversed processes to the concept of entropy and second law of thermodynamics.

## 2.2   Quantum mechanics

In quantum mechanics, each operation is associated with some operator which can act on the Hamiltonian, the physical states or another operator. Here, an operation is declared to be a symmetry of the system if the corresponding operator commutes with the Hamiltonian.

Parity and charge conjugation are represented by two *Hermitian as well as unitary* operators:

$$\mathbf{P} = \mathbf{P}^{-1} = \mathbf{P}^{\dagger} \qquad \text{and} \qquad \mathbf{C} = \mathbf{C}^{-1} = \mathbf{C}^{\dagger} \tag{2.3}$$

It readily follows from the above equation that squares of these two operators are identity; this means that acting on a state twice, these operators bring back the initial state. It also stipulates their eigen values to be $\pm 1$.

If $\vec{\mathcal{X}}$, $\vec{\mathcal{P}}$ and $\vec{\mathcal{J}}$ be the position, linear momentum and angular momentum operators respectively, then

$$\left\{ \mathbf{P}, \vec{\mathcal{X}} \right\} = 0, \qquad \left\{ \mathbf{P}, \vec{\mathcal{P}} \right\} = 0, \qquad \left[ \mathbf{P}, \vec{\mathcal{J}} \right] = 0. \tag{2.4}$$

The action of parity on a state $|\psi\rangle$ is given by:

$$\langle x| \mathbf{P} |\psi\rangle = \psi(-x) \tag{2.5}$$

However, the action of $\mathbf{C}$ operator is very limited in non-relativistic quantum mechanics; it only changes the signs of electric charge and electromagnetic four-potential and commutes with all other operators. A better understanding for this operator is provided in relativistic quantum mechanics and QFT.

Let us find the effects of these two transformations on Schrödinger equation. If $\mathbf{C}$ and $\mathbf{P}$ become symmetries of a quantum mechanical system, then the Hamiltonian $\mathbf{H}$ must commute with them, i.e., $[\mathbf{C}, \mathbf{H}] = 0$ and $[\mathbf{P}, \mathbf{H}] = 0$. It can only happen if the potential

energy *V* is symmetric under **C** and **P**.

On the other hand, time reversal is delineated by an *anti-unitary operator*, i.e. for any two states $|\psi_A\rangle$ and $|\psi_B\rangle$

$$\langle \psi_A | \mathbf{T}^\dagger \mathbf{T} | \psi_B \rangle = \langle \psi_B | \psi_A \rangle \tag{2.6}$$

Actually, all the observables in quantum mechanics can be expressed in terms of *transition probabilities* which are *modulus squared transition amplitudes*. All the transformations that preserve transition probabilities become symmetry of the system. Thus any "symmetry transformation" must be represented by a unitary or anti-unitary operator in Hilbert space[1].

The relations of time reversal with other operators are given by:

$$\left[\mathbf{T}, \vec{\mathcal{X}}\right] = 0, \qquad \left\{\mathbf{T}, \vec{\mathcal{P}}\right\} = 0, \qquad \left\{\mathbf{T}, \vec{\mathcal{J}}\right\} = 0. \tag{2.7}$$

The time reversal operator is generally described by:

$$\mathbf{T} = \exp\left(-i\frac{\pi}{\hbar}\mathbf{S}_y\right)\mathbf{K} \tag{2.8}$$

where $\mathbf{S}_y$ is the *y*-component of spin operator and **K** is the complex conjugate operator satisfying the following relations:

$$\mathbf{K}\left(\alpha |\psi_A\rangle + \beta |\psi_B\rangle\right) = \alpha^*\left(\mathbf{K}|\psi_A\rangle\right) + \beta^*\left(\mathbf{K}|\psi_B\rangle\right) \quad \text{and} \quad \mathbf{K}^2 = \mathbf{1} \tag{2.9}$$

Here the asterisk sign denotes complex conjugate. Due to presence of complex conjugate operator, it must satisfy: $\mathbf{T}^{-1} i \mathbf{T} = -i$. If the potential energy of a system is a function of position only, i.e. it does not contain linear or angular momentum or time explicitly, then $[\mathbf{T}, \mathbf{H}] = 0$. In that case, the Schrödinger equation transforms under time reversal operation as:

$$-i\hbar \frac{\partial}{\partial t}\psi^*(\vec{x}, t) = \mathbf{H}\psi^*(\vec{x}, t) \tag{2.10}$$

---

[1] *Wigner's theorem of automorphism*

An interesting fact about time reversal operator is that it can distinguish between bosons and fermions. It can be shown from Eq. (2.8) that

$$\mathbf{T^2} = \begin{cases} +1 & \text{for bosons} \\ -1 & \text{for fermions} \end{cases} \qquad (2.11)$$

It can also be proven that every energy state of a system with half-integer total spin is at least doubly degenerate if time reversal is a symmetry[2].

An important observable to search for $\mathbf{P}$ and $\mathbf{T}$ violations is *electric dipole moment* (EDM). As the corresponding operator is odd under parity, EDM must vanish for a parity conserved system. On the other hand, for a system with non-degenerate ground state, EDM must vanish for a $\mathbf{T}$ conservation. Several experimental searches have been done in this direction, however, no success has been achieved. An upper bound on neutron's electric dipole moment is measured as $d_n < 3.0 \times 10^{-26}$ with 90% confidence level [37].

## 2.3   Quantum field theory

For any symmetry in QFT, three quantities must be invariant under the transformation: i) the vacuum state, ii) the Lagrangian density and iii) the quantization conditions. If the vacuum is found to violate the symmetry, it is called *spontaneous breaking*. On the other hand, if the Lagrangian itself breaks the symmetry, it is called *explicit breaking*.

As electromagnetic interactions preserve $\mathbf{C}$, $\mathbf{P}$ and $\mathbf{T}$ individually, it can be used to determine the transformation properties of scalars, spinors and vectors. From the analogy with classical theories, we postulate the transformation properties for current density (four vactor) under $\mathbf{C}$, $\mathbf{P}$ and $\mathbf{T}$ as:

$$\mathbf{C}^{-1} J^\mu(\vec{x}, t) \, \mathbf{C} = -J^\mu(\vec{x}, t), \quad \mathbf{P}^{-1} J^\mu(\vec{x}, t) \, \mathbf{P} = J_\mu(-\vec{x}, t), \quad \mathbf{T}^{-1} J^\mu(\vec{x}, t) \, \mathbf{T} = J_\mu(\vec{x}, -t) \ (2.12)$$

---

[2] *Kramer's degeneracy theorem*

where, the lowering of Lorentz index must be noticed in case of parity and time reversal transformations since they change the sign of three vector only. Using these transformations, we find the operations of **C**, **P** and **T** on the annihilation and creation operators for different fields.

### 2.3.1   Charged scalar field

In terms of Fourier transform, the charged scalar field can be expressed[3] as:

$$\varphi(\vec{x}, t) = \int \frac{d^3 p}{\sqrt{(2\pi)^3 \, 2E_p}} \left[ \mathbf{b}(\vec{p}) \, e^{-ip \cdot x} + \mathbf{d}^\dagger(\vec{p}) \, e^{ip \cdot x} \right] \tag{2.13}$$

where $\mathbf{b}(\vec{p})$ and $\mathbf{d}(\vec{p})$ are the annihilation operators for particle and anti-particle with the dot product $p \cdot x \equiv p_\mu x^\mu$.

The quantization conditions are:

$$\left[ \varphi(\vec{x}, t), \, \varphi(\vec{y}, t) \right] = \left[ \varphi^\dagger(\vec{x}, t), \, \varphi^\dagger(\vec{y}, t) \right] = 0 \,, \tag{2.14}$$

$$\left[ \varphi(\vec{x}, t), \, \partial_t \, \varphi^\dagger(\vec{y}, t) \right] = \left[ \varphi^\dagger(\vec{x}, t), \, \partial_t \, \varphi(\vec{y}, t) \right] = i\delta^3(\vec{x} - \vec{y}) \,. \tag{2.15}$$

Excluding the coupling, the current for electromagnetic interaction in this case is:

$$J^\mu(\vec{x}, t) = i \left[ \varphi^\dagger(\vec{x}, t) \, \partial^\mu \varphi(\vec{x}, t) - \varphi(\vec{x}, t) \, \partial^\mu \varphi^\dagger(\vec{x}, t) \right]. \tag{2.16}$$

Let us postulate the following transformations of the charged scalar field:

$$\varphi_{\mathbf{C}}(\vec{x}, t) = \mathbf{C}^{-1} \varphi(\vec{x}, t) \, \mathbf{C} = \varphi^\dagger(\vec{x}, t) \,, \tag{2.17}$$

$$\varphi_{\mathbf{P}}(\vec{x}, t) = \mathbf{P}^{-1} \varphi(\vec{x}, t) \, \mathbf{P} = \varphi(-\vec{x}, t) \,, \tag{2.18}$$

$$\varphi_{\mathbf{T}}(\vec{x}, t) = \mathbf{T}^{-1} \varphi(\vec{x}, t) \, \mathbf{T} = \varphi^\dagger(\vec{x}, -t) \,. \tag{2.19}$$

---

[3]Different authors use different normalizations according to their convenience. This changes the commutation relations between $\mathbf{b}(\vec{p}_1)$ and $\mathbf{b}^\dagger(\vec{p}_2)$ (or $\mathbf{d}(\vec{p}_1)$ and $\mathbf{d}^\dagger(\vec{p}_2)$) by some factor in different conventions.

It can be shown easily that our ansatz about transformations of the charged scalar field provides correct transformation properties, as given by Eq.(2.12), for the electromagnetic current density in Eq. (2.16) under **C**, **P** and **T**. The transformed fields obey the quantization conditions in Eq. (2.14) too. Hence, our ansatz is correct and it forces the transformations for the annihilation operators of particle and antiparticle as:

$$\mathbf{C}^{-1}\mathbf{b}(\vec{p})\,\mathbf{C} = \mathbf{d}(\vec{p})\,, \tag{2.20}$$

$$\mathbf{P}^{-1}\mathbf{b}(\vec{p})\,\mathbf{P} = \mathbf{b}(-\vec{p})\,, \qquad \mathbf{P}^{-1}\mathbf{d}(\vec{p})\,\mathbf{P} = \mathbf{d}(-\vec{p})\,, \tag{2.21}$$

$$\mathbf{T}^{-1}\mathbf{b}(\vec{p})\,\mathbf{T} = \mathbf{b}(-\vec{p})\,, \qquad \mathbf{T}^{-1}\mathbf{d}(\vec{p})\,\mathbf{T} = \mathbf{d}(-\vec{p})\,. \tag{2.22}$$

### 2.3.2  Spinor field

Spinor field can be expressed through its Fourier components as:

$$\psi_a(\vec{x},t) = \int \frac{d^3 p}{(2\pi)^{\frac{3}{2}}} \sqrt{\frac{m}{E_p}} \sum_{s=\pm} \left[ \mathbf{b}(\vec{p},s)\,u_a(\vec{p},s)\,e^{-ip\cdot x} + \mathbf{d}^\dagger(\vec{p},s)\,v_a(\vec{p},s)\,e^{ip\cdot x} \right] \tag{2.23}$$

where, $a$ specifies the spinor index; $m$ and $s$ are the mass and spin of the fermion respectively; $\mathbf{b}(\vec{p},s)$ and $\mathbf{d}(\vec{p},s)$ are the annihilation operators for fermion and anti-fermion respectively; $u(\vec{p},s)$ and $v(\vec{p},s)$ are the four component Dirac spinors satisfying the following equations:

$$(\slashed{p} - m)\,u(\vec{p},s) = 0 \quad \text{and} \quad (\slashed{p} + m)\,v(\vec{p},s) = 0\,. \tag{2.24}$$

The canonical quantization relations are:

$$\left\{ \psi_a(\vec{x},t), \psi_b^\dagger(\vec{y},t) \right\} = \delta^3(\vec{x} - \vec{y})\,\delta_{ab}\,, \tag{2.25}$$

$$\left\{ \psi_a(\vec{x},t), \psi_b(\vec{y},t) \right\} = \left\{ \psi_a^\dagger(\vec{x},t), \psi_b^\dagger(\vec{y},t) \right\} = 0 \tag{2.26}$$

The electromagnetic current density in this case is: $J^\mu(\vec{x},t) = \overline{\psi}(\vec{x},t)\,\gamma^\mu\,\psi(\vec{x},t)\,.$ \hfill (2.27)

We make the following ansatz:

$$\psi_{\mathbf{C}}(\vec{x}, t) = \mathbf{C}^{-1}\psi(\vec{x}, t)\,\mathbf{C} = \mathcal{C}\,[\bar{\psi}(\vec{x}, t)]^{\text{Tr}}, \tag{2.28}$$

$$\psi_{\mathbf{P}}(\vec{x}, t) = \mathbf{P}^{-1}\psi(\vec{x}, t)\,\mathbf{P} = \gamma^0\,\psi(-\vec{x}, t), \tag{2.29}$$

$$\psi_{\mathbf{T}}(\vec{x}, t) = \mathbf{T}^{-1}\psi(\vec{x}, t)\,\mathbf{T} = \mathcal{U}\,\psi(\vec{x}, -t). \tag{2.30}$$

where the subscript "Tr" indicates transposition. It should be noted that the operators $\mathbf{C}$, $\mathbf{P}$ and $\mathbf{T}$ act on Dirac fields or more specifically on creation and annihilation operators[4] whereas $\mathcal{C}$ and $\mathcal{U}$ are two matrices acting on Dirac spinors ($u$ and $v$). This choice of transformations for Dirac field impart correct transformation properties to the electromagnetic current density as well as the transformed fields respect the quantization conditions too if:

$$\gamma^0\,\mathcal{C}^\dagger\,\gamma^0\,\gamma_\mu\,\mathcal{C} = \gamma_\mu^{\text{Tr}} \quad \text{and} \quad \mathcal{U}^{-1}\,\gamma_\mu^*\,\mathcal{U} = \gamma^\mu \tag{2.31}$$

It is easy to show that the above two conditions hold for following two matrices:

$$\mathcal{C} = i\gamma^2\,\gamma^0 \quad \text{and} \quad \mathcal{U} = \gamma^1\,\gamma^3 \tag{2.32}$$

Hence, $\mathcal{C} = -\mathcal{C}^{-1} = -\mathcal{C}^\dagger = -\mathcal{C}^{\text{Tr}}$ with $\mathcal{C}^2 = -1$

The matrix $\mathcal{U}$ also have similar properties like $\mathcal{C}$.

The transformation properties of Dirac field translet into the transformation of annihilation operators as:

$$\mathbf{C}^{-1}\mathbf{b}(\vec{p}, s)\,\mathbf{C} = s\,\mathbf{d}(\vec{p}, -s), \tag{2.33}$$

$$\mathbf{P}^{-1}\mathbf{b}(\vec{p}, s)\,\mathbf{P} = \mathbf{b}(-\vec{p}, s), \qquad \mathbf{P}^{-1}\mathbf{d}(\vec{p}, s)\,\mathbf{P} = -\mathbf{d}(-\vec{p}, s), \tag{2.34}$$

$$\mathbf{T}^{-1}\mathbf{b}(\vec{p}, s)\,\mathbf{T} = s\,\mathbf{b}(-\vec{p}, -s), \qquad \mathbf{T}^{-1}\mathbf{d}(\vec{p}, s)\,\mathbf{T} = s\,\mathbf{d}(-\vec{p}, -s). \tag{2.35}$$

---

[4]Though $\mathbf{T}$ changes other terms of Fourier transform into their complex conjugates since it is an anti-unitary operator.

This shows that fermions and antifermions carry opposite intrinsic parity.

### 2.3.3 Photon field

The photon field can be expanded in terms of creation and annihilation operators as:

$$A^\mu(\vec{x}, t) = \int \frac{d^3 p}{\sqrt{(2\pi)^3 \, 2E_p}} \sum_{s=\pm} \left[ \mathbf{a}(\vec{p}, s) \, \varepsilon_s^\mu \, e^{-ip \cdot x} + \mathbf{a}^\dagger(\vec{p}, s) \, \varepsilon_s^{\mu\,*} \, e^{ip \cdot x} \right] \qquad (2.36)$$

where $\mathbf{a}(\vec{p}, s)$ and $\varepsilon_s^\mu$ are the annihilation operator and polarization vector for photon with momentum $p^\nu$ and spin $s$. Photon has only two polarizations, as it is massless spin-1 particle. Since $A^\mu(\vec{x}, t)$ is also a four vector like current density, it should transform the same way as $J^\mu(\vec{x}, t)$. Hence, the annihilation operator should transform as:

$$\mathbf{C}^{-1} \mathbf{a}(\vec{p}, s) \, \mathbf{C} = -\mathbf{a}(\vec{p}, s), \qquad (2.37)$$

$$\mathbf{P}^{-1} \mathbf{a}(\vec{p}, s) \, \mathbf{P} = -\mathbf{a}(-\vec{p}, s), \qquad (2.38)$$

$$\mathbf{T}^{-1} \mathbf{a}(\vec{p}, s) \, \mathbf{T} = -\mathbf{a}(-\vec{p}, -s). \qquad (2.39)$$

Thus one-photon state carries odd intrinsic parity and **C**-parity:

$$\mathbf{P} \, |\gamma, \vec{p}\rangle = -|\gamma, -\vec{p}\rangle \quad \text{and} \quad \mathbf{C} \, |\gamma, \vec{p}\rangle = -|\gamma, \vec{p}\rangle \qquad (2.40)$$

However, other spin-1 fields (like gluons, $W^\pm$, some vector mesons, etc.) which carry internal quantum numbers (like colour, electric charge, strangeness, etc.) are not eigenstates of **C**. Hence, **C**-parity is not defined for them. Still, they carry intrinsic parity $\pm 1$ depending on whether the particle is axial vector or polar vector. For any composite system the parity is given by $\left[(-1)^L \prod_j \mathbf{P}_j\right]$ and the **C**-parity is given by $\left[(-1)^{L+S} \prod_j \mathbf{C}_j\right]$; here $\mathbf{P}_j$ and $\mathbf{C}_j$ are intrinsic parity and **C**-parity for individual particles, $L$ is orbital angular momentum and $S$ is spin.

## 2.4   Weak interaction and violation of symmetries

After the discovery of *strange-particles*, it had been found that one pseudoscalar charged strange meson has two different decay channels with opposite parity; one involves two pion, whereas the other includes three pions. Since parity violation had not been so far, it was assumed that the parent particles for those two decays must be different. The initial particle for the even-parity final state was given the name $\theta^+$ whereas the other one was named as $\tau^+$. However, no experiment could find significant difference in their masses or life-times which denies their existence as two separate particles[5]. This problem was termed as $\tau - \theta$ *puzzle.* In 1956, Lee and Yang [31] pointed out that *parity violation* could be the answer to $\tau - \theta$ puzzle and suggested a list of relevant tests. During the same time, Salam [32] showed that vanishing mass of neutrino can lead to violation of parity. In the following year, Wu and collaborators [33] discovered the experimental evidence for the breaking of parity and charge conjugation invariance by weak interactions in nuclear $\beta$ decay of $^{60}_{27}$Co. Similar results were confirmed by other groups too. This identified both the particles $\tau^+$ and $\theta^+$ as $K^+$ meson. To incorporate parity violation into theory, $(\mathbb{V} - \mathbb{A})$ Lagrangian for weak interaction was proposed by Sudarshan, Marshak, Feynman and Gell-Mann [38, 39] and later it had been included into SM too. After the violation of parity, it was thought that **CP** must be the symmetry of nature [34, 35]. However, Fitch and Cronin [36] found that:

$$\frac{\Gamma\left(K_L \rightarrow \pi^+\pi^-\right)}{\Gamma\left(K_L \rightarrow \text{all charged modes}\right)} = (2 \pm 0.4) \times 10^{-3}$$

which suggests **CP** violation in weak interactions. Theoretically, **CP** violation has great importance in explaining matter-antimatter asymmetry[6] . In SM, it occurs through the weak phase in CKM matrix only, however, it is not sufficient to explain the observed

---

[5]Particles with same mass and life-time can have separate existences only if one is the antiparticle of other. However, $\tau$ and $\theta$ cannot be considered as particle-antiparticle states, since they have same electric charges.

[6]*Sakharov conditions*

matter-antimatter asymmetry in our universe.

## 2.5   CPT symmetry

After the discovery of **CP** violation, it is now believed that the combined transformation **CPT**, which is given by an anti-unitary operator, is an exact symmetry of nature:

$$(\mathbf{CPT})^{-1} \mathcal{L}(\vec{x}, t) (\mathbf{CPT}) = \mathcal{L}(-\vec{x}, -t) \tag{2.41}$$

It is called ***CPT**-theorem*. The first proof of this theorem was given by Lüders and Pauli [40, 41] based on the Hamiltonian formulation of quantum field theory, which involves locality of the interaction, Lorentz invariance and Hermiticity of the Hamiltonian. Later on the theorem was proven rigorously by Jost and others [42–44] in the axiomatic formulation of quantum field theory based on the assumptions of: 1) Lorentz invariance, 2) existence of unique vacuum state and 3) weak local commutativity obeying 'right' statistics. There are some important consequences of this theorem:

1. *Any particle and its antiparticle have same masses.*

   **Proof:** If **H** be the Hamiltonian that contains every interaction involving a particle $|P\rangle$ and its antiparticle $|\overline{P}\rangle$, masses of them in their rest frame are given by:

   $$M(P) = \langle P | \mathbf{H} | P \rangle \quad \text{and} \quad M(\overline{P}) = \langle \overline{P} | \mathbf{H} | \overline{P} \rangle \tag{2.42}$$

   Now, the proof goes as follows:

   $$\langle P | \mathbf{H} | P \rangle$$
   $$= \langle P | \mathbf{H} (\mathbf{CPT})^{-1} (\mathbf{CPT}) | P \rangle$$
   $$= \left( \langle P | (\mathbf{CPT})^{\dagger} (\mathbf{CPT}) \, \mathbf{H} \, (\mathbf{CPT})^{-1} (\mathbf{CPT}) | P \rangle \right)^{*} \quad \text{[since \textbf{CPT} is antiunitary]}$$
   $$= \left( \langle \overline{P} | (\mathbf{CPT}) \, \mathbf{H} \, (\mathbf{CPT})^{-1} | \overline{P} \rangle \right)^{*} \quad [\because \mathbf{CPT} |P\rangle = e^{i\Theta} |\overline{P}\rangle, \ \Theta \text{ is a real number.}]$$

$$= \left( \langle \overline{P} | \ \mathbf{H} \ | \overline{P} \rangle \right)^{*} \quad [\text{If } \mathbf{CPT} \text{ becomes a symmetry, } (\mathbf{CPT}) \ \mathbf{H} \ (\mathbf{CPT})^{-1} = \mathbf{H}]$$

$$= \langle \overline{P} | \ \mathbf{H}^{\dagger} \ | \overline{P} \rangle$$

$$= \langle \overline{P} | \ \mathbf{H} \ | \overline{P} \rangle \quad [\because \ \mathbf{H} \text{ is Hermitian.}]$$

$$\implies M(P) = M(\overline{P}) \tag{2.43}$$

**2**. *Life times of any particle and its antiparticle are equal.*

**<u>Proof:</u>** The decay rates of particle and antiparticle in their rest frame are given by:

$$\Gamma(P) = 2\pi \sum_{f} \delta\left( M(P) - E_f \right) \left| \langle f; \ out | \ \mathbf{H} \ | P \rangle \right|^2 ,$$

$$\Gamma(\overline{P}) = 2\pi \sum_{f} \delta\left( M(P) - E_f \right) \left| \langle \overline{f}; \ out | \ \mathbf{H} \ | \overline{P} \rangle \right|^2 , \tag{2.44}$$

where $f$ and $\overline{f}$ indicate the final states for the decays of $P$ and $\overline{P}$ respectively. Now, using the same logics like the above proof we obtain:

$$\sum_{f} \delta\left( M(P) - E_f \right) \left| \langle f; \ out | \ \mathbf{H} \ | P \rangle \right|^2$$

$$= \sum_{f} \delta\left( M(P) - E_f \right) \left| \left( \langle f; \ out | \ (\mathbf{CPT})^{\dagger}(\mathbf{CPT}) \ \mathbf{H} \ (\mathbf{CPT})^{-1}(\mathbf{CPT}) \ | P \rangle \right)^{*} \right|^2$$

$$= \sum_{f} \delta\left( M(P) - E_f \right) \left| \left( \langle \overline{f}; \ in | \ (\mathbf{CPT}) \ \mathbf{H} \ (\mathbf{CPT})^{-1} \ | \overline{P} \rangle \right)^{*} \right|^2$$

$$= \sum_{f} \delta\left( M(P) - E_f \right) \left| \left( \langle \overline{f}; \ in | \ \mathbf{H} \ | \overline{P} \rangle \right)^{*} \right|^2$$

$$= \sum_{f} \delta\left( M(P) - E_f \right) \left| \langle \overline{f}; \ in | \ \mathbf{H} \ | \overline{P} \rangle \right|^2$$

$$\implies \Gamma(P) = \Gamma(\overline{P}) \tag{2.45}$$

In the above proof we have used the fact that both 'in' and 'out' states form complete sets, i.e.,

$$\sum_{f} | f; \ out \rangle \langle f; \ out | = \sum_{f} | \overline{f}; \ in \rangle \langle \overline{f}; \ in | = \mathbf{1} \tag{2.46}$$

3. *The magnetic moments for particle and its antiparticle are equal in magnitude, but opposite in sign.*

The magnetic moments for any particle and its antiparticle in their respective rest frame are given by:

$$\vec{\mu}(P) = c_1 \langle P, \vec{s}| \vec{\mathbf{S}} |P, \vec{s}\rangle \quad \text{and} \quad \vec{\mu}(\overline{P}) = c_1 \langle \overline{P}, \vec{s}| \vec{\mathbf{S}} |\overline{P}, \vec{s}\rangle \tag{2.47}$$

where $\vec{\mathbf{S}}$ is the spin operator, $\vec{s}$ is the spin vector of particle or antiparticle and $c_1$ is a constant. The Hamiltonian is given by $\mathbf{H} = \vec{\mathbf{S}} \cdot \vec{\mathbf{B}}$ where $\vec{\mathbf{B}}$ is the magnetic field. Now, using the same logic as in Eq. (2.43), we obtain:

$$\begin{aligned}
\vec{\mu}(P) \cdot \vec{\mathbf{B}} &= c_1 \left( \langle P, \vec{s}| \vec{\mathbf{S}} |P, \vec{s}\rangle \right) \cdot \vec{\mathbf{B}} \\
&= c_1 \langle P, \vec{s}| \mathbf{H} |P, \vec{s}\rangle \\
&= c_1 \left( \langle P, \vec{s}| (\mathbf{CPT})^\dagger (\mathbf{CPT}) \mathbf{H} (\mathbf{CPT})^{-1} (\mathbf{CPT}) |P, \vec{s}\rangle \right)^* \\
&= c_1 \left( \langle \overline{P}, -\vec{s}| (\mathbf{CPT}) \mathbf{H} (\mathbf{CPT})^{-1} |\overline{P}, -\vec{s}\rangle \right)^* \\
&= c_1 \left( \langle \overline{P}, -\vec{s}| \mathbf{H} |\overline{P}, -\vec{s}\rangle \right)^* \\
&= c_1 \langle \overline{P}, -\vec{s}| \mathbf{H}^\dagger |\overline{P}, -\vec{s}\rangle \\
&= c_1 \langle \overline{P}, -\vec{s}| \mathbf{H} |\overline{P}, -\vec{s}\rangle \\
&= c_1 \left( \langle \overline{P}, -\vec{s}| \vec{\mathbf{S}} |\overline{P}, -\vec{s}\rangle \right) \cdot \vec{\mathbf{B}} \\
&= -\vec{\mu}(\overline{P}) \cdot \vec{\mathbf{B}} \tag{2.48}
\end{aligned}$$

Since, the above relation is true for any arbitrary magnetic field, we must have:

$$\vec{\mu}(P) = -\vec{\mu}(\overline{P}) \tag{2.49}$$

About the source of **CPT** violation, Greenberg [1] argued that it arises from breaking of Lorentz invariance. However, this conclusion is debatable [45–52]. It is shown in Ref. [46–49] that QFT on non-commutative space-time can lead to breaking of Lorentz

invariance without **CPT** violation. On the other hand, a certain class of models has been proposed in Ref. [50–52] that breaks **CPT** symmetry through non-local interactions while preserving Lorentz invariance. Moreover, it has been shown in Ref. [52] that some Lorentz invariant but **CPT** violating models can provide equality of masses and decay widths for particles and anti-particles. Nevertheless, in the context of this thesis, we are not concerned about the theoretical formalism regarding the breaking of **CPT** symmetry, rather we are interested in measuring it experimentally if it exists at all in nature. The challenge here is that one cannot construct any **CPT**-violating observable relying on the corollaries of usual QFT, since our QFT is **CPT** invariant by construction.

⚜ ⚜ ⚜ ⚜ ⚜ ⚜ ⚜ ⚜

# A BRIEF DESCRIPTION OF SM

> " *God used beautiful mathematics in creating the world.*
>
> — **Paul Dirac**

In the early 1970s, enormous efforts of hundreds of physicists that spanned over four decades resulted in a beautiful mathematical interpretation for the fundamental structure of all matters in this universe: the Standard Model. It encapsulates our best understanding about the basic building blocks of this universe and there interplay with three fundamental forces of nature. Since its formulation, SM has to undergo copious experimental tests. However, it has successfully explained most of the experimental results and precisely predicted a wide variety of phenomena.

## 3.1 Elementary particles

The SM contains sixty one fundamental particles in total; twenty four of them are fermions, twenty four are anti-fermions and rest are bosons. However, according to flavour, there are twelve fermions and twelve anti-fermions. These spin-$\frac{1}{2}$ fermions and anti-fermions are the

elementary units for all the matters (excluding dark matter) in the universe, whereas twelve spin-1 gauge bosons are the mediators for strong and electroweak interactions among them. The last one is a spin-0 boson, responsible for masses of different elementary particles.

Depending on the interest in strong interaction, the fundamental fermions (anti-fermions) can be divided into two mutually exclusive categories: six flavours of them taking part in this interaction are termed as *quarks* (anti-quarks) and the rest six flavours, reluctant in it, are called *leptons* (anti-leptons). In terms of strong interaction, each flavour of quark or anti-quark can possess three different colours: red, blue, green, and hence they transform as *triplets*. The exchange particles for this interaction are eight gluons, each of which have two colour indices but no mass and electric charge, and together they form *colour octet*. *Colour confinement* ensures that any stable strongly interacting particle observed in nature must be a *colour singlet state*. Thus quarks and anti-quarks interact with each other through colour fields and produce bosonic *mesons* or fermionic *baryons* which are collectively called *hadrons*.

In the context of electroweak interaction, each of the sets accommodating six flavours of quarks or six leptons can be classified into three pairs, which are called *generations*. The lightest and most stable particles make up the first generation, whereas the heavier and less-stable particles belong to the second and third generations. Under weak isospin, the left-handed components of fermions transform as *doublets* whereas the right-handed components transform as *singlets*[1]. There are four gauge bosons for this interaction; among them two are massive and charged named *W*-boson, one is massive and neutral called *Z*-boson, and last one is massless and neutral photon. The massive spin-0 boson, commonly termed as *Higgs boson*, gives masses to different particles through *Higgs mechanism*. Properties of fundamental particles with respect to this interaction have been presented in Table 3.1.

---

[1]It should be noted that left-handed fermions and right-handed anti-fermions take part in weak interaction. That's why we observe left-handed neutrinos and right-handed anti-neutrinos, but not the reversed scenario. On the other hand, as $\begin{pmatrix} \nu_e \\ e^- \end{pmatrix}$ is an isospin doublet, the same with antiparticles will be $\begin{pmatrix} -e^+ \\ \bar{\nu}_e \end{pmatrix}$ [53].

| Type of particles | | Particles & generations | | | Electric charge, | Weak isospin, $\mathcal{T}_3$ | | Weak hypercharge, $Y$ | |
|---|---|---|---|---|---|---|---|---|---|
| | | 1st | 2nd | 3rd | $Q$ | L | R | L | R |
| Fermions | Leptons | $\nu_e$ | $\nu_\mu$ | $\nu_\tau$ | 0 | $+1/2$ | – | $-1$ | – |
| | | $e^-$ | $\mu^-$ | $\tau^-$ | $-1$ | $-1/2$ | 0 | $-1$ | $-2$ |
| | Quarks | $u$ | $c$ | $t$ | $+2/3$ | $+1/2$ | 0 | $+1/3$ | $+4/3$ |
| | | $d$ | $s$ | $b$ | $-1/3$ | $-1/2$ | 0 | $+1/3$ | $-2/3$ |
| Anti-Fermions | Anti-leptons | $e^+$ | $\mu^+$ | $\tau^+$ | $+1$ | 0 | $+1/2$ | $+2$ | $+1$ |
| | | $\bar{\nu}_e$ | $\bar{\nu}_\mu$ | $\bar{\nu}_\tau$ | 0 | – | $-1/2$ | – | $+1$ |
| | Anti-quarks | $\bar{d}$ | $\bar{s}$ | $\bar{b}$ | $+1/3$ | 0 | $+1/2$ | $+2/3$ | $-1/3$ |
| | | $\bar{u}$ | $\bar{c}$ | $\bar{t}$ | $-2/3$ | 0 | $-1/2$ | $-4/3$ | $-1/3$ |
| Bosons | Spin-1 | $W$ | | | $\pm1$ | $\pm1$ | | 0 | |
| | | $Z$, photon, gluons | | | 0 | 0 | | 0 | |
| | Spin-0 | $H$ | | | 0 | $-1/2$ | | $+1$ | |

Table 3.1: Quantum numbers of elementary particles in light of electroweak interaction.

## 3.2   Strong interaction

Strong interactions in SM are described by a local, non-Abelian $SU(3)_C$ gauge symmetry involving quarks and gluons only. The conserved quantity arising form this continuous symmetry is *colour*. Eight generators of this gauge group, denoted by $\mathcal{T}^a$ ($a = 1, 2, 3, ...., 8$), can be identified with Gell-Mann matrices in three dimensional representation. Three coloured quarks of each quark flavour form a *triplet* in the *fundamental representation* of the mentioned gauge group whereas eight gluons associated with this interaction form an *octate* in the *adjoint representation*.

The QCD Lagrangian density is given by:

$$\mathcal{L}_{QCD} = -\frac{1}{4} G^a_{\mu\nu} G^{\mu\nu a} + \sum_{\mathrm{f}} \overline{\psi}^{\mathrm{f}}_{\mathrm{i}} (i\gamma^\mu \mathcal{D}^{\mathrm{ij}}_\mu - m_{\mathrm{f}} \delta_{\mathrm{ij}}) \psi^{\mathrm{f}}_{\mathrm{j}} \tag{3.1}$$

where $G^a_{\mu\nu} = \partial_\mu \mathcal{A}^a_\nu - \partial_\nu \mathcal{A}^a_\mu + g_s f^{abc} \mathcal{A}^b_\mu \mathcal{A}^c_\nu$ and $\mathcal{D}^{\mathrm{ij}}_\mu = \delta_{\mathrm{ij}} \partial_\mu - i g_s \mathcal{A}^a_\mu \mathcal{T}^a_{\mathrm{ij}}$ with the following elucidation for different entities:

- i, j : colour indices in fundamental representation,

- $a, b, c$ : colour indices in adjoint representation,

- $\mu, \nu$ : Lorentz indices,

- f : different flavour of quarks,

- $\mathcal{A}^a_\mu$ : gluon field,

- $\psi^{\mathrm{f}}$ : quark field,

- $g_s$ : strong coupling constant,

- $f^{abc}$ : structure constant of the gauge group.

The generators and the structure constants of $SU(3)$ group obey the following relations:

$$[\mathcal{T}^a, \mathcal{T}^b] = i f^{abc} \mathcal{T}^c, \qquad \mathrm{Tr}(\mathcal{T}^a \mathcal{T}^b) = \frac{1}{2} \delta^{ab}, \qquad \sum_a (\mathcal{T}^a \mathcal{T}^a)_{\mathrm{ij}} = \frac{4}{3} \delta_{\mathrm{ij}}$$

$$\sum_a \mathcal{T}^a_{\mathrm{ij}} \mathcal{T}^a_{\mathrm{kl}} = \frac{1}{2} (\delta_{\mathrm{il}} \delta_{\mathrm{jk}} - \frac{1}{3} \delta_{\mathrm{ij}} \delta_{\mathrm{kl}}), \qquad f^{acd} f^{bcd} = 3 \delta^{ab}. \tag{3.2}$$

It can be easily shown that the QCD Lagrangian density, given by Eq. (3.1), is invariant under the following infinitesimal local gauge transformations:

$$\psi^{\mathrm{f}}_{\mathrm{i}} \rightarrow \left[ 1 - i g_s \alpha^a(x) \mathcal{T}^a_{\mathrm{ij}} \right] \psi^{\mathrm{f}}_{\mathrm{j}},$$

$$\mathcal{A}^a_\mu(x) \rightarrow \mathcal{A}^a_\mu(x) + \partial_\mu \alpha^a(x) + g_s f^{abc} \alpha^b(x) \mathcal{A}^c_\mu(x). \tag{3.3}$$

## 3.3    Electroweak interaction

The electroweak interactions in SM are described by a local $SU(2)_L \otimes U(1)_Y$ gauge symmetry. Under the non-Abelian $SU(2)_L$ gauge group, the left handed fermion fields, defined by: $\psi_L \equiv \frac{1}{2}(1 - \gamma_5)\psi$, transform as doublets, whereas the right handed fermion fields, described by: $\psi_R \equiv \frac{1}{2}(1 + \gamma_5)\psi$, transform as singlets; the corresponding conserved quantum number is *weak isospin* ($\mathcal{T}$). The three generators of this gauge group are denoted as $\mathcal{T}_j$ ($j = 1, 2, 3$) where $\mathcal{T}_j = \frac{1}{2}\sigma_j$ in two dimensional representation with $\sigma_j$ being the Pauli matrices. In addition to $SU(2)_L$ symmetry, an independent $U(1)_Y$ gauge symmetry has been introduced to encompass electromagnetic interaction into a common gauge structure. The conserved quantum number $Y$ for this symmetry is called *weak hypercharge*. In analogy with *Gell-Mann-Nishijima relation* from strong interaction, the weak hypercharge for different particles are specified by the formula: $Q = \mathcal{T}_3 + \dfrac{Y}{2}$, where $Q$ is the electric charge for the particle of interest in the unit of positron's charge. Unlike $SU(2)_L$ symmetry, both of the left and right handed components for fermion fields transform under $U(1)_Y$ symmetry (in general); but they transform differently since the weak hypercharges for those two components are different. An important point to mention here is that if left and right handed fermions possess different couplings to gauge bosons, usually there arises an awkward kind of divergence for the interaction of three gauge bosons via fermion loops which cannot be abolished by *renormalization*. This situation is entitled as *chiral anomaly problem*. However, with three colours of quarks and specific choices of quantum numbers for different particles, as described in Table 3.1, the chiral anomaly cancels for SM in a dramatic way.

The electroweak Lagrangian density for SM can be expressed as:

$$\mathcal{L}_{\text{EW}} = \mathcal{L}_{\text{kin}} + \mathcal{L}_{\text{Higgs}} + \mathcal{L}_{\text{Yuk}} \tag{3.4}$$

The first part, $\mathcal{L}_{\text{kin}}$, contains the kinetic terms for gauge bosons and fermions as well as all

the interactions among them. The second term, $\mathcal{L}_{\text{Higgs}}$ comprises interplay between Higgs and gauge bosons, and the self interaction of Higgs. The third portion $\mathcal{L}_{\text{Yuk}}$ indicates the interactions of fermions with Higgs. Let me discuss each term in more detail.

### 3.3.1 Kinetic part:

In terms of fermion fields and gauge boson fields the kinetic part of electroweak Lagrangian can be expressed as:

$$\mathcal{L}_{\text{kin}} = -\frac{1}{4} W_j^{\mu\nu} W_{j\mu\nu} - \frac{1}{4} B^{\mu\nu} B_{\mu\nu} + \sum_n \left[ \overline{\Psi}_n^{\mathbb{Q}} (i\gamma^\mu \mathcal{D}_\mu) \Psi_n^{\mathbb{Q}} + \overline{\Psi}_n^{\mathbb{L}} (i\gamma^\mu \mathcal{D}_\mu) \Psi_n^{\mathbb{L}} \right] \quad (3.5)$$

where the definitions of different mathematical entities, involved in this expression, are as follows:

$$W_j^{\mu\nu} = \partial^\mu W_j^\nu - \partial^\nu W_j^\mu - g\,\epsilon_{jkl} W_k^\mu W_l^\nu\,, \qquad B_j^{\mu\nu} = \partial^\mu B_j^\nu - \partial^\nu B_j^\mu\,,$$

$$\mathcal{D}_\mu = \partial_\mu + i\,g\,W_{j\mu}\,\mathcal{T}_j + \frac{i}{2}\,g'\,Y\,B_\mu\,. \quad (3.6)$$

Here, $W_{1,2,3}^\mu$ and $B^\mu$ are the massless gauge bosons associated to $SU(2)_L$ and $U(1)_Y$ gauge groups respectively; $g$ and $g'$ are corresponding coupling constants. While $B^\mu$ remains singlet under $SU(2)_L \otimes U(1)_Y$ gauge transformation, $W_{1,2,3}^\mu$ form a triplet. On the other hand, $\Psi$ is a column matrix consisting of two fermions from same generation; i.e., if $\psi^u$ and $\psi^d$ are *up* and *down* type quarks or leptons, respectively, belonging to same generation, then $\Psi$ can be represented as: $\Psi = \begin{pmatrix} \psi^u \\ \psi^d \end{pmatrix}$. The superscripts $\mathbb{Q}$ and $\mathbb{L}$ on $\Psi$ in Eq. (3.5) indicate quarks and leptons respectively, whereas the index $n$ signifies the generations of fermions. The generators of $SU(2)_L$ group transforming only the left-handed components of fermions, as discussed earlier, results in the condition:

$$\mathcal{T}_j \Psi_{n,R} = 0\,. \quad (3.7)$$

It can be shown easily that the Lagrangian $\mathcal{L}_{\text{kin}}$ is independently invariant under infinitesimal local gauge transformations $SU(2)_L$ and $U(1)_Y$, described by the following transformation rules:

$$\underline{SU(2)_L} \qquad\qquad \underline{U(1)_Y}$$

$$\Psi_{n,L} \rightarrow \left[ 1 - i\,g\,\mathcal{T}_j\,\alpha_j(x) \right] \Psi_{n,L} \qquad\qquad \Psi_n \rightarrow \left[ 1 - \frac{i}{2}\,g'\,Y\beta(x) \right] \Psi_n$$

$$\Psi_{n,R} \rightarrow \Psi_{n,R} \qquad\qquad B^\mu \rightarrow B^\mu + \partial^\mu \beta(x)$$

$$W_j^\mu \rightarrow W_j^\mu + \partial^\mu \alpha_j(x) + g\,\epsilon_{jkl}\,\alpha_k(x)\,W_l^\mu \qquad\qquad W_j^\mu \rightarrow W_j^\mu$$

$$B^\mu \rightarrow B^\mu$$

However, $W_j^\mu$ and $B^\mu$ fields are not generally used to describe electroweak interactions, rather their linear combinations are taken as the mediator of the gauge fields. Thus two charged fields ($W^{\pm\mu}$) and two neutral fields ($Z^\mu$ and photon $A^\mu$) are defined as:

$$\begin{pmatrix} W^{+\mu} \\ W^{-\mu} \end{pmatrix} = \frac{1}{\sqrt{2}} \begin{pmatrix} 1 & -i \\ 1 & i \end{pmatrix} \begin{pmatrix} W_1^\mu \\ W_2^\mu \end{pmatrix} \quad \text{and} \quad \begin{pmatrix} Z^\mu \\ A^\mu \end{pmatrix} = \begin{pmatrix} \cos\theta_W & -\sin\theta_W \\ \sin\theta_W & \cos\theta_W \end{pmatrix} \begin{pmatrix} W_3^\mu \\ B^\mu \end{pmatrix} \tag{3.8}$$

with $g'\cos\theta_W = g\sin\theta_W = e$ where $e$ is the electric charge of positron and the angle $\theta_W$ is the *Weinberg angle*, a parameter of the SM. The interaction of fermion anti-fermion pairs with $W^{\pm\mu}$ bosons are called *charged current interactions*, likewise the interactions involving photon or $Z^0$ and fermion anti-fermion pairs are labelled as *neutral current interactions*.

## 3.3.2  Spontaneous symmetry breaking

Though $\mathcal{L}_{\text{kin}}$ describes the self-interactions of gauge bosons as well as their interplay with fermions, it undergoes two serious problems. Firstly, non-zero masses of fermions break the $SU(2)_L$ symmetry of $\mathcal{L}_{\text{kin}}$ explicitly, which can be noticed from Eq. (3.5). On the other hand, the massive gauge bosons of weak interactions coerce the model into becoming non-renormalizable. To preserve the $SU(2)_L$ symmetry of Lagrangian as well

as the renormalizability of the model, an $SU(2)$ doublet scalar field $\Phi$ is introduced in the Lagrangian through $\mathcal{L}_{\text{Yuk}}$ and $\mathcal{L}_{\text{Higgs}}$ terms respectively. By preferring a particular direction in weak isospin plus hypercharge space through Higgs mechanism, the $SU(2)_L \times U(1)_Y$ symmetry for Lagrangian with massless particles remains intact whereas the same symmetry for the vacuum of the scalar field is *spontaneously broken* generating the masses to the elementary particles.

The Lagrangian density for scalar field is given by:

$$\mathcal{L}_{\text{Higgs}} = \left( \mathcal{D}^{\mu} \Phi \right)^{\dagger} \left( \mathcal{D}_{\mu} \Phi \right) - \lambda \left( \left| \Phi \right|^2 - \frac{1}{2} v^2 \right)^2 \tag{3.9}$$

where $\lambda$, $v$ are two positive quantities. The scalar potential $V(\Phi) = \lambda \left( \left| \Phi \right|^2 - \frac{1}{2} v^2 \right)^2$ has minima at $\left| \Phi \right| = \dfrac{v}{\sqrt{2}}$ and electroweak symmetry breaking occurs by preferring only one state with norm $\dfrac{v}{\sqrt{2}}$ as the vacuum state. In this process three massless, spin-zero *Goldstone bosons* appear. However, in *unitary gauge* they seem to disappear as separate degrees of freedom and essentially reappear as the longitudinal components of massless $W^{\pm}$ and $Z$ bosons of unbroken theory making the gauge mediators massive. In this gauge, scalar field takes the form: $\Phi = \dfrac{1}{\sqrt{2}} \begin{pmatrix} 0 \\ v + H(x) \end{pmatrix}$, where $H$ is called the *Higgs field*, with the masses for $W$, $Z$ and Higgs boson to be:

$$M_W = M_Z \cos \theta_W = \frac{1}{2} g v, \qquad m_H = \sqrt{2 v \lambda} \tag{3.10}$$

### 3.3.3  Yukawa interaction

To generate the masses of fermions, their interactions with the scalar field, which will be renormalizable as well as invariant under $SU(2)_L \times U(1)_Y$ gauge transformation, are introduced into the Lagrangian through the term:

$$\mathcal{L}_{\text{Yuk}} = -\sum_n \xi_n \left( \overline{\Psi}{}^{\mathbb{L}}_{n,L} \, \Phi \, \psi^{\mathbb{L},d}_n \right) - \sum_{n_1,n_2} \left\{ \xi^d_{n_1 n_2} \left( \overline{\Psi}{}^{\mathbb{Q}}_{n_1,L} \, \Phi \, \psi^{\mathbb{Q},d}_{n_2} \right) + \xi^u_{n_1 n_2} \left( \overline{\Psi}{}^{\mathbb{Q}}_{n_1,L} \, \widetilde{\Phi} \, \psi^{\mathbb{Q},u}_{n_2} \right) \right\} + h.c$$

$$(3.11)$$

where the indices ($n$, $n_1$, $n_2$) indicate different generations of doublets, the indices $\mathbb{L}$ and $\mathbb{Q}$ signify leptons and quarks respectively, the indices $u$ and $d$ indicate up-type and down-type fermions of a doublet respectively and $\widetilde{\Phi} = i\sigma_2 \Phi$.

After spontaneous symmetry breaking, all the neutrinos remain massless whereas the down-type lepton ($e$, $\mu$, $\tau$) of $n^{th}$ generation acquire mass $m_n = \dfrac{v\xi_n}{\sqrt{2}}$ under unitary gauge. On the other hand, two mass matrices of dimension ($3 \times 3$) with elements $\mathbb{M}^u_{n_1 n_2} = \dfrac{v}{\sqrt{2}} \xi^u_{n_1 n_2}$ and $\mathbb{M}^d_{n_1 n_2} = \dfrac{v}{\sqrt{2}} \xi^d_{n_1 n_2}$ emerge for up-type and down-type quarks respectively. Upon diagonalization[2] of these two mass matrices, quarks get their masses. However, there emerges generation mixing of mass eigenstates for the charged current interaction since the diagonalizing matrices for $\mathbb{M}^u$ and $\mathbb{M}^d$ are different, whereas no mixing occurs for the neutral current interaction. Conventionally, we associate this mixing to the unitary transformation of down-type quarks only through ($3 \times 3$) CKM matrix $V_{CKM}$, that contains four independent parameters including one **CP**-violating phase.

There are some important remarks to be made about both the strong and electroweak interactions [54]. The Lagrangian densities given by Eq. (3.1) and (3.4) do not depict the full picture. To eliminate the unphysical degrees of freedom for the respective gauge bosons, one must introduce proper gauge fixing terms along with Faddeev-Popov ghosts[3] for both of the interactions separately. Secondly, the attempt to renormalize these theories introduces several new mathematical entities and their relationships. For example, in perturbative approach of QFT, *counter terms* have to be inserted in the Lagrangian density in order to take care of the *ultraviolet divergences* arising from loops. Third, the coupling in both the interactions are not constants, rather they vary with energy scale respecting the *renormalization group equations*.

---

[2]According to *singular value decomposition (SVD) theorem* in linear algebra, any matrix can be diagonalized by multiplying two suitable unitary matrices on both sides of that matrix.

[3]hypothetical particles with spin-0 but obeying fermionic statistics.

# $B^0 - \bar{B}^0$ MIXING AND CPT VIOLATION

> "
> *There is no symmetry in nature. One eye is never exactly the same as the other.*
>
> **— Edouard Manet**

## 4.1 Prologue

**CPT** invariance is extensively believed to be one of the sacred principles of nature since according to **CPT** theorem, as described in section 2.5, any interaction described by Lorentz invariant local gauge theory must be **CPT** invariant. So, all physical processes are expected to respect this symmetry. Indeed, **CPT** violation would have a profound impact on physics in general, as it would might lead to a violation of Lorentz symmetry [1, 55]. Given its importance to the theoretical framework underlying all of particle physics, much attention has been devoted to experimentally testing the validity of **CPT** invariance.

One of the consequences of **CPT** invariance in quantum field theory is that a particle and its antiparticle should have the same mass and lifetime, as shown in section 2.5. The observed equality between masses and life times of particle and antiparticle with striking

precisions [56] obligates us to believe that **CPT** is a good symmetry of nature. But one can argue that there could be very small weak effects which are hard to measure in the differences between masses and lifetimes of particle and antiparticle since these quantities are mostly dominated by strong or electromagnetic interactions. Nevertheless, one must agree that if some **CPT** violating effects are there in nature at all, they must be very small, otherwise they would have been detected elsewhere. In this regard, neutral pseudoscalar meson mixing appears to be a promising area for testing **CPT** violation [2]. Since it is a second-order electroweak process governed by box diagrams, as shown in Fig. 4.1, small **CPT** violating effects may be easier to detect here. Moreover, as the most general mixing matrix involves **T** and **CP** violation too, it is impossible to study **CPT** alone without discriminating it from the effects of **CP** and **T** violations. That is, the effects of **T**, **CP** and **CPT** violation must be considered together.

The common method of measuring **CPT** violation has been developed in Refs. [57–64] where entangled $B^0\bar{B}^0$ states are produced from the decay of $\Upsilon(4S)$, with one meson decaying to a **CP** eigenstate ($J/\psi K_S$ or $J/\psi K_L$) and the other one being used to tag the flavour. Using this routine, true **T** and **CPT** violating asymmetries can be measured. The BaBar Collaboration implemented this strategy [65, 66], culminating in the measurement of **T** violation [67]. Though all the experimental results for **CPT** violating parameters are consistent with zero, an important improvement in statistics is expected in near future so that it will be possible to measure the **CP**, **T** and **CPT** violating parameters with greater precision.

In this chapter, we re-examine the possibilities for measuring **T** and **CPT** violation in $B^0 - \bar{B}^0$ mixing using the decays of $B^0$ or $\bar{B}^0$ to a **CP** eigenstate. As we will show, the time-dependent indirect **CP** asymmetry contains sufficient information to measure the conventional **CP** violating effects and extract the **T** and **CPT** violating parameters. Since no true **T** and **CPT** violating asymmetries are measured, this is an indirect determination of the **T** and **CPT** violating parameters. In this sense, this method is complementary to

that using entangled states. We also investigate the prospect to measure these parameters by fitting the individual decay rates of mode and conjugate mode separately.

We focus on $B_d^0 - \bar{B}_d^0$ mixing but the same approach can be modified and applied to the $B_s^0$ system. Note that we restrict the analysis to **T** and **CPT** violation arising from the $B^0 - \bar{B}^0$ mixing matrix alone. If there are new-physics contributions to $B$ decays, we assume they are **CPT** conserving.

## 4.2   General formalism for mixing

Particles and antiparticles are distinguished by different internal quantum numbers like charge, lepton number, baryon number, strangeness, beauty, charm, etc. Though strong and electromagnetic interactions conserve all of these internal quantum numbers, some of them are not conserved in different weak interactions. This drives a particle-antiparticle transition through changing some of these internal quantum numbers by two units. Since violation of electric charge conservation has not been seen yet, we restrict our analysis within the mixing of neutral particles $P^0 - \bar{P}^0$ only[1]. Suppose, non-conservation of internal quantum number $F$ induces this mixing. Then the Hamiltonian **H** can be divided into two parts as:

$$\mathbf{H} = \mathcal{H}_{SE} + \mathcal{H}_W \tag{4.1}$$

where, $\mathcal{H}_{SE}$ contains strong and electromagnetic interactions preserving $F$; $\mathcal{H}_W$ denotes the weak force mediated Hamiltonian that changes $F$.

In SM, dominant contribution in the mixing of neutral pseudoscalar mesons comes from box diagrams, as shown in Fig. 4.1 for $B_d^0 - \bar{B}_d^0$ mixing. However, we cannot use SM to construct **CPT** violating observable as QFT itself preserves **CPT** symmetry. On the other hand, to address the full dynamics of $P^0 - \bar{P}^0$ system, one has to consider the infinite-

---

[1]Here $P^0$ could be $B^0$, $D^0$, $K^0$, neutron. This analysis can be applied to neutrinos too, but there we have to study oscillations among three neutrinos rather than between neutrino and antineutrino.
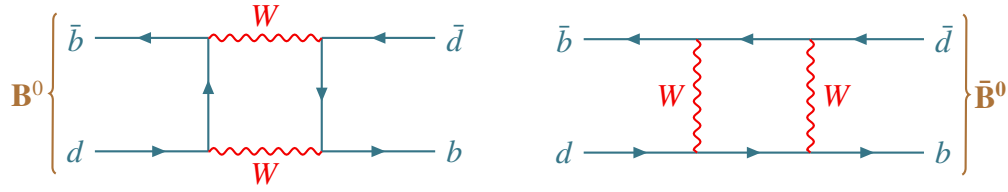
Figure 4.1: Box diagram for $B_d^0 - \bar{B}_d^0$ mixing in SM.

dimensional Hilbert space containing all the reactions that involve $P^0$ and $\bar{P}^0$. In that case **H** will be an infinite-dimensional Hermitian matrix. But, working with this Hamiltonian is immensely problematic since we have not achieved enough theoretical subjugation over strong dynamics and bound states. Nonetheless, we can circumvent these issues in the following way:

- A quantum mechanical approach will be implemented.

- The time scale involved in this context should be much longer than the typical strong interaction scale[2].

- The mixing phenomenon and decay of $P^0$ or $\bar{P}^0$ will be treated separately.

- For the mixing, we will consider a two dimensional vector-space comprising $P^0$ and $\bar{P}^0$ as two orthonormal basis vectors. However, the price to pay is that the mixing Hamiltonian $\mathcal{H}$ is no longer Hermitian. This occurs because the particles $P^0$ and $\bar{P}^0$ will decay eventually resulting in a decreasing probability for any state in the vector-space.

Taking the flavour eigenstates as basis-vectors, we write them as:

$$|P^0\rangle = \begin{pmatrix} 1 \\ 0 \end{pmatrix} \quad \text{and} \quad |\bar{P}^0\rangle = \begin{pmatrix} 0 \\ 1 \end{pmatrix}. \tag{4.2}$$

Then any state in the two dimensional vector-space can be expressed as:

---

[2]*Weisskopf-Wigner approximation.*

$$|\psi(t)\rangle = a(t)\,|P^0\rangle + b(t)\,|\bar{P}^0\rangle = \begin{pmatrix} a(t) \\ b(t) \end{pmatrix}. \tag{4.3}$$

The time evolution of this state is given by Schrödinger equation:

$$i\hbar\,\frac{\partial}{\partial t}\,|\psi(t)\rangle = \mathcal{H}\,|\psi(t)\rangle\,. \tag{4.4}$$

Now, every matrix can be written as a sum of one Hermitian matrix and one anti-Hermitian matrix. Hence, we can decompose the mixing matrix $\mathcal{H}$ as:

$$\mathcal{H} = \mathbf{M} - (i/2)\,\mathbf{\Gamma} \tag{4.5}$$

where the Hermitian matrices $\mathbf{M}$ and $\mathbf{\Gamma}$, defined in the $(P^0, \bar{P}^0)$ basis, are called the mass and decay matrices respectively. Again, together with identity matrix $\mathbf{1}$, the Pauli matrices form a basis for a vector-space of $2 \times 2$ matrices. This allows us to write:

$$\mathbf{M} - \frac{i}{2}\mathbf{\Gamma} = E_1\sigma_1 + E_2\sigma_2 + E_3\sigma_3 - iD\mathbf{1}\,. \tag{4.6}$$

It should be noted that the coefficients $E_1, E_2, E_3$ and $D$ are complex quantities in general as the mixing Hamiltonian is non-Hermitian. Comparing both sides of the above equation, we obtain the following relations:

$$\begin{aligned} E_1 &= \operatorname{Re}\mathbf{M}_{12} - \frac{i}{2}\operatorname{Re}\mathbf{\Gamma}_{12}\,, & E_3 &= \frac{1}{2}\left(\mathbf{M}_{11} - \mathbf{M}_{22}\right) - \frac{i}{4}\left(\mathbf{\Gamma}_{11} - \mathbf{\Gamma}_{22}\right), \\ E_2 &= -\operatorname{Im}\mathbf{M}_{12} + \frac{i}{2}\operatorname{Im}\mathbf{\Gamma}_{12}\,, & D &= \frac{i}{2}(\mathbf{M}_{11} + \mathbf{M}_{22}) + \frac{1}{4}(\mathbf{\Gamma}_{11} + \mathbf{\Gamma}_{22})\,. \end{aligned} \tag{4.7}$$

For convenience, we use spherical polar coordinate system and define three complex numbers $E, \theta$ and $\phi$ as follows:

$$E = \sqrt{E_1^2 + E_2^2 + E_3^2},\quad E_1 = E\sin\theta\cos\phi,\quad E_2 = E\sin\theta\sin\phi,\quad E_3 = E\cos\theta. \tag{4.8}$$

The flavour states are not the physical states since the mixing matrix $\mathcal{H}$ is not diagonal. Rather the physical states are the eigenvectors of the mixing matrix $\mathcal{H}$ and they can be written in terms of the flavour states as follows:

$$|P_L\rangle = p_1\,|P^0\rangle + q_1\,|\bar{P}^0\rangle\,, \qquad |P_H\rangle = p_2\,|P^0\rangle - q_2\,|\bar{P}^0\rangle\,. \tag{4.9}$$

where, $p_1 = N_1 \cos\frac{\theta}{2}$, $q_1 = N_1\, e^{i\phi} \sin\frac{\theta}{2}$, $p_2 = N_2 \sin\frac{\theta}{2}$ and $q_2 = N_2\, e^{i\phi} \cos\frac{\theta}{2}$. Here $N_1$ and $N_2$ are two normalization factors, given by: $N_1 = \frac{1}{\sqrt{|\cos\frac{\theta}{2}|^2 + |e^{i\phi}\sin\frac{\theta}{2}|^2}}$ , $N_2 = \frac{1}{\sqrt{|\sin\frac{\theta}{2}|^2 + |e^{i\phi}\cos\frac{\theta}{2}|^2}}$ . Hence, following Eq. (4.4), the time evolutions for the flavour eigenstates ($|B^0\rangle \equiv |B^0\rangle\,(t = 0)$ and $|\bar{B}^0\rangle \equiv |\bar{B}^0\rangle\,(t = 0)$) are given by:

$$|P^0(t)\rangle = (g_+ + g_-\cos\theta)\,|P^0\rangle + e^{i\phi}g_-\sin\theta\,|\bar{P}^0\rangle\,, \tag{4.10}$$

$$|\bar{P}^0(t)\rangle = e^{-i\phi}g_-\sin\theta\,|P^0\rangle + (g_+ - g_-\cos\theta)\,|\bar{P}^0\rangle\,,$$

with $g_+ = e^{-it\left(M - i\frac{\Gamma}{2}\right)} \cos\left[\left(\Delta M - i\frac{\Delta\Gamma}{2}\right)\frac{t}{2}\right]$ and $g_- = e^{-it\left(M - i\frac{\Gamma}{2}\right)} i\sin\left[\left(\Delta M - i\frac{\Delta\Gamma}{2}\right)\frac{t}{2}\right]$ . Here, $M \equiv (M_H + M_L)/2$, $\Delta M \equiv M_H - M_L$, $\Gamma \equiv (\Gamma_H + \Gamma_L)/2$ and $\Delta\Gamma \equiv \Gamma_H - \Gamma_L$ .

It should be noticed that:

$$\langle P_H|P_L\rangle = N_1 N_2 \left[\cos\frac{\theta}{2}\sin\frac{\theta^*}{2} - e^{i(\phi - \phi^*)}\sin\frac{\theta}{2}\cos\frac{\theta^*}{2}\right] \neq 0\,, \tag{4.11}$$

i.e., the inner product of the physical states does not vanish in general. This means, the physical states are not orthogonal. It happens because the Hamiltonian is non-Hermitian.

## 4.3   T and CPT violation

To obtain the conditions for **CPT** and **T** violations, we need to use the whole Hilbert space. Using perturbation theory, the elements of mass and decay matrices are given by [5, 68]:

$$\mathbf{M}_{\alpha\beta} = \langle\alpha|\mathbf{H}|\beta\rangle + \sum_n \mathcal{P}\left[\frac{\langle\alpha|\mathcal{H}_W|n;out\rangle\langle n;out|\mathcal{H}_W|\beta\rangle}{M_P - M_n}\right], \tag{4.12}$$

$$\mathbf{\Gamma}_{\alpha\beta} = 2\pi\sum_n \delta(M_P - M_n)\,\mathcal{P}\left[\langle\alpha|\mathcal{H}_W|n;out\rangle\langle n;out|\mathcal{H}_W|\beta\rangle\right], \tag{4.13}$$

with the constraints: $\mathbf{M}_{\alpha\beta} = \mathbf{M}^*_{\beta\alpha}$ and $\mathbf{\Gamma}_{\alpha\beta} = \mathbf{\Gamma}^*_{\alpha\beta}$ (since $\mathbf{M}$ and $\mathbf{\Gamma}$ are Hermitian), where $\mathcal{P}$ indicates the principal part.

The properties of $\mathbf{M}$ and $\mathbf{\Gamma}$ in light of $\mathbf{CPT}$ and $\mathbf{T}$ symmetries are given below [5]:

1. *If $\mathbf{CPT}$ invariance holds, independent of $\mathbf{T}$ symmetry, then*

$$\mathbf{M}_{11} = \mathbf{M}_{22} \quad\text{and}\quad \mathbf{\Gamma}_{11} = \mathbf{\Gamma}_{22} \tag{4.14}$$

The above relations can be proved easily by using the definition of $\mathbf{M}_{\alpha\beta}$ and $\mathbf{\Gamma}_{\alpha\beta}$ from Eq. (4.12), followed by same flow of logic as in Eq. (2.43) and Eq. (2.45). Applying this condition to Eq. (4.7) will result in:

$$E_3 = 0 \quad\Longrightarrow\quad \theta = \frac{\pi}{2}. \tag{4.15}$$

2. *If $\mathbf{T}$ invariance holds, then, independently of $\mathbf{CPT}$ symmetry,*

$$\frac{\mathbf{\Gamma}^*_{12}}{\mathbf{\Gamma}_{12}} = \frac{\mathbf{M}^*_{12}}{\mathbf{M}_{12}}. \tag{4.16}$$

Starting from Eq. (4.12), the above relation can be proved in the following way:

$$\begin{aligned}
\mathbf{\Gamma}^*_{12} &= 2\pi\sum_n \delta(M_P - M_n)\,\mathcal{P}\left[\left(\langle P^0|\mathcal{H}_W|n;out\rangle\right)^*\left(\langle n;out|\mathcal{H}_W|\bar{P}^0\rangle\right)^*\right] \\
&= 2\pi\sum_n \delta(M_P - M_n)\,\mathcal{P}\left[\langle P^0|\mathbf{T}^\dagger\mathbf{T}\mathcal{H}_W\mathbf{T}^{-1}\mathbf{T}|n;out\rangle\langle n;out|\mathbf{T}^\dagger\mathbf{T}\mathcal{H}_W\mathbf{T}^{-1}\mathbf{T}|\bar{P}^0\rangle\right]
\end{aligned}$$

$$\tag{4.17}$$

If $\mathbf{T}$ be a symmetry of the system, then: $\quad \mathbf{T}\mathcal{H}_W\mathbf{T}^{-1} = \mathcal{H}_W. \tag{4.18}$

Moreover, strong and electromagnetic interactions already obey **T** symmetry:

$$\mathbf{T}\,\mathcal{H}_{SE}\,\mathbf{T}^{-1} = \mathcal{H}_{SE}\,,\ \mathbf{T}\,|P^0\rangle = e^{i\omega}\,|P^0\rangle\,,\ \mathbf{T}\,|\bar{P}^0\rangle = e^{i\bar{\omega}}\,|\bar{P}^0\rangle\,,\ \mathbf{T}\,|n\rangle = e^{i\omega_n}\,|n\rangle\,,\quad (4.19)$$

where, $\omega$, $\bar{\omega}$ and $\omega_n$ are real phases. Thus, from Eq. (4.17), **T** symmetry implies:

$$\mathbf{\Gamma}_{12}^* = e^{\,i(\bar{\omega}-\omega)}\,\mathbf{\Gamma}_{12} \tag{4.20}$$

Likewise, it can be shown that **T** symmetry enforces:    $\mathbf{M}_{12}^* = e^{\,i(\bar{\omega}-\omega)}\,\mathbf{M}_{12}$ .   (4.21)

Using last two equations, we arrive at the **T** invariance condition in Eq. (4.16). In our formalism, this condition will translate as:

$$\mathrm{Im}\,(E_1 E_2^*) = 0 \quad \Longrightarrow \quad \mathrm{Im}\,\phi = 0, \tag{4.22}$$

which can be derived from Eq. (4.7) .

3. *Inner product of the physical states becomes real if **CPT** invariance holds and it turns into an imaginary entity if **T** symmetry is there.*

Using the condition for **CPT** symmetry from Eq. (4.15), the inner product of physical states, given by Eq. (4.11), becomes:

$$\langle P_H|P_L\rangle\Big|_{\theta=\pi/2} = \tanh\,[\mathrm{Im}(\phi)], \tag{4.23}$$

which is obviously real.. Now, if we use the **T** invariance condition from Eq. (4.22), the inner product in Eq. (4.11) turns into:

$$\langle P_H|P_L\rangle\Big|_{\mathrm{Im}(\phi)=0} = \frac{-\,i\,\sinh\,[\mathrm{Im}(\theta)]}{|\cos\frac{\theta}{2}|^2 + |\sin\frac{\theta}{2}|^2} \tag{4.24}$$

which is imaginary. It is obvious that $\langle P_H|P_L\rangle$ vanishes, i.e. physical states become orthogonal, if both **CPT** and **T** are good symmetries.

The above theorems signify that $[\text{Re}(\theta) - \pi/2]$ and $\text{Im}(\theta)$ are **CPT** violating parameters whereas $\text{Im}(\phi)$ is **T** violating parameter. Note that it is usually said that the absence of **CP** violation implies $|e^{i\phi}| = \sqrt{\left|\frac{\mathbf{M}_{12}^* - i\mathbf{\Gamma}_{12}^*/2}{\mathbf{M}_{12} - i\mathbf{\Gamma}_{12}/2}\right|} = 1$ (i.e. $\text{Im}(\phi) = 0$). However, strictly speaking, this is due to the absence of **T** violation. The two statements are equivalent only if **CPT** is conserved.

In the absence of both **T** and **CPT** violation in $B^0$-$\bar{B}^0$ mixing, the parameters $\theta$ and $\phi$ take the values $\theta = \frac{\pi}{2}$ and $\phi = -2\beta^{mix}$ where $\beta^{mix}$ is the weak phase describing $B^0 - \bar{B}^0$ mixing. In SM, $\beta^{mix} = \beta$ for the $B_d^0$ meson and it is $\beta_s$ for $B_s^0$ meson. But in the presence of **T** and **CPT** violation, the parameters $\theta$ and $\phi$ will deviate from these values. Now, we introduce **CPT** violating parameters $\epsilon_{1,2}$ and **T** violating parameter $\epsilon_3$ to express the mixing parameters $\theta$ and $\phi$ in terms of them as:

$$\theta = \frac{\pi}{2} + \epsilon_1 + i\,\epsilon_2\,, \quad \phi = -2\beta^{mix} + i\,\epsilon_3\,. \tag{4.25}$$

But one must be careful about the given names of $\epsilon_{1,2,3}$. The parameters $\epsilon_1$ and $\epsilon_2$ do not contribute *only* to observables measuring **CPT** violation, rather they also lead to **CP** and **T** violating effects. Similarly, the **T** violating parameter $\epsilon_3$ also contributes to **CP** violating observables. And the reverse is true: recall that, in Ref. [67], the BaBar Collaboration measured a large true **T** violating asymmetry. This does *not* suggest that $\epsilon_3$ is large, as there are also large contributions to the asymmetry coming from **CP** violating effects (assuming **CPT** invariance). The point is that $\epsilon_1$, $\epsilon_2$ and $\epsilon_3$ are also sources of **CP** violation, and it is this fact that allows their measurement in the time-dependent indirect **CP** asymmetry, as we will see below.

The values for $\epsilon_1$, $\epsilon_2$ and $\epsilon_3$ have been reported by the BaBar and Belle Collaborations [6]. Their notation is related to ours as follows:

$$\cos\theta \leftrightarrow -z\,, \quad \sin\theta \leftrightarrow \sqrt{1 - z^2}\,, \quad e^{i\phi} \leftrightarrow \frac{q}{p}\,, \tag{4.26}$$

$$\implies \quad \epsilon_1 = \text{Re}(z) \,, \quad \epsilon_2 = \text{Im}(z) \,, \quad \epsilon_3 = 1 - \left|\frac{q}{p}\right| \,. \tag{4.27}$$

Since $\epsilon_1$ and $\epsilon_2$ are **CPT** violating parameters, they are expected to be very small. As for $\epsilon_3$, note that $|q/p|$ has been measured at the $\Upsilon(4S)$ using the same-sign dilepton asymmetry, assuming **CPT** conservation [6]:

$$\left|\frac{q}{p}\right| = 1.0010 \pm 0.0008 \quad \implies \quad \epsilon_3 = -(1.0 \pm 0.8) \times 10^{-3} \,. \tag{4.28}$$

Thus, $\epsilon_3$ is also very small. The value of $y_d = \Delta\Gamma_d/2\Gamma_d$ has been measured to be small: $y_d = -0.003 \pm 0.015$ with the $B_d^0$ lifetime of $1.520 \pm 0.004$ ps [7]. This means that we can approximate $\sinh(\Delta\Gamma t/2) \simeq \Delta\Gamma t/2 = y_d\Gamma_d t$ and $\cosh(\Delta\Gamma t/2) \simeq 1$. In principle, for large enough times, this approximation will break down. However, even at time scales of $\mathcal{O}(10)$ ps, the approximation holds to $\sim 10^{-4}$, and by this time most of the $B_d^0$s will have decayed.

## 4.4    Time-dependent indirect CP asymmetry

Now, we consider a final state $f$ to which both $B^0$ and $\bar{B}^0$ can decay. Denoting the decay Hamiltonian by $\mathcal{H}_{\Delta F=1}$, we can express the time-dependent decay amplitudes for uncorrelated or tagged neutral mesons following Eq. (4.10) as:

$$\mathcal{A}(B^0(t) \to f) = \langle f | \mathcal{H}_{\Delta F=1} | B^0(t) \rangle = (g_+ + g_- \cos\theta)\,\mathcal{A}_f + e^{i\phi}g_- \sin\theta\,\bar{\mathcal{A}}_f \,, \tag{4.29}$$

$$\mathcal{A}(\bar{B}^0(t) \to f) = \langle f | \mathcal{H}_{\Delta F=1} | \bar{B}^0(t) \rangle = e^{-i\phi}g_- \sin\theta\,\mathcal{A}_f + (g_+ - g_- \cos\theta)\,\bar{\mathcal{A}}_f \,,$$

where, $\mathcal{A}_f \equiv \langle f | \mathcal{H}_{\Delta F=1} | B^0 \rangle$ and $\bar{\mathcal{A}}_f \equiv \langle f | \mathcal{H}_{\Delta F=1} | \bar{B}^0 \rangle$. The differential decay rates for any mode $d\Gamma/dt(B^0(t) \to f)$ and its conjugate mode $d\Gamma/dt(\bar{B}^0(t) \to f)$ are given by[3]:

$$\frac{d\Gamma}{dt}(B^0(t) \to f) = \frac{1}{2}e^{-\Gamma t}\left[\sinh\left(\Delta\Gamma t/2\right)\left\{2\,\text{Re}\left(\cos\theta|\mathcal{A}_f|^2 + e^{i\phi}\sin\theta\,\mathcal{A}_f^*\bar{\mathcal{A}}_f\right)\right\}\right.$$

---

[3]In Ref. [64] it was pointed out that the coefficient of $\cos(\Delta M t)$ includes a **CPT**-violating piece.

$$+ \cosh(\Delta\Gamma t/2)\Big\{|\mathcal{A}_f|^2 + |\cos\theta|^2 |\mathcal{A}_f|^2 + |e^{i\phi}\sin\theta|^2 |\bar{\mathcal{A}}_f|^2$$

$$+2\,\mathrm{Re}\Big(e^{i\phi}\cos\theta^*\sin\theta\,\mathcal{A}_f^*\bar{\mathcal{A}}_f\Big)\Big\} + \cos(\Delta M t)\Big\{|\mathcal{A}_f|^2 - |\cos\theta|^2 |\mathcal{A}_f|^2$$

$$-|e^{i\phi}\sin\theta|^2 |\bar{\mathcal{A}}_f|^2 - 2\,\mathrm{Re}\Big(e^{i\phi}\cos\theta^*\sin\theta\,\mathcal{A}_f^*\bar{\mathcal{A}}_f\Big)\Big\}$$

$$- \sin(\Delta M t)\Big\{2\,\mathrm{Im}\Big(\cos\theta\,|\mathcal{A}_f|^2 + e^{i\phi}\sin\theta\,\mathcal{A}_f^*\bar{\mathcal{A}}_f\Big)\Big\}\Big] , \qquad (4.30)$$

$$\frac{d\Gamma}{dt}(\bar{B}^0(t) \to f) = \frac{1}{2}\,e^{-\Gamma t}\Big[\sinh(\Delta\Gamma t/2)\Big\{2\,\mathrm{Re}\Big(-\cos\theta^*\,|\bar{\mathcal{A}}_f|^2 + e^{i\phi^*}\sin\theta^*\,\mathcal{A}_f^*\bar{\mathcal{A}}_f\Big)\Big\}$$

$$+ \cosh(\Delta\Gamma t/2)\Big\{|\bar{\mathcal{A}}_f|^2 + |\cos\theta|^2 |\bar{\mathcal{A}}_f|^2 + |e^{-i\phi}\sin\theta|^2 |\mathcal{A}_f|^2$$

$$-2\,\mathrm{Re}\Big(e^{i\phi^*}\cos\theta\sin\theta^*\,\mathcal{A}_f^*\bar{\mathcal{A}}_f\Big)\Big\} + \cos(\Delta M t)\Big\{|\bar{\mathcal{A}}_f|^2 - |\cos\theta|^2 |\bar{\mathcal{A}}_f|^2$$

$$-|e^{-i\phi}\sin\theta|^2 |\mathcal{A}_f|^2 + 2\,\mathrm{Re}\Big(e^{i\phi^*}\cos\theta\sin\theta^*\,\mathcal{A}_f^*\bar{\mathcal{A}}_f\Big)\Big\}$$

$$+ \sin(\Delta M t)\Big\{2\,\mathrm{Im}\Big(-\cos\theta^*\,|\bar{\mathcal{A}}_f|^2 + e^{i\phi^*}\sin\theta^*\,\mathcal{A}_f^*\bar{\mathcal{A}}_f\Big)\Big\}\Big] . \qquad (4.31)$$

If we set $\theta = \pi/2$ and $\mathrm{Im}\,\phi = 0$ in the above expressions, we recover expressions for the differential decay rates that are commonly found elsewhere in the literature.

The observable we will use to extract the **T** and **CPT** violating parameters $\epsilon_{1,2,3}$ is the time-dependent indirect **CP** asymmetry $\mathcal{A}_{\mathbf{CP}}^f(t)$ involving $B$-meson decays to a **CP** eigenstate. It is defined as:

$$\mathcal{A}_{\mathbf{CP}}^f(t) = \frac{d\Gamma/dt\,(\bar{B}_d^0(t) \to f_{\mathbf{CP}}) - d\Gamma/dt\,(B_d^0(t) \to f_{\mathbf{CP}})}{d\Gamma/dt\,(\bar{B}_d^0(t) \to f_{\mathbf{CP}}) + d\Gamma/dt\,(B_d^0(t) \to f_{\mathbf{CP}})} . \qquad (4.32)$$

In the limit of **CPT** and **T** conservation in the mixing, and $\Delta\Gamma = 0$, one has the familiar expression:

$$\mathcal{A}_{\mathbf{CP}}^f(t) = S\,\sin(\Delta M_d t) - C\,\cos(\Delta M_d t), \qquad (4.33)$$

where, $\quad \varphi \equiv -2\beta^{mix} - \arg[\mathcal{A}_f] + \arg[\bar{\mathcal{A}}_f],\ C \equiv \frac{|\mathcal{A}_f|^2 - |\bar{\mathcal{A}}_f|^2}{|\mathcal{A}_f|^2 + |\bar{\mathcal{A}}_f|^2},\ S \equiv \sqrt{1 - C^2}\,\sin\varphi. \quad (4.34)$

Here, $C$ is called *direct **CP** asymmetry* and $\varphi$ is the measured weak phase, which differs from the mixing phase $-2\beta^{mix}$ if $\arg[\mathcal{A}_f] \neq \arg[\bar{\mathcal{A}}_f]$. If there is no penguin pollution, then $\varphi$ cleanly measures a weak phase and $C = 0$. But if there is penguin pollution or any other

kind of new physics contribution that preserves **CPT**, then neither of these holds.

In the presence of **T** and **CPT** violation in the mixing, Eq. (4.33) does not hold. To obtain a more accurate form of $\mathcal{A}^f_{\mathbf{CP}}(t)$, we proceed in the following way. First, we insert the expressions for differential decay rates of mode and conjugate mode from Eq. (4.30) and (4.31) into Eq. (4.32). Then, keeping only terms at most linear in the small quantities $\epsilon_{1,2,3}$ and $\Delta\Gamma_d$, we obtain[4]:

$$\mathcal{A}^f_{\mathbf{CP}}(t) \simeq c_0 + c_1 \cos(\Delta M_d t) + c_2 \cos(2\Delta M_d t) + s_1 \sin(\Delta M_d t) + s_2 \sin(2\Delta M_d t)$$
$$+ c'_1 \Gamma_d t \cos(\Delta M_d t) + s'_1 \Gamma_d t \sin(\Delta M_d t) , \qquad (4.35)$$

where the coefficients are given by:

$$c_0 = \epsilon_1 \cos\varphi + \epsilon_3 - \frac{1}{2}\epsilon_3 \sin^2\varphi , \quad s_1 = \sqrt{1 - C^2} \sin\varphi - \epsilon_2 \cos^2\varphi - \epsilon_3 C \sin\varphi ,$$

$$c_1 = -C - \epsilon_3 - \epsilon_1 \cos\varphi - \epsilon_2 C \sin\varphi , \quad s_2 = -\frac{1}{2}\epsilon_2 \sin^2\varphi + \epsilon_3 C \sin\varphi ,$$

$$c_2 = \frac{1}{2}\epsilon_3 \sin^2\varphi + \epsilon_2 C \sin\varphi , \quad c'_1 = C y_d \cos\varphi , \quad s'_1 = -\frac{1}{2} y_d \sin 2\varphi . \qquad (4.36)$$

The seven pieces have different time dependences so that, by fitting $\mathcal{A}^f_{\mathbf{CP}}(t)$ to the seven time-dependent functions, all coefficients can be extracted. It should be noted for Eq. (4.36) that non-vanishing $c_0$, $c_2$ and $s_2$ indicate breaking of **T** or **CPT** symmetry in mixing. It is obvious that setting $\epsilon_{1,2,3}$ to zero in Eq. (4.35) and (4.36) brings back the usual form of **CP** asymmetry, as expressed in Eq. (4.33).

The five observables $c_0$, $c_1$, $c_2$, $s_1$ and $s_2$ can be used to solve for the five unknown parameters $C$, $\varphi$ and $\epsilon_{1,2,3}$. In practice, a fit will probably be used, but there is a way to solve analytically. The parameter $C$ is simply given by:

$$C = -(c_0 + c_1 + c_2) . \qquad (4.37)$$

---

[4]A time-dependent **CP** asymmetry having a complicated form with higher harmonics in $(\Delta M_d t)$, similar to that in Eq. (4.35), was noted in Ref. [62].

The solution for $\sin \varphi$ is obtained by solving the following quartic equation:

$$\sin^4 \varphi - 2 \left[ \frac{s_1 + 2s_2}{2 - C^2} \right] \sin^3 \varphi + 4C \left[ C + \frac{c_2}{2 - C^2} \right] \sin^2 \varphi$$
$$- 4 \left[ \frac{2C^2(s_1 + s_2) - s_2}{2 - C^2} \right] \sin \varphi - \left[ \frac{8C\, c_2}{2 - C^2} \right] = 0 \,. \qquad (4.38)$$

Of course, there are four solutions, but, since the $\epsilon_j$ are small, the correct solution is the one that is roughly $s_1/\sqrt{1 - C^2}$. Finally, $\epsilon_1, \epsilon_2, \epsilon_3$ are given by:

$$\epsilon_1 = c_0 \sec \varphi - \frac{(2 - \sin^2 \varphi)(c_2 \sin \varphi + 2C\, s_2)}{(4C^2 + \sin^2 \varphi)\, \sin \varphi \cos \varphi} \,,$$
$$\epsilon_2 = \frac{2\,(2C\, c_2 - s_2\, \sin \varphi)}{(4C^2 + \sin^2 \varphi)\, \sin \varphi} \,, \qquad \epsilon_3 = \frac{2\,(c_2\, \sin \varphi + 2C\, s_2)}{(4C^2 + \sin^2 \varphi)\, \sin \varphi} \,. \qquad (4.39)$$

Hence, it is possible to measure the parameters describing **T** and **CPT** violation in $B_d^0 - \bar{B}_d^0$ mixing using the time-dependent indirect **CP** asymmetry. Knowing $\varphi$, the value of $y_d$ can be found from measurements of $c_1'$ and $s_1'$. Note that, even if the width difference $\Delta \Gamma_d$ between the two $B$-meson eigenstates vanishes, the **T** violating parameter $\epsilon_3$ can still be extracted, which is contrary to the claim of Refs. [59] and [62].

We have described the above method for $B_d^0$ mesons, as $\Delta \Gamma_d$ is vanishingly small. In the case of $B_s^0$ mesons, $\Delta \Gamma_s$ is not that small; so the functions $\sinh(\Delta \Gamma_s\, t/2)$ and $\cosh(\Delta \Gamma_s\, t/2)$ must be kept throughout or one should truncate the series of $\sinh(\Delta \Gamma_s\, t/2)$ and $\cosh(\Delta \Gamma_s\, t/2)$ accordingly. This modifies the forms of Eq. (4.35), but the idea does not change.

## 4.5  CPT conserving scenario

We have another handle for probing **CPT** violation in $B_d^0 - \bar{B}_d^0$ mixing. Currently, we know that $\epsilon_3 = -(1.0 \pm 0.8) \times 10^{-3}$ [Eq. (4.28)]. Now, suppose that there is no **CPT** violation (i.e., $\epsilon_1 = \epsilon_2 = 0$). Then, the coefficients $c_0, c_2$ and $s_2$ can be expressed in terms of the

measured quantities $c_1$, $s_1$ and $\epsilon_3$ as follows:

$$c_0 = \epsilon_3\left[1 - \frac{2s_1^2}{(2 - c_1^2 + \epsilon_3^2)^2}\right], \quad c_2 = \frac{2s_1^2\,\epsilon_3}{(2 - c_1^2 + \epsilon_3^2)^2}, \quad s_2 = -\frac{2s_1\,(c_1 + \epsilon_3)\,\epsilon_3}{(2 - c_1^2 + \epsilon_3^2)}. \quad (4.40)$$

The values of $c_1$ and $s_1$ have been measured for several $B_d^0$ decays to **CP** eigenstates [6], and the value of $\epsilon_3$ is independent of the decay mode. Using these values, we can estimate $c_0$, $c_2$ and $s_2$ from Eq. (4.40), which assumes that **CPT** is conserved. We present the expected values for $c_0, c_2$ and $s_2$ in the absence of **CPT** violation for different modes in the Table 4.1. Should the measurements of $c_0$, $c_2$ and $s_2$ deviate significantly from the above values, this would indicate the presence of **CPT** violation in $B_d^0 - \bar{B}_d^0$ mixing.

| Modes | $c_0 \times 10^{-4}$ | $c_2 \times 10^{-4}$ | $s_2 \times 10^{-4}$ |
|---|---|---|---|
| $J/\psi K_S$ | $-15.18 \pm 15.50$ | $-4.31 \pm 4.41$ | $0.29 \pm 0.43$ |
| $J/\psi K_L$ | $-15.21 \pm 15.53$ | $-4.29 \pm 4.41$ | $-0.32 \pm 0.52$ |
| $\psi(2S)K_S$ | $-13.15 \pm 13.46$ | $-6.35 \pm 6.56$ | $-0.17 \pm 0.89$ |
| $\phi K_S$ | $-14.16 \pm 14.57$ | $-5.34 \pm 5.76$ | $-0.12 \pm 2.0$ |
| $K_S K_S K_S$ | $-14.14 \pm 14.71$ | $-5.36 \pm 6.17$ | $3.49 \pm 4.29$ |
| $\rho^0 K_S$ | $-16.65 \pm 17.23$ | $-2.85 \pm 4.08$ | $-0.65 \pm 2.25$ |
| $\omega K_S$ | $-14.58 \pm 15.16$ | $-4.92 \pm 5.81$ | $-0.58 \pm 2.05$ |

Table 4.1: Expected values with errors for $c_0, c_2$ and $s_2$ in the absence of **CPT** violation for different modes.

## 4.6   Fitting individual decay rates

Instead of going through time dependent indirect **CP** asymmetry, one can obtain **T** and **CPT** violating parameters by fitting the individual decay rates for mode and conjugate mode. Assuming $\epsilon_{1,2,3}$ and $\Delta\Gamma$ to be small, the differential decay rates for mode and

conjugate mode can be written as:

$$
\begin{aligned}
\frac{d\Gamma_f}{dt}(B_d^0(t) \to f) = \frac{1}{2} e^{-\Gamma t} &\left(|\mathcal{A}_f|^2 + |\bar{\mathcal{A}}_f|^2\right) \Bigg[ \cosh(\Delta\Gamma t/2) \Big\{ 1 - (1-C)\,\epsilon_3 - \sqrt{1-C^2}\,(\epsilon_1 \cos\varphi \\
&+ \epsilon_2 \sin\varphi) \Big\} + \sinh(\Delta\Gamma t/2) \Big\{ -(1+C)\,\epsilon_1 + \sqrt{1-C^2}\,(1-\epsilon_3)\cos\varphi \Big\} \\
&+ \cos(\Delta M t) \Big\{ C + (1-C)\,\epsilon_3 + \sqrt{1-C^2}\,(\epsilon_1 \cos\varphi + \epsilon_2 \sin\varphi) \Big\} \\
&+ \sin(\Delta M t) \Big\{ (1+C)\,\epsilon_2 + \sqrt{1-C^2}\,(-1+\epsilon_3)\sin\varphi \Big\} \Bigg] \\
= e^{-\Gamma t} &\left[ C_1^h \cosh(\Delta\Gamma t/2) + S_1^h \sinh(\Delta\Gamma t/2) + C_1 \cos(\Delta M t) + S_1 \sin(\Delta M t) \right], \quad (4.41)
\end{aligned}
$$

$$
\begin{aligned}
\frac{d\Gamma_f}{dt}(\bar{B}_d^0(t) \to f) = \frac{1}{2} e^{-\Gamma t} &\left(|\mathcal{A}_f|^2 + |\bar{\mathcal{A}}_f|^2\right) \Bigg[ \cosh(\Delta\Gamma t/2) \Big\{ 1 + (1+C)\,\epsilon_3 + \sqrt{1-C^2}\,(\epsilon_1 \cos\varphi \\
&- \epsilon_2 \sin\varphi) \Big\} + \sinh(\Delta\Gamma t/2) \Big\{ (1-C)\,\epsilon_1 + \sqrt{1-C^2}\,(1+\epsilon_3)\cos\varphi \Big\} \\
&+ \cos(\Delta M t) \Big\{ -C - (1+C)\,\epsilon_3 - \sqrt{1-C^2}\,(\epsilon_1 \cos\varphi - \epsilon_2 \sin\varphi) \Big\} \\
&+ \sin(\Delta M t) \Big\{ (-1+C)\,\epsilon_2 + \sqrt{1-C^2}\,(1+\epsilon_3)\sin\varphi \Big\} \Bigg] \\
= e^{-\Gamma t} &\left[ C_2^h \cosh(\Delta\Gamma t/2) + S_2^h \sinh(\Delta\Gamma t/2) + C_2 \cos(\Delta M t) + S_2 \sin(\Delta M t) \right]. \quad (4.42)
\end{aligned}
$$

Here, the coefficients $C_{1,2}^h$, $S_{1,2}^h$, $C_{1,2}$ and $S_{1,2}$ can be considered as observables. They can be determined directly from experiments by fitting the differential decay rates for mode and conjugate mode individually.

Now, we have eight observables to solve for six unknown quantities ($\varphi$, $|\mathcal{A}_f|$, $|\bar{\mathcal{A}}_f|$ and $\epsilon_{1,2,3}$). The solutions for $|\mathcal{A}_f|$ and $|\bar{\mathcal{A}}_f|$ are given by:

$$
|\mathcal{A}_f| = \sqrt{C_1^h + C_1} \qquad \text{and} \qquad |\bar{\mathcal{A}}_f| = \sqrt{C_2^h + C_2}\,. \qquad (4.43)
$$

$$
\implies C = \frac{C_1^h - C_2^h + C_1 - C_2}{C_1^h + C_2^h + C_1 + C_2} \qquad \text{and} \qquad |\mathcal{A}_f|^2 + |\bar{\mathcal{A}}_f|^2 = C_1^h + C_2^h + C_1 + C_2\,. \quad (4.44)
$$

We define: $\quad C'_j = \dfrac{C_j}{|\mathcal{A}_f|^2 + |\bar{\mathcal{A}}_f|^2}\quad$ and $\quad S'_j = \dfrac{S_j}{|\mathcal{A}_f|^2 + |\bar{\mathcal{A}}_f|^2}\,,\quad j \in \{1,2\}\,.$ $\qquad$ (4.45)

Then the value for $\sin\varphi$ can be obtained from the following cubic equation:

$$\sin^3\varphi + \frac{S'_1 - S'_2}{\sqrt{1 - C^2}}\,\sin^2\varphi + \left(\frac{C^2 - C'_1 - C'_2}{1 - C^2}\right)\sin\varphi - \frac{C}{\sqrt{1 - C^2}}\left[\frac{S'_1}{1 + C} + \frac{S'_2}{1 - C}\right] = 0\,. \quad (4.46)$$

The solutions for $\epsilon_{1,2,3}$ now become:

$$\epsilon_1 = -\left(\frac{2}{\sin 2\varphi}\right)\left[\frac{S'_1}{1 + C} + \frac{S'_2}{1 - C} - \left(\frac{C'_1 - C'_2}{\sqrt{1 - C^2}}\right)\sin\varphi\right]\,, \qquad (4.47)$$

$$\epsilon_2 = S'_1 - S'_2 + \sqrt{1 - C^2}\,\sin\varphi\,, \qquad (4.48)$$

$$\epsilon_3 = -C + \csc\varphi\left(S'_1\,\sqrt{\frac{1 - C}{1 + C}} + S'_2\,\sqrt{\frac{1 + C}{1 - C}}\right)\,. \qquad (4.49)$$

## 4.7  Summary

To sum up, we have shown that the time-dependent indirect **CP** asymmetries involving $B^0$ or $\bar{B}^0$ decaying to a **CP** eigenstate contain enough information to extract not only the **CP** violating weak phases, but also the parameters describing **T** and **CPT** violation in $B^0$-$\bar{B}^0$ mixing. It is also possible to extract these parameters by fitting the individual decay rates for modes and conjugate modes separately. Penguin pollutions and the width difference between light and heavy states need not be neglected. This procedure can be applied to both $B_d^0$ and $B_s^0$ meson decays.

# TESTING $WW\gamma$ VERTEX

> " *One accurate measurement is worth a thousand expert opinions.*
>
> — **Grace Hopper**

## 5.1 Prologue

The $SU(2)_L \otimes U(1)_Y$ theory of electroweak interactions has been tested extensively in last few decades and there is no doubt that it is the correct theory at least up to a TeVscale. This conviction is largely based on the precision measurements at LEP and the consistency of top and Higgs boson masses which could be predicted taking radiative corrections into account. The gauge boson and Higgs boson self interactions are, however, not as well probed either by direct measurement or by radiative corrections and it is possible that some deviations from the standard Model (SM) loop level values might still be seen. To ascertain the validity of SM it is critical that the $WW\gamma$ vertex, which is predicted uniquely in SM, be probed to an accuracy consistent with loop level corrections to it. Several experiments [69–76] have measured parameters that probe the $WW\gamma$ and $WWZ$ vertex, but the accuracy achieved is still insufficient to probe one loop corrections to it within the SM.

In this chapter, we have investigated how the **C** and **P** conserving dimension four $WW\gamma$ operator can be probed experimentally using radiative muon decays. The vertex factor for this operator is usually denoted by $\kappa_\gamma$ and is uniquely predicted in the SM. At tree level $\kappa_\gamma = 1$ in the SM and the absolute value of the one loop corrections to the tree level values of $\kappa_\gamma$ is restricted to be less than $1.5 \times 10^{-2}$ [10]. However, the current global average $\kappa_\gamma = 0.982 \pm 0.042$ [7] has too large an uncertainty to probe the SM up to one loop accuracy. Of the experimentally measured values of $\kappa_\gamma$, only ATLAS and CMS collaborations use the data for real on-shell photon emission in hadron colliders [69, 70], probing the true magnetic moment of the $W$-boson.

One can expect $\kappa_\gamma$ to deviate from its SM value by only a few percent, hence, we must choose the mode to be studied very carefully. Radiative muon decay $\mu \rightarrow e\gamma\nu_\mu\bar{\nu}_e$ is a promising mode to measure the true magnetic moment (due to real photon in the final state) of the $W$-boson in this regard. At first sight the measurement of $W$-boson gauge coupling using low energy decay process may seem impossible, since the effect is suppressed by two powers of the $W$-boson mass. The process has two missing neutrinos in the final state and on integrating their momenta the partial differential decay rate shows no radiation-amplitude zero [77]. Moreover, the differential decay rate does not show enough sensitivity to a deviation of the $WW\gamma$ vertex from that of the SM. We show, however, that an easily separable part the normalized differential decay rate (odd under the exchange of photon and electron energies) does have a zero in the case of SM. The vanishing of the odd contribution under the exchange of final state electron and photon energies in the decay rate is a *new type of zero*, hitherto not been studied in literature. A suitably constructed asymmetry using this fact enables adequate sensitivity to probe the $WW\gamma$ vertex beyond the SM. We consider a very restricted part of the phase space where the asymmetry is larger than statistical errors for our study. Large number of muons are expected to be produced for COMET, MEG and Mu2e collaborations [3] to probe lepton flavour violating processes like $\mu \rightarrow e\gamma$. The radiative muon decay $\mu \rightarrow e\gamma\nu_\mu\bar{\nu}_e$, which has been discussed in Ref. [78] in a great detail, is the dominant background process for this case. The large sample of

$\mu \rightarrow e\gamma\nu_\mu\bar{\nu}_e$ produced at such facilities make them an ideal environment to probe $WW\gamma$ vertex, with reduced statistical uncertainty, as discussed in this chapter. In a simulation using $\eta_\gamma \equiv \kappa_\gamma - 1 = 0.01$, we find that the asymmetry constructed by us, can probe this $\eta_\gamma$ value with a $3.9\sigma$ significance.

The rest of the chapter is organized as follows. In Sec. 5.2 we briefly discuss the decay kinematics and relevant expressions for decay rate. These results are used to construct the observables in Sec. 5.3, where we also explain why a zero in odd amplitude is expected. In sec. 5.4, we have discussed the effects of electron mass. Sec. 5.5 deals with the numerical analysis to probe the $WW\gamma$ vertex and finally we conclude in Sec. 5.6.

## 5.2   Theoretical Framework

### 5.2.1   Dynamics

The most general couplings of $W$ to the neutral gauge bosons $\gamma$ and $Z$ can be described by the following effective Lagrangian [8]:

$$\mathcal{L}_{eff}^V = -ig_V\left[ g_1^V\,(W_{\mu\nu}^\dagger W^\mu - W^{\dagger\mu}W_{\mu\nu})V^\nu + \kappa_V\,W_\mu^\dagger W_\nu V^{\mu\nu} + \left(\frac{\lambda_V}{m_W^2}\right)W_{\lambda\mu}^\dagger W_\nu^\mu V^{\nu\lambda} + if_4^V\,W_\mu^\dagger W_\nu\,(\partial^\mu V^\nu \right.$$

$$\left. + \partial^\nu V^\mu) - if_5^V\,\epsilon^{\mu\nu\rho\sigma}(W_\mu^\dagger \overleftrightarrow{\partial}_\rho W_\nu)V_\sigma + \widetilde{\kappa}_V\,W_\mu^\dagger W_\nu \widetilde{V}^{\mu\nu} + \left(\frac{\widetilde{\lambda}_V}{m_W^2}\right)W_{\lambda\mu}^\dagger W_\nu^\mu \widetilde{V}^{\nu\lambda}\right]. \quad (5.1)$$

Here, $V$ corresponds to $\gamma$ or $Z$, $g_\gamma = e$ and $g_Z = e\cot\theta_W$ where $\theta_W$ is the weak mixing angle and $e$ is electric charge of positron. The other definitions are: $W_{\mu\nu} = \partial_\mu W_\nu - \partial_\nu W_\mu$, $V_{\mu\nu} = \partial_\mu V_\nu - \partial_\nu V_\mu$, $\widetilde{V}_{\mu\nu} = \frac{1}{2}\epsilon_{\mu\nu\rho\sigma}V^{\rho\sigma}$, $(A\overleftrightarrow{\partial}_\mu B) = A(\partial_\mu B) - (\partial_\mu A)B$ and Bjorken-Drell metric is taken as $\epsilon_{0123} = -\epsilon^{0123} = +1$. In the SM, at tree level, $g_1^V = \kappa_V = 1$ and all other coupling parameters are zero.

In the case of radiative muon decay, $V$ stands for photon. According to charge conjugation and parity the seven coupling constants associated with most general $WW\gamma$ effective

Lagrangian can divided into four categories:

- Coupling of **C** & **P** conserving operator: $g_1^\gamma$, $\kappa_\gamma$, $\lambda_\gamma$ .

- Coupling of **C** conserving but **P** violating operator: $\widetilde{\kappa}_\gamma$, $\widetilde{\lambda}_\gamma$ .

- Coupling of **C** violating but **P** conserving operator: $f_4^\gamma$ .

- Coupling of **C** & **P** violating but **CP** conserving operator: $f_5^\gamma$ .

These coupling parameters are directly involved in the electromagnetic properties of $W$ boson in the following way [79–81][1]:

- Magnetic moment: $\mu_W = \dfrac{e}{2m_W}(1 + \kappa_\gamma + \lambda_\gamma)$

- Electric dipole moment: $d_W = \dfrac{e}{2m_W}(\widetilde{\kappa}_\gamma + \widetilde{\lambda}_\gamma)$

- Electric quadrupole moment: $Q_W = -\dfrac{e}{m_W^2}(\kappa_\gamma - \lambda_\gamma)$

- Magnetic quadrupole moment: $\widetilde{Q}_W = -\dfrac{e}{m_W^2}(\widetilde{\kappa}_\gamma - \widetilde{\lambda}_\gamma)$

where $m_W$ is the mass of $W$ boson.



$$W_\rho^-(q_2) \qquad W_\sigma^-(q_1) \quad = -ie\Gamma_{\rho\sigma\delta}(q_2, q_1, p)$$
$$A_\delta(p)$$
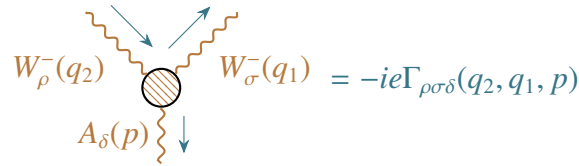
Figure 5.1: Feynman rule for effective $WW\gamma$ vertex.

Among the seven coupling parameters, the ones with **CP** violating interactions, i.e. $f_4^\gamma$, $\widetilde{\kappa}_\gamma$ and $\widetilde{\lambda}_\gamma$, are constrained to be less than $\sim (10^{-4})$ [9] due to the measurements of neutron electric dipole moment in case of direct **CP** violation. Due to the **CP** violating nature of

---

[1]As pointed out by Kim and Tsai [81], the expression for $Q_W$ given by Aronson [80] contains an error.

these couplings, deviations from the SM contributions are proportional to square of these couplings and thus are highly suppressed, as compared to **CP** conserving contributions. Hence, we neglect the **CP** violating parameters for the rest of the discussion of the chapter. Moreover, we can expect the interaction of photon with $W$ boson to preserve **C** and **P** symmetry separately, since it can be thought of as an electromagnetic interaction. The demand of **C** and **P** to be conserved separately in the Lagrangian allows us to choose vanishing $f_5^\gamma$. On the other hand, it is obvious that the radiative muon decay will not be sensitive to the dimension six-operator involving $\lambda_\gamma$, due to an additional $m_W^2$ suppression. The measurement of $\lambda_\gamma$ is possible only at high energy colliders. Hence, we can safely neglect the deviation of $\lambda_\gamma$ from its SM value of zero. Furthermore, the value of the coupling $g_1^\gamma$ is fixed to be unity due to electromagnetic gauge invariance. Thus, in momentum space the $WW\gamma$ vertex can be expressed as (in the unit of electron's charge):

$$\Gamma_{\rho\sigma\delta}(q_2, q_1, p) = g_{\rho\sigma}(q_2 + q_1)_\delta + g_{\sigma\delta}(p - q_1)_\rho - g_{\delta\rho}(p + q_2)_\sigma + \eta_\gamma (p_\rho g_{\sigma\delta} - p_\sigma g_{\rho\delta}), \quad (5.2)$$

where $\eta_\gamma \equiv \kappa_\gamma - 1$ and $q_2, q_1, p$ are the four momenta of incoming $W^-$, outgoing $W^-$ and outgoing photon respectively, as depicted in Fig. 5.1.

The radiative muon decay proceeds through three Feynman diagrams, shown in Fig. 5.2, where the photon in the final state can either arise from any of the initial and final state leptons (excluding neutrinos) or the $W$ boson in the propagator. The later process is of our particular interest.
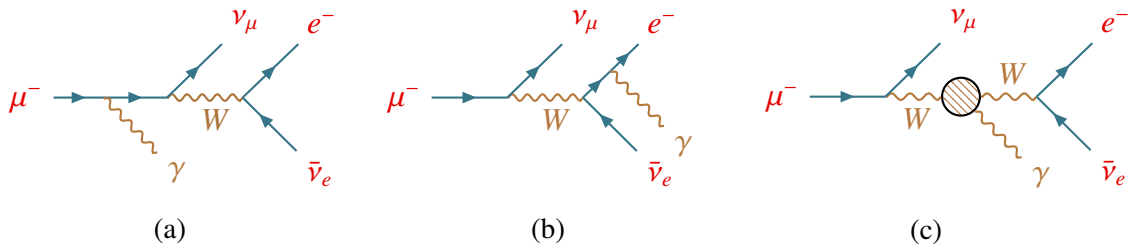


Figure 5.2: Feynman diagrams for radiative muon decay.

We define the four momenta of incoming $\mu^-$, outgoing $e^-$, $\gamma$, $\nu_\mu$, $\bar{\nu}_e$ as $p_m$, $p_e$, $p$, $k$ and $k'$,

respectively, and the masses of muon and electron are denoted by $m_\mu$ and $m_e$, respectively. Defining the $W$-propagator of momentum $q_j$ as $-i\,\mathbb{W}^{\mu\nu}(q_j)$, the amplitudes corresponding to these three diagrams (from top to bottom), labelled with subscript 1 to 3, can be expressed as:

$$i\mathcal{M}_1 = \left(\frac{-ieg^2}{8}\right)\left[\bar{u}(p_e)\,\gamma_\beta(1-\gamma_5)\,v(k')\right]\mathbb{W}^{\alpha\beta}(q_1)\left[\bar{u}(k)\,\gamma_\alpha(1-\gamma_5)\left(\frac{1}{\not{p}_m - \not{p} - m_\mu}\right)\gamma_\delta\,u(p_m)\right]\epsilon^{*\delta}, \qquad (5.3)$$

$$i\mathcal{M}_2 = \left(\frac{-ieg^2}{8}\right)\left[\bar{u}(k)\,\gamma_\alpha(1-\gamma_5)\,u(p_m)\right]\mathbb{W}^{\alpha\beta}(q_2)\left[\bar{u}(p_e)\,\gamma_\delta\left(\frac{1}{\not{p}_e + \not{p} - m_e}\right)\gamma_\beta(1-\gamma_5)\,v(k')\right]\epsilon^{*\delta}, \qquad (5.4)$$

$$i\mathcal{M}_3 = \left(\frac{-ieg^2}{8}\right)\left[\bar{u}(k)\,\gamma_\alpha(1-\gamma_5)\,u(p_m)\right]\mathbb{W}^{\alpha\rho}(q_2)\,\mathbb{W}^{\sigma\beta}(q_1)\left[\bar{u}(p_e)\,\gamma_\beta(1-\gamma_5)\,v(k')\right]\Gamma_{\rho\sigma\delta}(q_2,q_1,p)\,\epsilon^{*\delta}, \quad (5.5)$$

where $g$ is the weak coupling constant; $q_1^\mu = p_e^\mu + k'^\mu$ and $q_2^\mu = p_m^\mu - k^\mu$.

It is apparent from Fig. 5.2 as well as Eqs. (5.3)-(5.5), that amplitude ($\mathcal{M}_3$) containing effective vertex $\Gamma_{\rho\sigma\delta}$ is $1/m_W^2$ suppressed compared to the other two contributions $\mathcal{M}_1$ and $\mathcal{M}_2$. Hence, within the SM, the first two Feynman-diagrams in Fig. 5.2 are sufficient to study the process. On the other hand, the third diagram only is sensitive to $\eta_\gamma$. Thus, in order to retain sensitivity to $\eta_\gamma$ in $\Gamma_{\rho\sigma\delta}$, it is necessary and sufficient to keep contributions up to $\mathcal{O}(1/m_W^4)$, in the amplitudes. To achieve this we expand the $W$ boson propagator in the power series of $(q_j^2/m_W^2)$ as:

$$-i\,\mathbb{W}^{\alpha\beta}(q_j) = -i\left[\frac{g^{\alpha\beta} - \left(q_j^\alpha q_j^\beta/m_W^2\right)}{q_j^2 - m_W^2}\right] \approx \frac{i}{m_W^2}\left[g^{\alpha\beta} + \frac{q_j^2}{m_W^2}\left(g^{\alpha\beta} - \frac{q_j^\alpha q_j^\beta}{q_j^2}\right)\right]. \qquad (5.6)$$

The total amplitude can be expressed as $\mathcal{M} = \mathcal{M}_1 + \mathcal{M}_2 + \mathcal{M}_3$ and we calculate differential cross section keeping all the amplitudes up to $\mathcal{O}(1/m_W^4)$.

## 5.2.2 Kinematics

Since the neutrinos $\nu_\mu$ and $\bar{\nu}_e$ cannot be observed we integrate the $\nu_\mu$ and $\bar{\nu}_e$ momenta using the following formulae for phase space integration[2]:

---

[2]First three relations are given in the Ref. [82]. The remaining two can easily derived by writing the general structure of the result and multiplying both sides by $q^\mu$ or $g^{\mu\nu}$.

$$\int d^2\Phi(k, k') = \frac{\pi}{2}, \tag{5.7}$$

$$\int k^\mu \, d^2\Phi(k, k') = \frac{\pi}{4} \, q^\mu, \tag{5.8}$$

$$\int k^\mu k^\nu \, d^2\Phi(k, k') = \frac{\pi}{6} \left[ q^\mu q^\nu - \frac{q^2}{4} g^{\mu\nu} \right], \tag{5.9}$$

$$\int k^\mu k^\nu k^\rho \, d^2\Phi(k, k') = \frac{\pi}{6} \left[ q^\mu q^\nu q^\rho - \frac{q^2}{8} (g^{\mu\nu} q^\rho + g^{\rho\nu} q^\mu + g^{\mu\rho} q^\nu) \right], \tag{5.10}$$

$$\int k^\mu k^\nu k^\rho k^\sigma \, d^2\Phi(k, k') = \frac{\pi}{10} \left[ q^\mu q^\nu q^\rho q^\sigma + \frac{q^4}{48} (g^{\mu\nu} g^{\rho\sigma} + g^{\mu\rho} g^{\nu\sigma} + g^{\mu\sigma} g^{\nu\rho}) \right.$$
$$\left. - \frac{q^2}{8} (g^{\mu\nu} q^\rho q^\sigma + g^{\mu\rho} q^\nu q^\sigma + g^{\mu\sigma} q^\rho q^\nu + g^{\nu\rho} q^\mu q^\sigma + g^{\nu\sigma} q^\rho q^\mu + g^{\rho\sigma} q^\mu q^\nu) \right], \tag{5.11}$$

where $\Phi(k, k')$ and $q$ indicate the two dimensional phase space and invariant momentum for the $\nu_\mu \bar{\nu}_e$ system respectively. Since the decay now looks like a 3-body decay it is meaningful to define effective Mandelstam like variable constructed from the invariant momentum square of $e^- \nu_\mu \bar{\nu}_e$ system as $t$ and that of $\gamma \nu_\mu \bar{\nu}_e$ system as $u$. Hence, $(p_e + q)^2 = t$ and $(p_\gamma + q)^2 = u$. Notice that, $q^2$ is not a constant for our decay. It is, however, much more convenient to define normalized parameters:

$$x_p = \frac{t + u}{2(q^2 + m_\mu^2)}, \qquad y_p = \frac{t - u}{2(q^2 + m_\mu^2)}, \qquad q_p^2 = \frac{q^2}{(q^2 + m_\mu^2)}, \tag{5.12}$$

which can be written in terms of the observable quantities, the photon energy $E_\gamma$, the electron energy $E_e$ and the angle between the electron and photon $\theta$ as follows:

$$x_p = \frac{m_\mu(m_\mu - E_e - E_\gamma)}{2[m_\mu^2 - E_\gamma m_\mu - E_e m_\mu + E_e E_\gamma(1 - \cos\theta)]}, \tag{5.13}$$

$$y_p = \frac{m_\mu(E_e - E_\gamma)}{2[m_\mu^2 - E_\gamma m_\mu - E_e m_\mu + E_e E_\gamma(1 - \cos\theta)]}, \tag{5.14}$$

$$q_p^2 = \frac{m_\mu^2 - 2E_\gamma m_\mu - 2E_e m_\mu + 2E_e E_\gamma(1 - \cos\theta)}{2[m_\mu^2 - E_\gamma m_\mu - E_e m_\mu + E_e E_\gamma(1 - \cos\theta)]}. \tag{5.15}$$

The parameters of interest for the derivation, $x_p$, $y_p$ and $q_p^2$ can easily be inverted in terms of the observables $E_e$, $E_\gamma$ and $\cos\theta$ as:

$$E_e = \frac{m_\mu}{2}\left(\frac{1 - q_p^2 - x_p + y_p}{1 - q_p^2}\right), \tag{5.16}$$

$$E_\gamma = \frac{m_\mu}{2}\left(\frac{1 - q_p^2 - x_p - y_p}{1 - q_p^2}\right), \tag{5.17}$$

$$\cos\theta = \frac{(q_p^2 - x_p)^2 + 2x_p - y_p^2 - 1}{(1 - q_p^2 - x_p)^2 - y_p^2}. \tag{5.18}$$

We notice that replacing $y_p$ by $-y_p$ while keeping $q_p^2$ and $x_p$ unchanged actually results in swapping the energies of photon and electron keeping the angle between them unaltered. This feature will play a very crucial role in defining the observable asymmetry in Sec. 5.3.

We have ignored the electron mass, $m_e$, starting from Eq. (5.12) as it results in significant simplification of analytic expressions. It is of course well-known that neglecting the electron mass results in the persistence of wrong helicity right-handed electron [83, 84] in this decay as a result of inner bremsstrahlung from the electron (see second diagram of Fig. 5.2). The results are in obvious disagreement depending on whether $m_e$ is retained or not. We will therefore very carefully consider the issue of electron mass to justify the neglect of $m_e$ for our limited purpose of extracting $\eta_\gamma$, while acknowledging that $m_e$ should not be ignored in general. In order to retain maximum sensitivity to $\eta_\gamma$ the kinematic domain is chosen to minimize the soft photon and collinear singularity contributions; the effect of $m_e$ is found to be insignificant in the kinematic domain sensitive to $\eta_\gamma$. Our calculations have been verified retaining $m_e$ throughout. Critical expressions including $m_e$ contributions are presented in the section 5.4 for clarity. Expressions for $x_p$ and $y_p$ are modified to accommodate effects of $m_e$, while retaining an *apparent exchange symmetry* between $E_\gamma$ and $E_e$ under the newly defined variables $x_n$ and $y_n$ in Eq. (5.34).

In terms of these new normalized variables, the phase space for this process is bounded by three surfaces: $q_p^2 = 0$, $x_p = 1/2$ and $(q_p^4 - q_p^2 + x_p^2 - y_p^2) = 0$. It is easily seen from Eq. (5.18), the plane $x_p = 1/2$ corresponds to $\theta = 0°$ and the curved surface $(q_p^4 - q_p^2 + x_p^2 - y_p^2) = 0$ signifies $\theta = 180°$. The physical region in $q_p^2$, $x_p$ and $y_p$ parameter space is given by:

$$q_p \sqrt{1 - q_p^2} \leq x_p \leq \frac{1}{2}; \quad |y_p| \leq (\frac{1}{2} - q_p^2); \quad 0 \leq q_p^2 \leq \frac{1}{2}; \quad (q_p^4 - q_p^2 + x_p^2 - y_p^2) \geq 0. \quad (5.19)$$

The whole phase space region is depicted in the Fig. 5.3 . The red triangle at right side signifies $x_p = 1/2$ plane, the red triangle at base indicates $q_p^2 = 0$ and the intersection curve of $x_p - q_p^2$ plane with the curved surface $C$ (that indicates $\cos \theta = -1$ or $(q_p^4 - q_p^2 + x_p^2 - y_p^2) = 0$) is shown as the black curve.
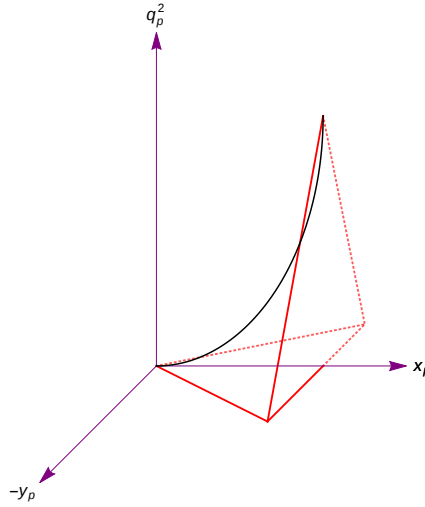


Figure 5.3: A pictorial view for the allowed phase space region.

## 5.3    Observable and asymmetry

We consider only the normalized differential decay rate $\overline{\Gamma}(x_p, y_p, q_p^2)$ obtained after integrating the $\nu_\mu$ and $\bar{\nu}_e$ momenta which is defined as:

$$\overline{\Gamma}(x_p, y_p, q_p^2) = \frac{1}{\Gamma_\mu} \cdot \frac{d^3\Gamma}{dq_p^2 \, dx_p \, dy_p}, \quad (5.20)$$

where, $\Gamma_\mu$ is the total decay width of muon.

Form Eq. (5.12) and Eq. (5.19), it is clear that both $q_p^2$ and $x_p$ are positive valued functions whereas $y_p$ can have a positive value or a negative value and the physical region allows $y_p$ to have a range symmetric about $y_p = 0$. So, if $(x_p, y_p, q_p^2)$ be a point inside physical

region, $(x_p, -y_p, q_p^2)$ will also lie inside the allowed region. This motivates us to investigate the properties of odd and even part of $\overline{\Gamma}(x_p, y_p, q_p^2)$ under the variable $y_p$.

The 'odd' and 'even' part $\overline{\Gamma}_o(x_p, y_p, q_p^2)$ and $\overline{\Gamma}_e(x_p, y_p, q_p^2)$, respectively, of the normalized differential decay rate (Eq. (5.20)) with respect to $y_p$ are defined as:

$$\overline{\Gamma}_o(x_p, y_p, q_p^2) = \frac{1}{2}\left[\overline{\Gamma}(x_p, y_p, q_p^2) - \overline{\Gamma}(x_p, -y_p, q_p^2)\right] \approx F_o(x_p, y_p, q_p^2) + \eta_\gamma\, G_o(x_p, y_p, q_p^2), \quad (5.21)$$

$$\overline{\Gamma}_e(x_p, y_p, q_p^2) = \frac{1}{2}\left[\overline{\Gamma}(x_p, y_p, q_p^2) + \overline{\Gamma}(x_p, -y_p, q_p^2)\right] \approx F_e(x_p, y_p, q_p^2) + \eta_\gamma\, G_e(x_p, y_p, q_p^2), \quad (5.22)$$

where the small $\eta_\gamma^2$ terms are ignored.

As we have obtained $\overline{\Gamma}(x_p, y_p, q_p^2)$ by integrating a positive valued function $|\mathcal{M}|^2$, it is obvious that both $\overline{\Gamma}(x_p, y_p, q_p^2)$ and $\overline{\Gamma}(x_p, -y_p, q_p^2)$ will be positive. Hence, $\overline{\Gamma}_e(x_p, y_p, q_p^2)$, which is proportional to the sum of $\overline{\Gamma}(x_p, y_p, q_p^2)$ and $\overline{\Gamma}(x_p, -y_p, q_p^2)$, as well as $F_e(x_p, y_p, q_p^2)$, which is $\eta_\gamma \rightarrow 0$ limit of $\overline{\Gamma}_e(x_p, y_p, q_p^2)$, will always be greater than or equal to zero inside the physical region. On the other hand, $\overline{\Gamma}_o(x_p, y_p, q_p^2)$, which is proportional to subtraction of two positive quantities, as well as $F_o(x_p, y_p, q_p^2)$, which is $\eta_\gamma \rightarrow 0$ limit of $\overline{\Gamma}_o(x_p, y_p, q_p^2)$, could be positive, zero or negative inside the allowed region.

We now define an observable as: $\quad \mathcal{R}_\eta(x_p, y_p, q_p^2) = \dfrac{\overline{\Gamma}_o}{\overline{\Gamma}_e} \approx \dfrac{F_o}{F_e}\left[1 + \eta_\gamma\left(\dfrac{G_o}{F_o} - \dfrac{G_e}{F_e}\right)\right], \quad (5.23)$

and the asymmetry in $\mathcal{R}_\eta$ as: $\quad \mathcal{A}_\eta(x_p, y_p, q_p^2) = \left(\dfrac{\mathcal{R}_\eta}{\mathcal{R}_{\text{SM}}} - 1\right) \approx \eta_\gamma\left(\dfrac{G_o}{F_o} - \dfrac{G_e}{F_e}\right), \quad (5.24)$

where, $\quad \mathcal{R}_{\text{SM}} = \left.\dfrac{\overline{\Gamma}_o}{\overline{\Gamma}_e}\right|_{\eta_\gamma=0} = \dfrac{F_o}{F_e}.$

Since, $F_o$ and $G_o$ are the zeroth order and first order terms respectively in the expansion of the odd part of $\overline{\Gamma}(x_p, y_p, q_p^2)$ with respect to $\eta_\gamma$ (see Eq. (5.21)), both of them are expected to be proportional to odd powers of $y_p$, rendering the ratio $(G_o/F_o)$ to be finite at $y_p = 0$.

We will now show that $F_o$ i.e. the odd part of SM, has a zero for this mode for all $q_p^2$. For simplicity, to describe the situation mathematically, we consider only the dominant contributions arising from the first and second Feynman diagrams in Fig. 5.2. Retaining

only relevant terms upto $\mathcal{O}(1/m_W^4)$, we can write:

$$F_o \propto y_p\, h(x_p, y_p, q_p^2)\, f(x_p, y_p, q_p^2) \tag{5.25}$$

where,
$$h = \left[ \frac{1 + q_p^2}{(1 - q_p^2)^5(1 - 2x_p)\{(1 - q_p^2 - x_p)^2 - y_p^2\}^2} \right], \tag{5.26}$$

$$
\begin{aligned}
f = \Big[ & 7\,q_p^8 - 4(4 - x_p)\,q_p^6 + (11 - 4x_p + 6x_p^2 - 6y_p^2)\,q_p^4 - 2\,(1 - x_p + 8x_p^2 - 6x_p^3 \\
& - 4y_p^2 + 2x_p y_p^2)\,q_p^2 + 3x_p^4 - 12x_p^3 + x_p^2(11 - 2y_p^2) - x_p(2 - 4y_p^2) - y_p^2(3 + y_p^2) \Big].
\end{aligned}
\tag{5.27}
$$

As can be seen from the inequalities in Eq. (5.19), $h(x_p, y_p, q_p^2)$ is always positive inside the physical region and it contains all the divergent terms in $F_o$. Hence, the deciding factor on the sign of $F_o$ is only $f(x_p, y_p, q_p^2)$. Now, on $x_p = 1/2$ surface, we have:

$$f\left(\frac{1}{2}, y_p, q_p^2\right) = \frac{7}{16}(1 - 2q_p^2)^4 - \frac{3}{2}(1 - 2q_p^2)^2\, y_p^2 - y_p^4, \tag{5.28}$$

which after using the upper limit of $|y_p|$ from Eq. (5.19), implies that:

$$f\left(\frac{1}{2}, y_p, q_p^2\right) \geq 0 \quad \Longrightarrow \quad F_o\left(\frac{1}{2}, |y_p|, q_p^2\right) \geq 0 \quad \text{and} \quad F_o\left(\frac{1}{2}, -|y_p|, q_p^2\right) \leq 0. \tag{5.29}$$

Likewise, for any point on the curved surface $(q_p^4 - q_p^2 + x_p^2 - y_p^2) = 0$, denoted as $C$, we have $y_p^2 = (q_p^4 - q_p^2 + x_p^2)$ and hence,

$$f(x_p, y_p, q_p^2)\Big|_C = (1 - q_p^2)(1 - 2x_p)^2\,(q_p^2 - 2x_p). \tag{5.30}$$

On using the limits of $x_p$ and $q_p^2$ from Eq. (5.19), it can easily be shown that:

$$f(x_p, y_p, q_p^2)\Big|_C \leq 0 \quad \Longrightarrow \quad F_o(x_p, |y_p|, q_p^2)\Big|_C \leq 0 \quad \text{and} \quad F_o(x_p, -|y_p|, q_p^2)\Big|_C \geq 0. \tag{5.31}$$

We have concluded that $f(x_p, y_p, q_p^2) < 0$ along the curved surface $C$ and $f(x_p, y_p, q_p^2) > 0$ at the other boundary surface $x_p = 1/2$. It is obvious therefore that there must be at least one surface within the allowed phase space region where $f(x_p, y_p, q_p^2) = 0$. In the first plot

of Fig. 5.4, the blue region signifies $f(x_p, y_p, q_p^2) < 0$ and the brown region symbolizes $f(x_p, y_p, q_p^2) > 0$ whereas the black curve indicates $f(x_p, y_p, q_p^2) = 0$. In the second plot of Fig. 5.4, the yellow region signifies $F_o(x_p, y_p, q_p^2) < 0$ and the green region symbolizes $F_o(x_p, y_p, q_p^2) > 0$ while the red curve indicates $F_o(x_p, y_p, q_p^2) = 0$.
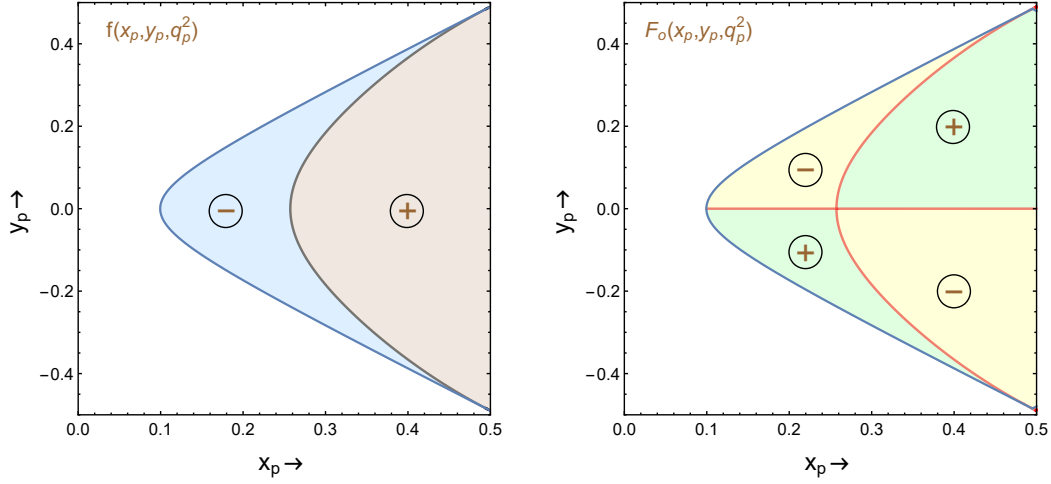


Figure 5.4: The variations of functions $f(x_p, y_p, q_p^2)$ and $F_o(x_p, y_p, q_p^2)$ are shown in $x_p - y_p$ plane in left and right panel, respectively, where $q_p^2 = 0.01$. The blue line in both the panels indicates one boundary of phase space with $\cos\theta = -1$ or $(q_p^4 - q_p^2 + x_p^2 - y_p^2) = 0$. In the left panel, the blue region signifies negative valued $f(x_p, y_p, q_p^2)$, the brown region symbolizes positive valued $f(x_p, y_p, q_p^2)$ and the black curve indicates $f(x_p, y_p, q_p^2) = 0$. In the right panel, the yellow region signifies negative valued $F_o(x_p, y_p, q_p^2)$, the green region symbolizes positive valued $F_o(x_p, y_p, q_p^2)$ and the red curve indicates $F_o(x_p, y_p, q_p^2) = 0$.

The odd ($\overline{\Gamma}_o$) and even ($\overline{\Gamma}_e$) parts of differential rate as well as the four functions $F_o$, $F_e$, $G_o$, $G_e$ contain soft collinear divergences arising due to $E_\gamma = 0$ or $\cos\theta = 1$ and divergence due to vanishing $E_e$ if $m_e$ is ignored. It is obvious form Eq. (5.17) that soft photon dominate in the region corresponding to $(x_p + y_p) \approx (1 - q_p^2)$, which implies $(x_p + y_p)$ is close to its maximum value. Hence, events with small photon energy lie at the top corner in Fig. 5.4 where the blue curve meets $x_p = 1/2$ line. Similarly, one can see from Eq. (5.16) that small electron energy implies $(x_p - y_p) \approx (1 - q_p^2)$ and these events lie at the bottom corner in Fig. 5.4 where the blue curve meets $x_p = 1/2$ line. For any value of $q_p^2$, the collinear divergence occurs along $x_p = 1/2$ line as can easily be seen from Eq. (5.18). These singularities are evident from Eq. (5.26) and occur in each of $\overline{\Gamma}$, $\overline{\Gamma}_o$, $\overline{\Gamma}_e$ as well as the four functions $F_o$, $F_e$, $G_o$, $G_e$. It is only in these regions that an expansion in powers of $m_e/m_\mu$

is not valid; the electron mass needs to be retained and ignoring it alters the differential decay rates. To deal with the $x_p = 1/2$ collinear singularity, we choose an appropriate cut on $x_p$ which is also necessitated by experimental resolution. It can be seen from Eq. (5.24), however, that with in SM, $\mathcal{A}_\eta$ is finite and zero, even in the regions plagued by collinear soft photon singularities and the ones that arise due to neglect of $m_e$. Note, that in $\mathcal{A}_\eta$ the $h$-function in Eq. (5.26) carrying the singular denominator cancels. The zero observed in $F_o$ and the consequent singularity in the asymmetry $\mathcal{A}_\eta$ has nothing to do with the well know collinear soft photon and $m_e \rightarrow 0$ singularities. The zero observed in $F_o$ is genuine and looks like an apparent exchange symmetry between $E_e$ and $E_\gamma$ only for the appropriately chosen parameters, $x_p$ and $y_p$ (or $x_n$ and $y_n$ defined in Eq. (5.34)) with $m_e$ retained.

We have explicitly demonstrated that there exists a surface (besides $y_p = 0$ plane) where $F_o(x_p, y_p, q_p^2) = 0$; we refer to this surface corresponding to the *'new type of zero'* as "null-surface". This means that at each point on this surface the differential decay rate $\overline{\Gamma}(x_p, y_p, q_p^2)$ remains unaltered if we interchange the energies of photon and electron. Hence, $\mathcal{A}_\eta(x_p, y_p, q_p^2)$ diverges on null-surface for any non-zero value of $\eta_\gamma$ and becomes zero everywhere in the phase space for $\eta_\gamma$ being zero. The null-surface divides the phase space into two regions, one where $\mathcal{A}_\eta$ is positive and the other where $\mathcal{A}_\eta$ is negative. For $\eta_\gamma > 0$, $\mathcal{A}_\eta < 0$ for $x_p$ values smaller than the values indicated by the null-surface, whereas, $\mathcal{A}_\eta > 0$ for $x_p$ values larger than the values indicated by the null-surface. However, if $\eta_\gamma < 0$, an opposite behaviour in the signs of $\mathcal{A}_\eta$ is indicated. This feature can be used to determine the sign of $\eta_\gamma$. To measure the value of $\eta_\gamma$ experimentally, one must average $\mathcal{A}_\eta$ over specified regions of phase space where it could be positive or negative. Such averages are necessitated by the experimental resolutions for $q_p^2$, $x_p$ and $y_p$ and will in general reduce the asymmetry. Hence, it is convenient to use $|\mathcal{A}_\eta|$ as the asymmetry.

## 5.4 Retaining mass of electron

In presence of electron mass $m_e$, we have $s + t + u = q^2 + m_\mu^2 + m_e^2$ where the Mandelstam variables are defined as: $(p_e + p_\gamma)^2 = s$, $(p_e + q)^2 = t$ and $(p_\gamma + q)^2 = u$. The physical region is determined by the following inequalities [85]:

$$m_e^2 \le s \le (m_\mu - \sqrt{q^2})^2, \quad q^2 \le u \le (m_\mu - m_e)^2, \quad (m_e + \sqrt{q^2})^2 \le t \le m_\mu^2,$$

$$G[s, u, m_\mu^2, 0, m_e^2, q^2] \le 0, \tag{5.32}$$

where, 
$$G[x, y, z, u, v, w] = -\frac{1}{2}\begin{vmatrix} 0 & 1 & 1 & 1 & 1 \\ 1 & 0 & v & x & z \\ 1 & v & 0 & u & y \\ 1 & x & u & 0 & w \\ 1 & z & y & w & 0 \end{vmatrix}. \tag{5.33}$$

We define variables $x_n, y_n$ and $q_n^2$, which reduce to $x_p, y_p$ and $q_p^2$ at $m_e \to 0$ limit, in the following way:

$$x_n = \frac{t + u}{2(q^2 + m_\mu^2 + m_e^2)}, \quad y_n = \frac{t - u + m_e^2}{2(q^2 + m_\mu^2 + m_e^2)}, \quad q_n^2 = \frac{q^2}{(q^2 + m_\mu^2 + m_e^2)}. \tag{5.34}$$

The energy of electron and photon are obtained from the above definitions as:

$$E_e = \frac{(2m_\mu^2 + m_e^2)(1 - q_n^2 - x_n + y_n) - m_e^2(x_n - y_n)}{4m_\mu(1 - q_n^2)}, \tag{5.35}$$

$$E_\gamma = \frac{(2m_\mu^2 + m_e^2)(1 - q_n^2 - x_n - y_n) - m_e^2(x_n + y_n)}{4m_\mu(1 - q_n^2)}. \tag{5.36}$$

Under the replacement $y_n \to -y_n$ electron and photon energies get exchanged and one separate the odd and even parts differential decay rate as follows:

$$\overline{\Gamma}_o(x_n, y_n, q_n^2) = \frac{1}{2}\left[\overline{\Gamma}(x_n, y_n, q_n^2) - \overline{\Gamma}(x_n, -y_n, q_n^2)\right], \tag{5.37}$$

$$\overline{\Gamma}_e\left(x_n, y_n, q_n^2\right) = \frac{1}{2}\left[\overline{\Gamma}(x_n, y_n, q_n^2) + \overline{\Gamma}(x_n, -y_n, q_n^2)\right]. \tag{5.38}$$

The *h*-function in Eq. (5.26) containing singular denominator, now, becomes:

$$h \propto \frac{1}{E_e^2\, E_\gamma^2\, (m_\mu^2(1 - 2x_n) + m_e^2(q_n^2 - 2x_n))}. \tag{5.39}$$

In the region around $F_o = 0$, which are denoted by red dots in Fig. 5.5, a legitimate expansion in powers of $(m_e/m_\mu)$ for the expressions of $\overline{\Gamma}_o$ and $\overline{\Gamma}_e$ can be carried out in the following way:

$$\overline{\Gamma}_o \approx \left(F_o + (m_e/m_\mu)^2\, \delta F_o\right) + \eta_\gamma\left(G_o + (m_e/m_\mu)^2\, \delta G_o\right), \tag{5.40}$$

$$\overline{\Gamma}_e \approx \left(F_e + (m_e/m_\mu)^2\, \delta F_e\right) + \eta_\gamma\left(G_e + (m_e/m_\mu)^2\, \delta G_e\right), \tag{5.41}$$

where the small $\eta_\gamma^2$ terms are ignored. Here, $\delta F_o$, $\delta G_o$, $\delta F_e$ and $\delta G_e$ are the leading order correction terms due to non zero electron mass. The observable $\mathcal{R}_\eta$ gets modified as:

$$\begin{aligned}
\mathcal{R}_\eta(x_n, y_n, q_n^2) &= \frac{\overline{\Gamma}_o(x_n, y_n, q_n^2)}{\overline{\Gamma}_e(x_n, y_n, q_n^2)} \\
&\approx \left(\frac{F_o + (m_e/m_\mu)^2\, \delta F_o}{F_e + (m_e/m_\mu)^2\, \delta F_e}\right) \cdot \left[1 + \eta_\gamma\left(\frac{G_o + (m_e/m_\mu)^2\, \delta G_o}{F_o + (m_e/m_\mu)^2\, \delta F_o} - \frac{G_e + (m_e/m_\mu)^2\, \delta G_e}{F_e + (m_e/m_\mu)^2\, \delta F_e}\right)\right].
\end{aligned} \tag{5.42}$$

Hence, the asymmetry, $\mathcal{A}_\eta(x_p, y_p, q_p^2)$, in $\mathcal{R}_\eta$ becomes,

$$\begin{aligned}
\mathcal{A}_\eta(x_n, y_n, q_n^2) &= \left(\frac{\mathcal{R}_\eta}{\mathcal{R}_{\text{SM}}} - 1\right) \approx \eta_\gamma\left(\frac{G_o + (m_e/m_\mu)^2\, \delta G_o}{F_o + (m_e/m_\mu)^2\, \delta F_o} - \frac{G_e + (m_e/m_\mu)^2\, \delta G_e}{F_e + (m_e/m_\mu)^2\, \delta F_e}\right) \\
&\approx \eta_\gamma\left[\left(\frac{G_o}{F_o} - \frac{G_e}{F_e}\right) + \left(\frac{m_e}{m_\mu}\right)^2\left(\frac{G_e\, \delta F_e}{F_e^2} - \frac{G_o\, \delta F_o}{F_o^2} + \frac{\delta G_o}{F_o} - \frac{\delta G_e}{F_e}\right)\right]
\end{aligned} \tag{5.43}$$

where, $\mathcal{R}_{\text{SM}} = \left.\frac{\overline{\Gamma}_o}{\overline{\Gamma}_e}\right|_{\eta_\gamma=0} = \left(\frac{F_o + (m_e/m_\mu)^2\, \delta F_o}{F_e + (m_e/m_\mu)^2\, \delta F_e}\right).$

Note that the above expansion in $\mathcal{O}(m_e/m_\mu)$ fails in the region where collinear or soft photon divergences occurs.

## 5.5 Simulation and analysis

In order to study the sensitivity of muon radiative decay mode we need to include the resolutions for energy of photon, energy of electron and the angle between them. We take them to be 2%, 0.5% and 10 Milli-radian, respectively [11]. As can be seen from Eq. (5.16)-(5.18), the resolutions for $x_p$, $y_p$ and $q_p^2$ will also vary at different point in phase space due to the functional form of these parameters. We begin by evaluating the resolutions for $x_p$, $y_p$ and $q_p^2$ for the entire allowed phase space. We find that the resolutions for $x_p$ $y_p$ and $q_p^2$ are always less than 0.01, 0.02 and 0.02 respectively. For simplicity, in our simulation, we take the worst possible scenario and assume constant resolutions for each of $x_p$, $y_p$ and $q_p^2$, corresponding to their largest value of 0.01, 0.02 and 0.02 respectively throughout the entire allowed phase space, which allows us to choose equal size bins. Hence, the phase space region $0 \leq q_p^2 \leq 1/2$, $0 \leq x_p \leq 1/2$, $-1/2 \leq y_p \leq 1/2$ is divided into 24 bins in $q_p^2$ and 50 bins in both $x_p$ and $y_p$ – all equal in size. Among these bins, only 6378 number of bins lie inside the physical phase space region. Now, assuming $\eta_\gamma = 0.01$, we estimate the systematic and statistical error for $|\mathcal{A}_\eta|$ in each of these bins.

To find the systematic error in $|\mathcal{A}_\eta|$ for a particular $i$-th bin, we evaluate it at $62, 500$ equally spaced points in that bin to estimate $|\mathcal{A}_\eta|_i^j$ where $j$ is the index of a point inside the $i$-th bin. However, for the bins near to the boundary of phase space, all of these points will not be inside the physical region and hence, we denote the number of physical points inside $i$-th bin as $n_i$. We now, calculate the average of $|\mathcal{A}_\eta|_i^j$ inside a bin

$$\langle |\mathcal{A}_\eta|_i \rangle = \frac{1}{n_i} \sum_j |\mathcal{A}_\eta|_i^j,$$

and take this as the asymmetry of that bin. Then we take the systematic error as the average deviation of $|\mathcal{A}_\eta|_i^j$, i.e.

$$\sigma_i^{\text{sys}} = \frac{1}{n_i} \sum_j \left| \langle |\mathcal{A}_\eta|_i \rangle - |\mathcal{A}_\eta|_i^j \right|.$$

Ideally the errors can and should have been calculated using a standard Monte-Carlo

technique with more number of sample points. However, The approach followed in this chapter is to express the integral as a Riemann sum[3] only for simplicity.

The statistical error for $|\mathcal{A}_\eta|$ in each bin is also estimated by averaging it at the same $62, 500$ equally spaced points. Note that, while $\mathcal{A}_\eta$ is divergent on the null-surface the average value of $|\mathcal{A}_\eta|$ for the $i$-th bin, i.e. $\langle|\mathcal{A}_\eta|_i\rangle$, estimated from Monte Carlo studies is never larger than $10^{-6}$ for any bin. Hence,

$$\sigma_i^{\text{sta}} = \sqrt{\frac{1 - \langle|\mathcal{A}_\eta|_i\rangle^2}{N_i}} \approx \frac{1}{\sqrt{(N_{SM})_i}},$$

where $i$ is the index of the bins and $N_i$ represents the number of events inside $i$-th bin which is almost the same as $(N_{SM})_i$ the number of SM events for the $i$-th bin. We have also assumed that both $\mathcal{A}_\eta$ and the effects of $\eta_\gamma$ on $N_i$ are small and can be ignored. If this were not the case $N_i$ would itself be sensitive to $\eta_\gamma$, contrary to our simulation results. Hence, we simply take the statistical error for all practical purposes to be that in the case of SM events. The number of events in each bin is calculated by taking total number of muons to be $10^{19}$. To avoid the singularities in the number of SM events for the bins near $x_p = 1/2$ plane, we ignore the bins with $0.49 \leq x_p \leq 0.5$.

The total error in $|\mathcal{A}_\eta|$ for any particular bin is then given by $\delta|\mathcal{A}_\eta|_i = \sqrt{(\sigma_i^{\text{sta}})^2 + (\sigma_i^{\text{sys}})^2}$. This error in $|\mathcal{A}_\eta|$ will affect the measurement of $\eta_\gamma$. Using Eq. (5.24), we observe that the error in the measurement of $\eta_\gamma$ in each bin as

$$\left|\frac{\delta\eta_\gamma}{\eta_\gamma}\right|_i = \frac{\delta|\mathcal{A}_\eta|_i}{|\mathcal{A}_\eta|_i} \tag{5.44}$$

where, $|\mathcal{A}_\eta|_i \equiv \langle|\mathcal{A}_\eta|_i\rangle$ and we take the theoretical function $\left(G_o/F_o - G_e/F_e\right)$ to be free from experimental uncertainties. It is obvious from Eq. (5.44), that the highest sensitivity is achieved in bins close to the null-surface where $|\mathcal{A}_\eta|_i$ is the largest. Hence, to determine $\eta_\gamma$,

---

[3]Definite integral as Riemann sum: $\displaystyle\int_a^b f(x)dx = \lim_{\Delta x \to 0} \sum_{j=1}^{(b-a)/\Delta x} \Delta x \, f(a + j\Delta x)$

we consider the region around the null-surface only by applying a cut $\left(\delta|\mathcal{A}_\eta|_i\,/\,|\mathcal{A}_\eta|_i\right) \leq 10$.
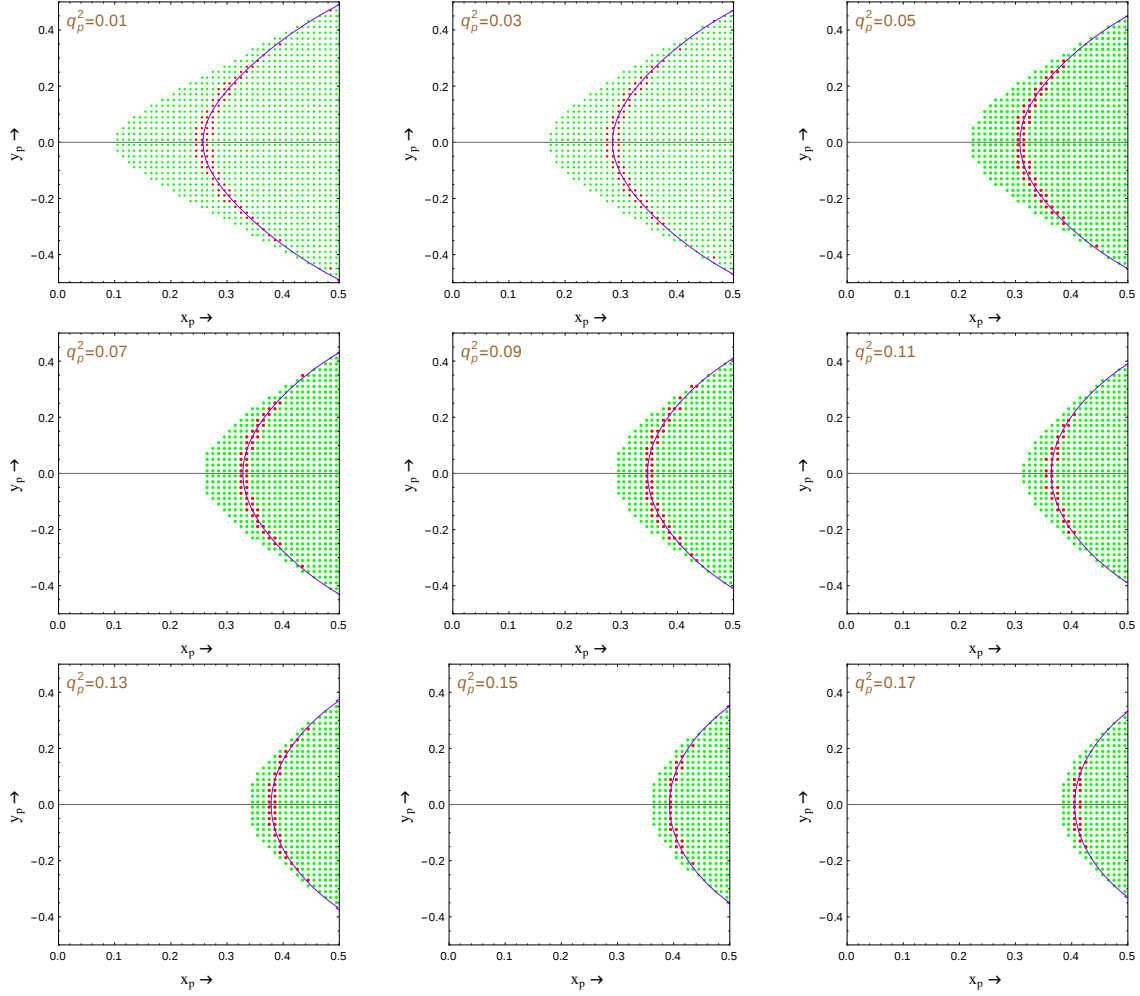


Figure 5.5: The variation of $F_o(x_p, y_p, q_p^2)$ for different $q_p^2$ in the $x_p$-$y_p$ plane. Each green dot represents a bin according to experimental resolution of photon energy, electron energy and angle between them. The red dots stand for the bins having $\left(\delta|\mathcal{A}_\eta|_i\,/\,|\mathcal{A}_\eta|_i\right) \leq 10$ in that bin. The purple curve signifies $F_o(x_p, y_p, q_p^2) = 0$ in different $q_p^2$ plane. Our numerical analysis includes the bins corresponding to the red dots only. This results in an optimal sensitivity to $\eta_\gamma$.

In Fig. 5.5, we depict the bins, which satisfy the above cut, with red dots for different $q_p^2$ values, whereas, the green dots signify all the other bins inside the physical region; the purple curve indicates the null-surface where $F_o = 0$ for the corresponding $q_p^2$ value. Including only the bins, which satisfy the above cut, for a simulated value of $\eta_\gamma = 0.01$ (at one loop in SM, $|\eta_\gamma| \lesssim 0.015$), we estimate an error of $\delta\eta_\gamma = 2.6 \times 10^{-3}$, implying a $3.9\sigma$ significance for the measurement. A total of $10^{19}$ muons are aimed for in the long term future. The next-round of experiments are aiming at $10^{18}$ muons /year. This reduces

the sensitivity from $3.9\sigma$ to $1.4\sigma$. To appreciate the advantage of radiative muon decays in measuring $WW\gamma$ vertex one needs to note that the current global average of $\kappa_\gamma$ differs from unity only by $0.4\sigma$. We note that the significance of the measured value of $\eta_\gamma$ may in principle be improved by optimizing the chosen cut and binning procedure. However, we refrain from such intricacies as our approach is merely to present a proof of principle.

We have shown that the sensitivity to $\eta_\gamma$ arises due to the vanishing of the odd differential decay rate in the standard model denoted by $F_o$. The observed singularity in $\mathcal{A}_\eta$ is unrelated to soft photon and collinear singularities or the singularity arising due to neglect of $m_e$ in calculations. The most sensitive region to measure $\eta_\gamma$ is where $\mathcal{A}_\eta$ is large and obviously lies along the zero of $F_o$ as indicated by Eq. (5.24). The region around $F_o = 0$ for which $\left(\delta|\mathcal{A}_\eta|_i / |\mathcal{A}_\eta|_i\right) \leq 10$, is where a legitimate expansion in powers of $m_e/m_\mu$ can be carried out and is distinct from the singular regions in the differential decay rates where such an expansion cannot be done. However, in order to verify the accuracy of sensitivity achievable in $\eta_\gamma$ measurement the calculations have been redone by numerically retaining $m_e$. We find that for the bins represented by red dots in Fig. 5.5 the maximum correction in $\eta_\gamma$ is $\mathcal{O}(10^{-4})$, which is an order of magnitude smaller than the error in it, $\delta\eta_\gamma = 2.6 \times 10^{-3}$.

Finally, we discuss possible sources of inaccuracies in our estimation of uncertainty. Higher order electroweak corrections to the process considered will modify the decay rate and alter $F_o$. While higher order electroweak corrections have not been included in our analysis they have been worked out in detail [86–89]. However, this is unlikely to affect our analysis technique as we have selected bins to be included in estimating $\eta_\gamma$ purely based on the criterion $\left(\delta|\mathcal{A}_\eta|_i / |\mathcal{A}_\eta|_i\right) \leq 10$ and not on the location and validity of the null-surface. A possible source of uncertainty that we have ignored in our analysis is the assumption that the muon decays at rest or with known four-momenta. While facilities that produce large numbers of muons are designed to bring the muon to rest, a fraction of them may decay with a finite but unknown 4-momenta, rendering the exact measurement of $q_p^2$ inaccurate. This effect can in-principle be considered by including additional systematic errors in $q_p^2$.

## 5.6  Summary

In order to probe lepton flavour violating process $\mu \rightarrow e\gamma$, facilities that produce large numbers of muons are being designed. We show that radiative muon decay $\mu \rightarrow e\gamma\nu_\mu\bar{\nu}_e$ is a promising mode to probe loop level corrections in the SM to the **C** and **P** conserving dimension four $WW\gamma$ vertex with good accuracy. The process has two missing neutrinos in the final state and on integrating their momenta the partial differential decay rate removes the well known radiation-amplitude-zero. We show, however, that the normalized differential decay rate, odd under the exchange of photon and electron energies, does have a zero in the case of standard model (SM). This *new type of zero* had hitherto not been studied in literature. A suitably constructed asymmetry using this fact enables a sensitive probe for the $WW\gamma$ vertex beyond the SM. The large number of muons produced keeps the statistical error in control for a tiny part of the physical phase space, enabling us to measure $\eta_\gamma = 0.01$ with $3.9\sigma$ significance.

CONCLUSION

> ❝
> *To understand the actual world as it is, not as we should wish it to be, is the beginning of wisdom.*
>
> — **Bertrand Russell**

In spite of various meticulous aspects and multiple precise predictions, there are enough compelling evidences projecting the incompleteness of SM. This obligates us to extend our theory beyond the realm of SM such that all natural phenomena lie under the same roof. However, the absence of any conspicuous hint from collider experiments about the existence of new physics particles has perplexed the situation by providing no transparent direction for the augmentation of the theory. In this scenario, precise measurement of various theoretical parameters that are uniquely predicted in SM is indispensable. Any deviation observed from their predictions in SM will act as indirect evidence for the existence of BSM physics. New measurement techniques along with advancements in experimental methods are required in this regard. In this thesis we have investigated new techniques to measure two different classes of BSM parameters.

First, we focus on measuring **T** and **CPT** violating parameters in $B^0 - \bar{B}^0$ mixing through

time dependent indirect **CP** asymmetry. **CPT** invariance is a very important notion of QFT due to its affinity to Lorentz symmetry. Though all the experimental data to date are compatible with **CPT** conservation, improvement in statistics is expected in forthcoming years and hence we should explore this possibility too. In this context, we establish that departure of mixing parameter $\theta$ from value $\pi/2$ indicates **CPT** whereas non-vanishing imaginary part of other mixing parameter $\phi$ signifies braking of **T** symmetry. We expand the time dependent indirect **CP** asymmetry assuming that breaking of **T** and **CPT** symmetry in $B^0 - \bar{B}^0$ mixing, if it exists at all, must be very small. Higher harmonics in $(\Delta Mt)$ and a constant piece emanate from the expansion of time dependent **CP** asymmetry along with usual $\cos(\Delta Mt)$ and $\sin(\Delta Mt)$ pieces. All the theoretical parameters like direct **CP** asymmetry ($C$), effective **CP** violating phase ($\varphi$), and **T** and **CPT** violating parameters ($\epsilon_{1,2,3}$) can be measured using the coefficients of these harmonics. We notice that the presence of those unconventional terms in the expansion confirms the existence of **T** or **CPT** violation in mixing. We show that it is also possible to measure all the theoretical parameters by fitting the differential decay rates for mode and conjugate mode separately instead of constructing time dependent **CP** asymmetry. In our analysis, penguin pollution and the width difference between the light and heavy states are not neglected; it also does not require $B^0\bar{B}^0$ entangled states. Though we have performed this analysis for $B^0_d$ only, it is equally applicable to $B^0_s$ too with some minor modifications.

Next, we have proposed a new method to probe **C** and **P** conserving dimension four $WW\gamma$ vertex with higher accuracy using radiative muon decay. The associated coupling constant is very important in determining the electromagnetic properties of $W$ boson. However, it has not been measured so far with a good accuracy to probe at least one loop correction to it within the framework of SM. Though our proposal in this regard looks non-viable at first glimpse due to $1/m_W^2$ suppression of our desired amplitude than the leading one, large number of muons produced at experiments to probe lepton flavour violating processes like $\mu \to e\gamma$ can materialize this possibility. Differential decay rate neither shows enough sensitivity to probe the vertex, nor it involves any zeros of radiation amplitude inside the

allowed phase space. Nevertheless, we establish the appearance of a new type of zero inside the physical region in the odd part of normalised differential decay rate under the exchange of electron and photon energies within the framework of SM. We also show that a suitably constructed asymmetry based on this fact can enable us a sensitive probe for $WW\gamma$ vertex beyond SM. The null-surface divides the phase space into two separate regions depending on the sign of function $f_o$. On this surface our proposed asymmetry diverges, however, this divergence has nothing to do with the usual infinities coming from soft photon or vanishing electron mass or collinearity of photon and electron since all of those events occur on $x_p = {}^1\!/_2$ plane. On the other hand, the error in the asymmetry for the region surrounding null-surface remains in control. We have shown that by using a suitable cut on the relative error in the asymmetry, one can measure $\eta_\gamma = 0.01$ with $3.9\sigma$ significance which is far better than the current global average of $\kappa_\gamma$ differing from unity with only $0.4\sigma$ significance. Repeating the whole analysis keeping non-vanishing electron mass does not alter this result significantly.

Let me now discuss the prospect of these techniques. The method used in our first project can be applied to other neutral meson mixing to find the signals of **T** and **CPT** violations there. It is also a good idea to check with the modes where neutral mesons decay to two vectors.Large number of observables, involved in those modes, can help in finding other kinds of new physics effects along with contribution from **T** and **CPT** violations. Talking about the method of our second project, it would be very interesting to investigate the null-surface in other radiative decay modes. Similar strategy can also be taken for $e^+e^-$ colliders involving two particles in the final state associated with a photon. It is also intriguing to inspect the scope of this procedure for the modes involving more number of particles or different massive particles in the final states.

# BIBLIOGRAPHY

BIBLIOGRAPHY

[1] *"CPT violation implies violation of Lorentz invariance"*, O. W. Greenberg, *Phys. Rev. Lett. 89 (2002) 231602*.

[2] *"Disentangling violations of CPT from other new physics effects"*, L. Lavoura and J. P. Silva, *Phys. Rev. D 60 (1999) 056003*.

[3] Collaborations: COMET, MEG, Mu2e.

[4] *"Magnetic Moment of Weak Bosons Produced in $pp$ and $p\bar{p}$ collisions"*, K. O. Mikaelian, M. A. Samuel and D. Sahdev, *Phys. Rev. Lett. 43, 746 (1979)*.

[5] *Particle Physics and Introduction to Field Theory, Contemporary Concepts in Physics, volume 1*, (Harwood Academic, 1st edition, 1981), T.D. Lee

[6] *"Search for time-dependent CPT violation in hadronic and semileptonic B decays"*, T. Higuchi, et al., *Phys. Rev. D 85 (2012) 071105*; *"Study of CP asymmetry in $B^0 - \bar{B}^0$ mixing with inclusive dilepton events"*, J.P. Lees, et al., BaBar Collaboration, *Phys. Rev. Lett. 114 (8) (2015) 081801*; HFLAV Collaboration.

[7] *"Review of Particle Physics"*, C. Patrignani *et al.* [Particle Data Group], *Chin. Phys. C 40, no. 10, 100001 (2016)*.

[8] *"Probing the weak boson sector in $e^+e^- \rightarrow W^+W^-$"*, K. Hagiwara, R. D. Peccei and D. Zeppenfeld, *Nucl. Phys. B 282, 253 (1987)*.

[9] *"Bound on the W-boson electric dipole moment"*, W. J. Marciano and A. Queijeiro, *Phys. Rev. D 33, 3449 (1986)*.

[10] *"Heavy fermion contributions to the anomalous magnetic dipole and quadrupole moments of theW-boson"*, G. Couture and J. N. Ng, *Z. Phys. C 35, 65 (1987)*.

[11] Y. Kuno (private communication)

[12] *"An attempt of a theory of beta radiation. 1 (In German)"*, E. Fermi, *Z. Phys. 88, (1934) 161 – 177*.

[13] *"Partial Symmetries of Weak Interactions"*, S. L. Glashow, *Nucl. Phys. 22 (1961) 579 – 588*.

[14] *"A Model of Leptons"*, S. Weinberg, *Phys. Rev. Lett. 19 (1967) 1264 – 1266*.

[15] *"Weak and Electromagnetic Interactions"*, Abdus Salam, *Conf. Proc. C 680519 (1968) 367 – 377*.

[16] *"Renormalizable Lagrangians for massive Yang-Mills fields"*, G. 't Hooft, *Nucl. Phys. B 35 (1971) 167-188*.

[17] *"A Schematic Model of Baryons and Mesons"*, M. Gell-Mann, *Phys. Lett. 8 (1964) 214 – 215*.

[18] *"An SU(3) model for strong interaction symmetry and its breaking. Version 2"*, G. Zweig, Published in 'Developments in the Quark Theory of Hadrons'. Volume 1, Hadronic Press, 1980. pp. 22-101, *CERN-TH-412, NP-14146, PRINT-64-170*.

[19] *"The Connection Between Spin and Statistics"*, W. Pauli, *Phys. Rev. 58 (1940) 716 – 722*.

[20] *"Spin and unitary spin independence in a paraquark model of baryons and mesons"*, O. W. Greenberg, *Phys. Rev. Lett. 13, 598 – 602 (1964)*.

[21] *"Three-Triplet Model with Double SU(3) Symmetry"*, M. Y. Han and Y. Nambu, *Phys. Rev. 139, B1006 – B1010 (1965)*.

[22] *"Advantages of the color octet gluon picture"*, H. Fritzsch, M. Gell-Mann, H Leutwyler, *Phys. Lett. 47 B (1973) 365 – 368*.

[23] *"Conservation of Isotopic Spin and Isotopic Gauge Invariance"*, C. N. Yang and R. L. Mills, *Phys. Rev. 96, 191 (1954)*.

[24] *"Precision electroweak measurements on the Z resonance"*, ALEPH and DELPHI and L3 and OPAL and SLD Collaborations and LEP Electroweak Working Group and SLD Electroweak Group and SLD Heavy Flavour Group, *Phys.Rept. 427 (2006) 257 – 454*.

[25] *"Electroweak Measurements in Electron-Positron Collisions at W-Boson-Pair Energies at LEP"*, ALEPH and DELPHI and L3 and OPAL and LEP Electroweak Collaborations, *Phys. Rept. 532 (2013) 119 – 244*.

[26] *"Observation of Top Quark Production in $\bar{p}p$ Collisions with the Collider Detector at Fermilab"*, F. Abe *et al.* (CDF Collaboration), *Phys. Rev. Lett. 74 (1995) 2626-2631*.

[27] *"Observation of the Top Quark"*, S. Abachi *et al.* (D0 Collaboration), *Phys. Rev. Lett. 74, 2632 (1995)*.

[28] *"Observation of tau neutrino interactions"*, K. Kodama *et al.* (DONUT Collaboration), *Phys. Lett. B 504 (2001) 218 – 224*.

[29] *"Observation of a new boson at a mass of 125 GeV with the CMS experiment at the LHC"*, S. Chatrchyan *et al.* (CMS Collaboration), *Phys. Lett. B 716 (2012) 30 – 61*.

[30] *"Observation of a New Particle in the Search for the Standard Model Higgs Boson with the ATLAS Detector at the LHC"*, G. Aad *et al.* (ATLAS Collaboration), *Phys. Lett. B 716 (2012) 1 − 29*.

[31] *"Question of Parity Conservation in Weak Interactions"*, T. D. Lee and C. N. Yang, *Phys. Rev. 104, 254 (1956)*.

[32] *"On parity conservation and neutrino mass"*, Abdus Salam, *Nuovo Cim. 5 (1957) 299 − 301*.

[33] *"Experimental Test of Parity Conservation in Beta Decay"*, C. S. Wu, E. Ambler, R. W. Hayward, D. D. Hoppes, and R. P. Hudson, *Phys. Rev. 105, 1413 (1957)*.

[34] *"On the conservation laws for weak interactions"*, L Landau, *Nucl Phys. 3, 127 (1957)*.

[35] *"Parity nonconservation and a two-component theory of the neutrino"*, T. D. Lee and C. N. Yang, *Phys. Rev. 105, 1671 (1957)*.

[36] *"Evidence for the $2\pi$ decay of the $K_2^0$ meson"*, J. H. Christenson, J. W. Cronin, V. L. Fitch and R. Turlay, *Phys. Rev. Lett. 13 138 (1964)*.

[37] *"Revised experimental upper limit on the electric dipole moment of the neutron"*, J. M. Pendlebury *et al.*, *Phys. Rev. D 92 (2015) no. 9, 092003*.

[38] *"The nature of the four-fermion interaction"*, E. C. G. Sudarshan and R. E. Marshak, Proceedings of the Padua-Venice Conference on Mesons and Newly Discovered Particles, 22-27 September 1957, Bologna 1958, p. V-14.

[39] *"Theory of the Fermi Interaction"*, R. P. Feynman and M. Gell-Mann, *Phys. Rev. 109, 193 (1958)*.

[40] *"On the Equivalence of Invariance under Time-Reversal and under Particle-Antiparticle Conjugation for Relativistic Field Theories"*, G. Lüders, *Kong. Dan. Vid. Sel. Mat. Fys. Med. 28N5 (1954) no.5, 1-17*.

[41] *Niels Bohr and the Development of Physics*, (Pergamon Press, New York, 1955), W. Pauli.

[42] *"A remark on the C.T.P. theorem"*, R. Jost, **Helv. Phys. Acta 30 (1957) 409**.

[43] *PCT, Spin & Statistics, and All That*, (Princeton University Press, 2000), R. F. Streater and A. S. Wightman.

[44] *Introduction to Axiomatic Quantum Field Theory*, (W.A. Benjamin, 1975), N. N. Bogoliubov, A. A. Logunov and I. T. Todorov.

[45] *"CPT and Lorentz Invariance: Their Relation and Violation"*, A. Tureanu, *J. Phys. Conf. Ser. 474 (2013) 012031*.

[46] *"Spin statistics and CPT theorems in noncommutative field theory"*, M. Chaichian, K. Nishijima and A. Tureanu, *Phys. Lett. B 568 (2003) 146*.

[47] *"General properties of noncommutative field theories"*, L. Álvarez-Gaumé and M. A. Vázquez-Mozo, *Nucl. Phys. B 668 (2003) 293*.

[48] *"Towards an axiomatic formulation of noncommutative quantum field theory"*, M. Chaichian, M. N. Mnatsakanova, K. Nishijima, A. Tureanu and Yu. S. Vernov, *J. Math. Phys. 52 (2011) 032303*.

[49] *"C, P, and T invariance of noncommutative gauge theories"*, M. M. Sheikh-Jabbari, *Phys. Rev. Lett. 84 (2000) 5265-5268*.

[50] *"CPT Violation Does Not Lead to Violation of Lorentz Invariance and Vice Versa"*, M. Chaichian, A. D. Dolgov, V. A. Novikov and A. Tureanu, *Phys. Lett. B 699 (2011) 177-180*.

[51] *"Lorentz invariant CPT violation: Particle and antiparticle mass splitting"*, M. Chaichian, K. Fujikawa and A. Tureanu, *Phys. Lett. B 712 (2012) 115*.

[52] *"Lorentz invariant CPT violation"*, M. Chaichian, K. Fujikawa and A. Tureanu, *Eur. Phys. J. C 73 (2013) 2349*.

[53] *Quarks and Leptons: An Introductory Course in Modern Particle Physics*, (Wiley, 1st Edition, 1984), F. Halzen and A. D. Martin, page 42.

[54] *An introduction to quantum field theory*, M. E. Peskin and D. V. Schroeder.

[55] *"Gravity, Lorentz violation, and the standard model"*, V. A. Kostelecky, *Phys. Rev. D 69, 105009 (2004)*.

[56] *"Search for violations of Lorentz invariance and CPT symmetry in $B^0_{(s)}$ mixing"*, R. Aaij *et al.* [LHCb Collaboration], *Phys. Rev. Lett. 116, no. 24, 241601 (2016)*.

[57] *"CP, T and CPT versus temporal asymmetries for entangled states of the $B_d$ system"*, M. C. Bañuls and J. Bernabéu, *Phys. Lett. B 464, 117 (1999)*.

[58] *"Studying indirect violation of CP, T and CPT in a B factory"*, M. C. Bañuls and J. Bernabéu, *Nucl. Phys. B 590, 19 (2000)*.

[59] *"Correlated neutral B meson decays into CP eigenstates"*, E. Alvarez and J. Bernabéu, *Phys. Lett. B 579, 79 (2004)*.

[60] *"CPT violation in entangled $B^0$-$\bar{B}^0$ states and the demise of flavor tagging"*, E. Alvarez, J. Bernabéu, N. E. Mavromatos, M. Nebot and J. Papavassiliou, *Phys. Lett. B 607, 197 (2005)*.

[61] *"Direct test of time reversal invariance violation in B mesons"*, E. Alvarez and A. Szynkman, *Mod. Phys. Lett. A 23, 2085 (2008)*.

[62] *"Time Reversal Violation from the entangled $B^0$-$\bar{B}^0$ system"*, J. Bernabéu, F. Martinez-Vidal and P. Villanueva-Perez, *JHEP 1208, 064 (2012)*.

[63] *"Subtleties in the BABAR measurement of time-reversal violation"*, E. Applebaum, A. Efrati, Y. Grossman, Y. Nir and Y. Soreq, *Phys. Rev. D 89, no. 7, 076011 (2014)*.

[64] *"Genuine T, CP, CPT asymmetry parameters for the entangled $B_d$ system"*, J. Bernabéu, F. J. Botella and M. Nebot, *JHEP 1606, 100 (2016)*.

[65] *"Limits on the decay-rate difference of neutral B mesons and on CP, T, and CPT violation in $B^0 \bar{B}^0$ oscillations"*, B. Aubert *et al.* (BaBar Collaboration), *Phys. Rev. Lett. 92, 181801 (2004)*.

[66] *"Limits on the decay rate difference of neutral$-B$ mesons and on CP, T, and CPT violation in $B^0 \bar{B}^0$ oscillations"*, B. Aubert *et al.* (BaBar Collaboration), *Phys. Rev. D 70, 012007 (2004)*.

[67] *"Observation of Time Reversal Violation in the $B^0$ Meson System"*, J. P. Lees *et al.* (BaBar Collaboration), *Phys. Rev. Lett. 109, 211801 (2012)*.

[68] *CP violation, Cambridge Monographs on Particle Physics Nuclear Physics and Cosmology*, (Cambridge University Press, 2 edition, 2009), I. I. Bigi and A. I. Sanda.

[69] *"Measurement of the $W\gamma$ and $Z\gamma$ inclusive cross sections in pp collisions at $\sqrt{s} = 7$ Tev and limits on anomalous triple gauge boson couplings"*, S. Chatrchyan *et al.* (CMS Collaboration), *Phys. Rev. D 89, 092005 (2014)*.

[70] *"Measurements of $W\gamma$ and $Z\gamma$ production in pp collisions at $\sqrt{s} = 7$ Tev with the ATLAS detector at the LHC"*, G. Aad *et al.* (ATLAS Collaboration), *Phys. Rev. D 87, 112003 (2013)*.

[71] *"Limits on anomalous trilinear gauge boson couplings from WW, WZ and $W\gamma$ production in $p\bar{p}$ collisions at $\sqrt{s} = 1.96$ Tev"*, V. M. Abazov *et al.* (D0 Collaboration), *Phys. Lett. B 718 (2012) 451-459*.

[72] *"Measurement of the $W^+W^-$ production cross section and search for anomalous $WW\gamma$ and $WWZ$ couplings in $p\bar{p}$ collisions at $\sqrt{s}$ = 1.96 Tev"*, T. Aaltonen et al. (CDF Collaboration), *Phys. Rev. Lett. 104 (2010) 201801*.

[73] *"Measurements of CP-conserving trilinear gauge boson couplings WWV ($V \equiv \gamma, Z$) in $e^+e^-$ collisions at LEP2"*, J. Abdallah et al. (DELPHI Collaboration), *Eur. Phys. J. C 66 (2010) 35 − 56*.

[74] *"Improved measurement of the triple gauge-boson couplings $\gamma$WW and ZWW in $e^+e^-$ collisions"*, S. Schael et al. (ALEPH Collaboration), *Phys. Lett. B 614 (2005) 7 − 26*.

[75] *"Measurement of charged current triple gauge boson couplings using W pairs at LEP"*, G. Abbiendi et al. (PAL Collaboration), *Eur. Phys. J. C 33 (2004) 463 − 476*.

[76] *"Measurement of triple-gauge-boson couplings of the W boson at LEP"*, P. Achard et al. (L3 Collaboration), *Phys. Lett. B 586 (2004) 151 − 166*.

[77] *"Magnetic Moment of Weak Bosons Produced in pp and $p\bar{p}$ Collisions"*, K. O. Mikaelian, M. A. Samuel and D. Sahdev, *Phys. Rev. Lett. 43, 746 (1979)*.

[78] *"Muon decay and physics beyond the standard model"*, Y. Kuno, Y. Okada, *Rev. Mod. Phys. 73 (2001) 151 − 202*.

[79] *"Theory of Charged Vector Mesons Interacting with the Electromagnetic Field"*, T.D. Lee, C.N. Yang, *Phys. Rev. 128 (1962) 885 − 898*.

[80] *"Spin-1 Electrodynamics with an Electric Quadrupole Moment"*, H. Aronson, *Phys. Rev. 186 (1969) 1434 − 1441*.

[81] *"Magnetic Dipole and Electric Quadrupole Moments of the $W^\pm$ Meson"*, K. J. Kim, Y. S. Tsai, *Phys. Rev. D 7 (1973) 3710*.

[82] *Collider Physics, Frontiers in Physics*, (Addison-Wesley, updated edition, 1996), V. D. Barger and R. J. N. Phillips, page 562.

[83] *"Right-handed electrons in radiative muon decay"*, L. M. Sehgal, *Phys. Lett. B 569 (2003) 25 – 29*.

[84] *"Wrong helicity electrons in radiative muon decay"*, V. S. Schulz and L. M. Sehgal, *Phys. Lett. B 594 (2004) 153 – 163*.

[85] *Particle Kinematics*, (Wiley, 1973), E. Byckling and K. Kajantie, page 106.

[86] *"One loop corrections to radiative muon decay"*, A. B. Arbuzov, E. S. Scherbakova, *Phys. Lett. B 597 (2004) 285 – 290*.

[87] *"W-propagator corrections to $\mu$ and $\tau$ leptonic decays"*, M. Fael, L. Mercolli, M. Passera, *Phys. Rev. D 88 (2013) no. 9, 093011*.

[88] *"Radiative $\mu$ and $\tau$ leptonic decays at NLO"*, M. Fael, L. Mercolli, M. Passera, *JHEP 1507 (2015) 153*.

[89] *"Fully differential NLO predictions for the radiative decay of muons and taus"*, G. M. Pruna, A. Signer, Y. Ulrich, *Phys. Lett. B 772 (2017) 452 – 458*.